

DOE/PC/93215--T8

FINAL REPORT

**NOVEL MICROORGANISM FOR SELECTIVE  
SEPARATION OF COAL FROM PYRITE AND ASH**

DOE Grant No. DE-FG22-93PC93215

Submitted to :

The Department of Energy  
Pittsburgh Energy Technology Center  
P. O. Box 10940, MS 921-118  
Pittsburgh, PA 15236-0940

by:

Manoranjan Misra  
Department of Chemical and Metallurgical Engineering  
Mackay School of Mines  
University of Nevada, Reno  
Reno, NV 89557

**CLEARED BY  
PATENT COUNSEL**

September 1995

THE ATTACHED REPORTS HAVE BEEN  
ENTERED INTO THE DTS AND DISTRIBUTED  
ON 2-1-96  
THIS IS THE COPY FOR THE AWARD FILE  
DOCUMENT CONTROL CENTER

DISTRIBUTION OF THIS DOCUMENT IS UNLIMITED

**MASTER**

## PROJECT PERSONNEL

Principal Investigator : Dr. Manoranjan Misra

Co-principal Investigator : Dr. Ross W. Smith

Students : Ashok M. Raichur (Graduate Student)  
Amy Mouat (UCR Intern)

Visiting Scholar : Dr. K. Bukka

## DISCLAIMER

This report was prepared as an account of work sponsored by an agency of the United States Government. Neither the United States Government nor any agency thereof, nor any of their employees, makes any warranty, express or implied, or assumes any legal liability or responsibility for the accuracy, completeness, or usefulness of any information, apparatus, product, or process disclosed, or represents that its use would not infringe privately owned rights. Reference herein to any specific commercial product, process, or service by trade name, trademark, manufacturer, or otherwise does not necessarily constitute or imply its endorsement, recommendation, or favoring by the United States Government or any agency thereof. The views and opinions of authors expressed herein do not necessarily state or reflect those of the United States Government or any agency thereof.

## PROJECT SUMMARY

The project "Novel Microorganism for Selective Separation of Coal from Pyrite and Ash" was conducted with a support from the Department of Energy, Pittsburgh Energy Technology Center under the University Coal Research program. This final report describes the results and findings of this project during the performance period of September 1, 1993 through August 31, 1995.

In keeping with the main objective of the project, the separation of fine coal from ash and pyrite was conducted using a microorganism *Mycobacterium phlei* (*M. phlei*). The surface hydrophobicity and surface charge of *Mycobacterium phlei* and its sonicated products (extracellular soluble fractions) were established using contact angle and electrophoretic measurements. *Mycobacterium phlei* was highly hydrophobic and point-of-zero charge was around pH 2. The hydrophobic character and negative surface charge of the microorganism above pH 2 were due to the presence of excessive fatty groups at the surface and corresponding carboxylate groups. In addition, soluble fractions derived from the cell exhibited the presence of varying amounts of fatty acids ranging from C<sub>14</sub> - C<sub>20</sub> carbon chain and phosphate groups.

The surface chemistry analyses of coal, coal-pyrite, mineral pyrite and quartz were conducted. The adhesion of *Mycobacterium phlei* onto coal, coal-

pyrite and quartz was measured as a function of pH and *Mycobacterium phlei* concentration. It was noticed that *Mycobacterium phlei* selectively attached to hydrophobic coal particles and did not attach to hydrophilic mineral fractions. Adhesion was strongly dependent on pH and maximum adhesion was observed in an acidic pH range of 3-4.

On the basis of the detailed surface chemistry analysis, adhesion and contact angle measurements, a series of flocculation and flotation experiments were conducted. The experimental results showed that *Mycobacterium phlei* was an excellent flotation collector and flocculating agent. However, the soluble fraction derived from *Mycobacterium phlei* by sonication was a better flotation collector and flocculating agent for fine coal than whole cells of *Mycobacterium phlei*. In order to selectively separate the coal-*Mycobacterium phlei* entities, a modified floc-flotation technique was used. At an optimized experimental condition, more than 70 percent pyritic sulfur and 60 percent of ash could be rejected with a combustible (clean coal) recovery of 90 percent. During this investigation, it was established that *Mycobacterium phlei* and more importantly its sonication products had a strong potential to be used for selective flocculation and separation of fine coal from associated mineral matters.

## TABLE OF CONTENTS

Project Summary .....	iii
Table of Contents .....	v
List of Figures .....	viii
List of Tables .....	xiii
<b>CHAPTER 1. INTRODUCTION .....</b>	<b>1</b>
1.1 Objective and Scope of the Work .....	5
<b>CHAPTER 2. BACKGROUND .....</b>	<b>7</b>
2.1 Physical Coal Cleaning .....	8
2.1.1 Froth Flotation .....	8
2.1.2 Selective Agglomeration .....	11
2.1.3 Selective Flocculation .....	13
2.2 Chemical Coal Cleaning .....	15
2.3 Microbial Coal Cleaning .....	16
2.4 Bioflocculation .....	21
2.4.1 <i>Mycobacterium phlei</i> .....	21
2.4.2 <i>Mycobacterium phlei</i> in Mineral Processing .....	25
<b>CHAPTER 3. EXPERIMENTAL MATERIALS AND METHODS .....</b>	<b>28</b>
3.1 Materials .....	28
3.2 Techniques and Procedures .....	30
3.2.1 Culture of <i>M. phlei</i> .....	30
3.2.2 Sonication of <i>M. phlei</i> cells .....	32
3.2.3 Zeta potential measurements .....	32
3.2.4 Contact Angle Measurements .....	33
3.2.5 Adhesion Experiments .....	35

3.2.6	Scanning Electron Microscopy Studies	37
3.2.7	Sedimentation and Flocculation Experiments	37
3.2.8	Floc Separation	40
3.2.9	Analysis of Coal	41
3.3	Bulk Physical and Chemical Properties of Samples	42
<b>CHAPTER 4. RESULTS AND DISCUSSION</b>		<b>48</b>
4.1	Characterization of <i>Mycobacterium phlei</i>	48
4.1.1	Growth Kinetics	48
4.1.2	Morphology of <i>M. phlei</i>	50
4.1.3	Cell Wall Composition of <i>M. phlei</i>	52
4.1.4	Surface properties of <i>M. phlei</i>	57
4.2	Characterization of Coal and Mineral Samples	60
4.3	Adhesion Experiments	64
4.3.1	Adhesion of <i>M. phlei</i> whole cells	67
4.3.2	Adhesion of sonicated cells of <i>M. phlei</i>	72
4.4	Effect of Adhesion on Hydrophobicity	74
4.5	Scanning Electron Microscopy (SEM) Studies	81
4.6	Sedimentation and Flocculation Experiments	88
4.6.1	Effect of time	88
4.6.2	Effect of concentration on flocculation efficiency	92
4.6.3	Effect of pH on flocculation efficiency	96
4.7	Floc-Separation	101
4.7.1	Settling	101
4.7.2	Flotation	102
4.8	Interaction Energy Calculations	115
4.8.1	Columbic Interaction Energy	115
4.8.2	Hydrophobic Interaction Energy	136

<b>CHAPTER 5. CONCLUSIONS</b> .....	<b>143</b>
<b>REFERENCES</b> .....	<b>148</b>

## LIST OF FIGURES

Figure 2.1	Cellular structure of procaryotic microorganisms . . . . .	22
Figure 2.2	Schematic diagram of the cell membrane showing the arrangement of proteins and phospholipids . . . . .	23
Figure 3.1	Schematic of the graduated cylinder used in sedimentation and flocculation experiments . . . . .	38
Figure 3.2	SEM-EDX Analysis of Illinois No.6 Coal . . . . .	46
Figure 3.3	SEM-EDX Analysis of Coal-pyrite . . . . .	47
Figure 4.1	Growth curve for <i>Mycobacterium phlei</i> as a function of time .	49
Figure 4.2	Scanning Electron Microphotograph of <i>M. phlei</i> whole cells . .	51
Figure 4.3	Scanning Electron Microphotograph of <i>M. phlei</i> sonicated cells . . . . .	53
Figure 4.4	FTIR spectra of <i>M. phlei</i> whole cells . . . . .	54
Figure 4.5	Amount of extracellular surfactant released as a function of sonication time . . . . .	56
Figure 4.6	Zeta potential measurements of whole and sonicated cells of <i>M. phlei</i> . . . . .	59
Figure 4.7	Zeta potential measurements of coal, coal-pyrite, mineral pyrite and quartz as a function of pH . . . . .	61
Figure 4.8	Advancing contact angle measurements of coal and pyrite as as function of pH in the absence of <i>M. phlei</i> . . . . .	63



Figure 4.9	Calibration plot for <i>M. phlei</i> whole cells .....	65
Figure 4.10	Calibration plot for sonicated cells of <i>M. phlei</i> .....	66
Figure 4.11	Effect of conditioning time on the amount of whole cells adhering onto coal, pyrite and quartz surfaces .....	68
Figure 4.12	Effect of concentration of whole cells of <i>M. phlei</i> on the amount adhering onto coal, pyrite and quartz .....	69
Figure 4.13	Effect of pH on the amount of whole cells of <i>M. phlei</i> adhering to coal, pyrite and quartz .....	71
Figure 4.14	Effect of concentration on the amount of sonicated cells of <i>M. phlei</i> adhering to coal, pyrite and quartz .....	73
Figure 4.15	Effect of pH on the amount of sonicated cells of <i>M. phlei</i> adhering to coal, pyrite and quartz .....	75
Figure 4.16	Comparison of advancing contact angle measurements for IL No.6 coal in the presence and absence of <i>M. phlei</i> .....	76
Figure 4.17	Comparison of advancing contact angle measurements for KY No.9 coal in the presence and absence of <i>M. phlei</i> .....	77
Figure 4.18	Contact angle measurements of coal-pyrite in the presence and absence of whole cells of <i>M. phlei</i> as a function of pH .....	79
Figure 4.19	Contact angle measurements of mineral pyrite in the presence and absence of whole cells of <i>M. phlei</i> as a function of pH ...	80
Figure 4.20	Scanning electron microphotograph of <i>M. phlei</i> adhering to IL No.6 coal (pH 3.5; 180 ppm concentration) .....	82
Figure 4.21	Scanning electron microphotograph of <i>M. phlei</i> adhering to IL No.6 coal (pH 8.2; 180 ppm concentration) .....	83

Figure 4.22	Scanning electron microphotograph of <i>M. phlei</i> adhering to coal-pyrite (pH 3.5; 180 ppm concentration) .....	84
Figure 4.23	Scanning electron microphotograph of <i>M. phlei</i> adhering to mineral pyrite (pH 3.5; 180 ppm concentration) .....	85
Figure 4.24	Scanning electron microphotograph of <i>M. phlei</i> adhering to mineral pyrite (pH 8.2; 180 ppm concentration) .....	86
Figure 4.25	Scanning electron microphotograph of <i>M. phlei</i> adhering to quartz (pH 3.5; 180 ppm concentration) .....	87
Figure 4.26	Amount of IL No.6 coal settled as a function of time in the presence of different flocculants .....	89
Figure 4.27	Amount of KY No.9 coal settled as a function of time in the presence of different flocculants .....	91
Figure 4.28	The effect of concentration of different flocculants on the flocculation efficiency of IL No.6 coal .....	93
Figure 4.29	Scanning electron microphotograph of coal floc formed with whole cells of <i>M. phlei</i> .....	95
Figure 4.30	Effect of concentration of different flocculants on the flocculation efficiency of KY No.9 coal .....	97
Figure 4.31	The effect of different flocculants on the flocculation efficiency of IL No.6 coal as a function of pH .....	98
Figure 4.32	The effect of different flocculants on the flocculation efficiency of KY No.9 coal as a function of pH .....	100
Figure 4.33	The amount of coal and coal-pyrite settled in the presence and absence of <i>M. phlei</i> whole cells as a function of time ...	103

Figure 4.34	The effect of gas (nitrogen) flow rate on the combustible recovery and pyritic sulfur/ash rejection for IL No.6 coal . . .	105
Figure 4.35	The effect of frother (MIBC) dosage on the combustible recovery and pyritic sulfur/ash rejection for IL No.6 coal . . .	106
Figure 4.36	Combustible recovery for IL No.6 coal in the presence of different reagents as a function of pH . . . . .	112
Figure 4.37	Pyritic sulfur rejection for IL No.6 coal in the presence of different reagents as a function of pH . . . . .	113
Figure 4.38	Ash rejection for IL No.6 coal in the presence of different reagents as a function of pH . . . . .	114
Figure 4.39	Combustible recovery for KY No.9 coal in the presence of different reagents as a function of pH . . . . .	116
Figure 4.40	Pyritic sulfur rejection for KY No.9 coal in the presence of different reagents as a function of pH . . . . .	117
Figure 4.41	Ash rejection for KY No.9 coal in the presence of different reagents as a function of pH . . . . .	118
Figure 4.42	The variation of total interaction energy as a function of separation distance at different pH values for IL No.6 coal and whole cells . . . . .	126
Figure 4.43	Effect of pH on the total interaction energy for IL No.6 coal and whole cells of <i>M. phlei</i> . . . . .	127
Figure 4.44	Comparison of total interaction energies for coal, coal-pyrite and quartz with whole cells of <i>M. phlei</i> as a function of pH . . . . .	128
Figure 4.45	Comparison of total interaction energies for coal, coal-pyrite	

	and quartz with sonicated cells of <i>M. phlei</i> as a function of pH .....	130
Figure 4.46	Comparison of interaction energies for whole cell/coal and sonicated cell/coal interface for IL No.6 coal .....	131
Figure 4.47	Comparison of interaction energies for whole cell/coal and sonicated cell/coal interface for KY No.9 coal .....	133
Figure 4.48	Comparison of interaction energies for whole cell/coal-pyrite and sonicated cell/coal-pyrite interface .....	134
Figure 4.49	Comparison of interaction energies for whole cell/quartz and sonicated cell/quartz interface .....	135

## LIST OF TABLES

Table 2.1	Contact angle and electrophoretic mobilities of various microorganisms .....	26
Table 3.1	List of different samples used in this study .....	29
Table 3.2	List of chemicals used in this study .....	29
Table 3.3	Procedure for calculating combustible recovery .....	42
Table 3.4	Proximate and Ultimate Analysis of Illinois No.6 Coal .....	44
Table 3.5	Proximate and Ultimate Analysis of Kentucky No.9 Coal ...	45
Table 4.1	The fatty acid composition of the extracellular surfactant ...	57
Table 4.2	The contact angle of <i>M. phlei</i> before and after sonication ...	58
Table 4.3	Analysis of IL No.6 coal before and after flocculation with whole cells of <i>M. phlei</i> .....	101
Table 4.4	Flotation results of IL No.6 coal at pH 3.6 .....	108
Table 4.5	Flotation results of KY No.9 coal at pH 3.9 .....	110
Table 4.6	The $\gamma_s^d$ values and Hamaker constants ( $A_{11}$ ) for different minerals .....	124
Table 4.7	Zeta potential values of different samples used for DLVO calculations .....	124
Table 4.8	Potential energies of interaction for IL No.6 coal and <i>M. phlei</i> whole cells .....	140

Table 4.9	Potential energies of interaction for KY No.9 coal and <i>M. phlei</i> whole cells .....	140
Table 4.10	Potential energies of interaction for coal-pyrite and <i>M. phlei</i> whole cells .....	141

## CHAPTER 1

### INTRODUCTION

Coal is the nation's most abundant fossil energy resource. It is also the largest domestic source of energy. It has been estimated that there are more than 1 trillion tons of coal which can be potentially recovered for commercial use. At the current consumption level of coal for power generation, this constitutes close to 1,000 years of coal supply. During 1994, the total U.S. coal production was 934 million tons and electric utilities accounted for 88% of coal consumption. It is projected that the demand for coal from utilities will rise sharply in the coming years.

Most of the U.S. coals, especially those in the Illinois coal basin, have high amounts of sulfur and ash forming minerals associated with them. The utilization of these high sulfur coals is of particular concern as current and newer, potentially more stringent, regulations require reduction in sulfur dioxide emissions. According to the 1990 Clean Air Act Amendments (CAAA),

utilities must comply with an average emission standard of 2.5 pounds of sulfur dioxide per million Btu by the year 1995 and 1.2 pounds of sulfur dioxide per million Btu by the year 2000. Release of particulates,  $\text{NO}_x$ , and other pollutants during the coal-use cycle is also of concern. Sulfur dioxide together with nitrogen oxides are primarily responsible for acid rain.

The impurities occurring in coal may be classified broadly into those that form ash and those that contribute sulfur. From the standpoint of coal cleaning, both the ash-forming and the sulfur-containing impurities may be subdivided into two categories - inherent and extraneous. The inherent impurities are inseparably combined with the coal. The extraneous impurities are segregated and can be eliminated by the available cleaning methods.

Sulfur occurs in coal in three different forms. It is present in organic compounds as part of the coal substance, as sulfides, generally pyrite or marcasite, and as sulfate. The amount of organic sulfur normally is not over 3%. The sulfates, mainly calcium and iron, rarely exceed a few hundredths percent except in highly weathered and oxidized samples. Pyrite and marcasite constitute the principal mineral form of sulfur found in coals. The principal ash-forming minerals include various clay minerals, carbonates, oxides and hydroxides.



The current practice of controlling sulfur dioxide, nitrogen oxides and particulate emissions in the coal-use cycle is limited mainly to coal preparation by physical beneficiation and, to a smaller extent, to post utilization cleanup. Commonly used physical beneficiation methods include jigs, dense-medium baths, cyclone systems, and concentrating tables. Coal needs to be ground to finer sizes to liberate the associated mineral matter and pyrite. Conventional coal cleaning methods are ineffective at these fine sizes. In particular the rejection of pyrite is a very difficult problem. It was reported by Hucko et al. (1988) that approximately two-thirds of the coal from states east of the Mississippi is physically cleaned; whereas, only 15% to 20% of the operating boilers in the utility industry are equipped with scrubbers to desulfurize the flue gas. Therefore, to comply with the 1990 CAAA, the utilities will have to make a choice between installing scrubbers or switching to low-sulfur coals. Installing scrubbers might not be economically feasible for all existing power plants. Therefore, the demand for low sulfur coal is expected to rise in the coming years, and pre-combustion cleaning of coal is expected to play a major role in the reduction of sulfur dioxide emissions from utility boilers.

Over the past decade, several processes have been studied for removing sulfur and ash-forming minerals to produce compliance quality coal. These methods may be broadly classified into chemical, biological and physical cleaning methods. Most chemical cleaning technologies can remove ash-forming

minerals and sulfur very effectively, however, the operating costs are very high due to very high temperatures and pressures involved. In addition, some of the processes involve the generation of toxic wastes. Biological coal cleaning technologies can effectively remove both organic and inorganic sulfur from coal, but are ineffective in removing ash-forming minerals.

Advanced physical coal cleaning technologies such as column flotation, oil agglomeration, selective flocculation, etc. have received considerable attention due to their lower operating costs. A prerequisite for these processes is that the feed coal needs to be ground to micron size to liberate all the mineral matter and pyrite from coal. As the particle size decreases ( $<75 \mu\text{m}$ ), the effect of particle size becomes small and the role of surface properties becomes important i.e., hydrophobicity of coal versus hydrophilicity of mineral matter. Advanced coal cleaning processes may be inefficient in terms of pyrite and ash rejection due to the variable surface properties of mineral matter. Effective control of the surface properties of coal and mineral matter is required in order to obtain an effective separation of pyrite and ash from coal. Of all the advanced coal cleaning technologies studied so far, only froth flotation has been commercialized so far. However, at very fine sizes, even froth flotation has its limitations. The efficiency of separation of coal by flotation decreases at ultra-fine sizes, therefore, there is a need to develop new processes or modify existing processes

in order to produce compliance quality coal from high sulfur, high ash coals.

### 1.1 Objective and Scope of the Work

The objective of the present work was to study a novel method for selectively flocculating coal by using a hydrophobic microorganism, *Mycobacterium phlei*, and to separate the coal flocs from pyrite and ash by column flotation. The scope of the present work involved studying the surface chemistry of coal, pyrite and *Mycobacterium phlei* in detail. The adhesion of *Mycobacterium phlei* onto coal and pyrite and its effect on the hydrophobicity were studied by spectrophotometric and contact angle measurements. Zeta potential measurements were used to study the surface electrical properties of coal, pyrite and *Mycobacterium phlei*. The effect of various parameters such as pH, concentration of microorganism, etc. on the adhesion and hence flocculation behavior of coal were studied. The surface chemical composition of the microorganism was determined by sonication of the cells. Also, the effect of sonication on the surface properties of the bacterium were studied.

The role of extracellular surfactants present on the cell wall of *Mycobacterium phlei* in the flocculation of coal were also investigated. Separation of coal flocs were conducted using column flotation and the effect of gas flow rate and frother dosage on combustible recovery and pyrite/ash

rejection were studied. The contributions due to van der Waal's attractive energy and electrical repulsive energy in the flocculation of coal was evaluated by using the extended Derjaguin-Landau-Verwey-Overbeek (DLVO) theory. The importance of hydrophobic interaction energy in the coal-*Mycobacterium phlei* system was examined. Finally, an attempt was made to correlate the flocculation efficiency, adhesion results and hydrophobicity measurements with the interaction energy calculations.

## CHAPTER 2

### BACKGROUND

As discussed in chapter one, removal of sulfur and ash-forming minerals from high-sulfur, high ash coal is essential in order to meet the requirements of the 1990 Clean Air Act. In high-sulfur coals, roughly 55-80% of the total sulfur is due to pyritic sulfur (Yoon, 1991). This sulfur can be removed substantially by advanced physical coal cleaning processes such as flotation, flocculation and oil agglomeration. Conventional coal cleaning processes, on the other hand, are not designed to remove more than 10 to 50% of the pyritic sulfur (Yoon, 1991). Chemical and microbial coal cleaning processes have been shown to remove both pyritic and organic sulfur, but at significantly higher operating costs than the physical cleaning processes. It should be noted that a prerequisite to all advanced physical coal cleaning processes is that the feed coal has to be pulverized to a size at which mineral matter is sufficiently liberated from the coal.

Thus, advanced cleaning processes have two major impetuses for their

development, i.e., producing super-clean or ultra-clean coals for increased utilization and helping to solve the SO<sub>2</sub> abatement problem. In this chapter, many of the advanced coal cleaning processes that are under development along with their advantages and disadvantages will be discussed.

## 2.1 Physical Coal Cleaning

### 2.1.1 *Froth Flotation*

Froth flotation is a physico-chemical separation process that depends on the attachment of hydrophobic particles to air bubbles. Other hydrophilic particles are wetted by the aqueous phase and do not attach to the air bubbles. Conventional coal flotation is typically used to clean either the minus 28 mesh (minus 500 μm) or minus 100 mesh (minus 150 μm) raw coal fines. The process involves the addition of a modifier (No.2 fuel oil) which adsorbs onto coal rendering the coal surface hydrophobic. Methyl isobutyl carbinol (MIBC) is used as a frother. A very high grade product can be obtained from flotation provided all the conditions are satisfied.

Historically, this process has been used to treat the coal fines naturally occurring after mining and a minimal amount of crushing at the preparation

plant. However, over the past few years, flotation has been studied as a potential technique that can be used to clean micronized coal to produce compliance quality coal. But it has some disadvantages. When the particle size is too small or when the coal contains a large amount of clay, froth flotation becomes ineffective. Small particles have a low probability of collision with air bubbles, resulting in a low coal recovery. Another serious problem is that of entrainment or entrapment. As bubbles laden with hydrophobic coal particles enter the froth phase, a significant amount of pulp water is recovered into the froth phase. Along with this water, the fine clay particles dispersed in it will be entrained to the froth product, resulting in poor grade. Many investigators (Engelbrecht and Woodburn, 1975; Bishop and White, 1976; Lynch et al., 1981) have shown that the amount of entrained gangue material is proportional to the amount of water recovered in the froth phase. Also coal-pyrites have some natural hydrophobicity which makes it difficult to reject these pyrites by conventional flotation.

The above mentioned problems associated with conventional mechanical flotation can be overcome by using column flotation. Most of the current designs for column froth flotation cells have been described by Miller (1988) and by Finch and Dobby (1990). The main advantage of column flotation is that it provides a very quiescent zone for the attachment of fine coal to bubbles, which in turn, keeps ash entrainment in the froth to a minimum (Parekh et al., 1990).

The quiescent conditions are created by passing low pressure air through porous metal or rubber spargers. Further, wash water is added to the froth phase to create a net downward flow of water. Therefore, a column is an ideal device for producing superclean coals, in which case achieving product quality rather than Btu recovery is of more concern. However, columns do not necessarily give higher recoveries than conventional cells at a given gas rate and retention time. To increase the recovery, smaller bubbles must be used. Luttrell et al. (1988) have shown that by generation of "microbubbles" the selectivity of column flotation can be significantly improved. Several microbubble flotation columns have been developed in recent years. One of the most prominent has been the Microcel™ column developed at Virginia Tech (Yoon and Luttrell, 1989).

The other approach to improve the efficiency of conventional flotation has been in the area of reagents schedule. For example, Miller and Misra (1985) used carbon dioxide instead of air for flotation of coal and found that recovery of coal increased substantially with carbon dioxide when compared to air. Also, Miller and coworkers (1989) used a chemically-modified flotation process for cleaning fine coal. In this process, the coal is conditioned with potassium monopersulfate or other peroxy compounds for a short time before or during flotation. After such conditioning, the separation of coal from mineral matter is accomplished by conventional flotation technology. These results showed that improved ash and pyritic sulfur rejections could be obtained with the



chemically-modified flotation process.

In spite of all these studies and development, froth flotation has achieved limited success in the flotation of high sulfur coals.

### *2.1.2 Selective Agglomeration*

Higher rank coals are naturally hydrophobic and, therefore, more wettable by oily substances (i.e., oleophilic) than the hydrophilic mineral matter present in coal. Thus, if an oil is added to an aqueous suspension of pulverized coal, the coal particles will be collected into the oil phase, while the mineral matter will remain in the aqueous phase, allowing them to be separated from each other. When a sufficient amount of oil is added, the coal particles form agglomerates larger than 1 to 2 mm in diameter, which can be screened off from the dispersed mineral matter for separation. This process is generally referred to as selective agglomeration.

The major advantage of the selective agglomeration process is that it is capable of recovering coal particles as small as a few microns in diameter. The ability to separate micron size particles is an important advantage when coal must be pulverized to very fine sizes to liberate the mineral matter more completely. Another advantage with selective agglomeration is the ease with

which the product coal can be dewatered. However, selective oil agglomeration suffers from one major disadvantage, that is, the large amount of oil consumption. Typically, 10% or more of oil by weight of feed solids is required for cleaning coal containing large portions of minus 325 mesh (45  $\mu\text{m}$ ) material. Various researchers (Cheh et al., 1982; Bensley et al., 1977; Schubert, 1974) have worked on reducing the oil consumption by using emulsified oil. The main reason that a large amount of oil is used for selective agglomeration is to have the convenience of separating the agglomerates from the dispersed mineral matter by simple screening. However, Capes (1989) has reported that when the agglomerants are separated by flotation about 1% oil is sufficient for agglomeration.

Another approach of selectively agglomerating coal was reported by Chi et al. (1989). This process, known as the LICADO (LIquid CARbon DiOxide) process, utilizes liquid  $\text{CO}_2$  (6 Mpa) at room temperature to separate mineral matter from coal. The LICADO process relies on the preferential wettabilities of clean coal and mineral particles with liquid  $\text{CO}_2$  and water, respectively. When liquid  $\text{CO}_2$  is dispersed into a coal-water slurry, it tends to form agglomerates with the clean coal particles which float to the liquid  $\text{CO}_2$  phase. The mineral particles, on the other hand, remain in the water phase. Although this process is capable of producing ultra-clean coal, it entails a high capital cost because of the high pressure operation.

### *2.1.3 Selective Flocculation*

Several investigators have studied the use of polymeric flocculants for separating ash forming minerals from coal, and have reported that certain flocculants exhibit some degree of selectivity for coal against mineral matter. Various flocculants used for coal beneficiation include partially hydrolyzed polyacrylamide (Blaschke, 1975), nonionic polyacrylamide (Hucko, 1977), polystyrene sulfonate (Attia and Fuerstenau, 1982), and polyacrylamide containing chelating and complexing groups (Brookes et al., 1982). Although many of these results are encouraging, the selective flocculation processes using these common flocculants suffer from relatively low selectivity. Two reasons may be given. First, the settled coal flocs entrap mineral particles, resulting in poor product grade. For this reason, selective flocculation processes are usually run in multiple stages to remove the entrained ash-forming minerals. Second, these flocculants may adsorb not only onto coal, but also significantly onto minerals, as many of these reagents are used for destabilizing clay suspensions. However, the advantage of selective flocculation may be found in the low reagent dosage and the simplicity of the operation.

Numerous researchers have attempted to improve the selectivity of the separation process. Attia et al. (1987) used a totally hydrophobic flocculant that can adsorb specifically on coal. This reagent, FR-7A, is insoluble in water and,

therefore, requires proper emulsification before use. Using a minus 500 mesh Upper Freeport coal assaying 10.5% ash and 1.6% total sulfur, a three-stage selective flocculation process reduced the ash and sulfur contents to 3.5 and 1.1% total sulfur, respectively. The best selectivity was achieved at neutral pH. Although a good ash rejection was obtained, the sulfur reduction was very poor. Part of the reason may be attributed to the hydrophobic nature of pyrite present in coal. Adsorption kinetics showed that the hydrophobic flocculant adsorbed much faster onto coal than onto pyrite and shale. However, equilibrium adsorption density measurements of FR-7A on coal and pyrite indicated the adsorption of FR-7A on pyrite was also high. These results show the difficulty in separating pyrite from coal in a selective flocculation process using FR-7A as a flocculant. In a similar series of experiments, Palmes and Laskowski (1993) examined the effect of coal surface properties and flocculant type on coal flocculation. They found that FR-7A flocculated hydrophobic coal effectively in comparison to lesser hydrophobic coal, while semi-hydrophobic and hydrophilic flocculants flocculated all types of coal irrespective of their hydrophobicities.

To overcome this problem, Attia and coworkers (1988) have used a selective dispersant to modify the pyrite surface to render it hydrophilic in order to minimize adsorption of FR-7A. Polyxanthate was used as a dispersant (200 mg/L) and experiments were performed at pH 8. Using Pittsburgh No.8 coal, the sulfur content was reduced from 3.6% to 0.95% in a two stage selective

flocculation-dissolved air flotation cleaning process.

Attia (1985) and Palmes and Laskowski (1993) also used partially hydrophobic polymeric flocculants, which are more water-soluble than totally hydrophobic polymers. The semi-hydrophobic flocculant is a copolymer of acrylamide (85%), acrylic acid (5%) and methyl acrylate (10%). Using this flocculant, the ash content of coal was reduced to less than 3% with 68-93% Btu recovery. The adsorption of totally or partially hydrophobic polymeric flocculants on coal was reported to occur mainly through hydrophobic interactions (Attia, 1985).

## 2.2 Chemical Coal Cleaning

While physical coal cleaning is efficient in removing most of the ash-forming minerals and a significant part of the inorganic sulfur in coal, its efficiency in sulfur rejection is limited, particularly with regard to organic sulfur removal. Organic sulfur in coal can be mainly divided into 2 classes, aliphatic or aromatic compounds and heterocyclic compounds (Markuszewski et al., 1980). Since the heterocyclic compounds are more stable than the others, many of the chemical cleaning processes are capable of removing only the aliphatic or aromatic compounds of sulfur. Most of the chemical desulfurization techniques are based on the selective oxidation of these compounds over the hydrocarbons.

Of the several chemical cleaning processes proposed in recent years, the molten caustic leaching (MCL) process developed by TRW Inc. has received the most attention. A detailed description of this process has been given by Meyers (1989). From a coal containing 4% sulfur and 10 to 11% ash, the MCL process can typically produce ultra-clean coal with 0.4 to 0.7% sulfur and 0.1 to 0.65% ash. In general, the more severe the operating conditions, i.e., high operating temperature, long retention time, and high KOH/NaOH ratio, the lower the ash and sulfur content in the coal produced. Other chemical processes that have been tested include the microwave process developed by General Electric (Zavitsanos et al., 1982; Richardson et al., 1986) and the oxydesulfurization process (Agarwal et al., 1976; Friedman et al., 1977). Although chemical cleaning methods produce ultra-clean coal, the conditions used are very severe and toxic, which puts these processes at a serious disadvantage in comparison with physical cleaning methods.

### 2.3 Microbial Coal Cleaning

Parallel to the physical and chemical cleaning methods described above, alternative bio-techniques have been the subject of much investigation during the last decades. These include desulfurization, liquefaction, and gasification procedures, which have been summarized in different reviews (Kargi, 1986; Olson and Brinckman, 1986; Gouch, 1987; Bos and Kuenen, 1990). The most

widely studied technique to date has been microbiological desulfurization. Zurubina et al. (1959) and Silverman et al. (1963) carried out the experiments on coal by extracting pyrite in aqueous phase of low pH, using the bacteria *Thiobacillus ferrooxidans*. The principle of biodesulfurization lies in the capacity of certain microorganisms to oxidize the compounds of sulfur found in coal and convert them into products which are soluble in an aqueous medium.

In general, different types of bacteria are used to eliminate pyrite and organic sulfur since the principle of solubilization is different. Those which dissolve pyrite use sulfur as an energy source, while those which eliminate organic sulfur do so as a secondary metabolic function. Microorganisms, then, can be classified into three groups according to their capacity to eliminate different types of sulfur (Kargi, 1986) :

- a) Obligate autotrophs, which oxidize only pyritic sulfur;
- b) Facultative autotrophs, which oxidize pyritic sulfur and some compounds of organic sulfur; and
- c) Heterotrophs, which oxidize organic compounds only.

Most of the high-sulfur coals contain nearly 50 to 80% pyritic sulfur. Removal of pyrite should be able to reduce sulfur levels in coal to produce compliance quality coal. Therefore studies related to microbes which can oxidize

pyrite or depress pyrite by adhesion will be discussed here.

Microorganisms that oxidize iron and/or sulfur are acidophilic, the most important being the species of *Thiobacillus ferrooxidans* (*T. ferrooxidans*) (Eligwe, 1988; Ballester et al., 1988; Torma, 1977). These bacteria are mesophilic (optimum development temperature of 28 to 35°C) and capable of extracting large quantities of pyritic sulfur (more than 90% in some cases). It has been used in pure, mixed and natural cultures, in which there are other species in smaller proportions; i.e., *T. thiooxidans*, *Leptospirillum ferrooxidans* and *Thiobacillus acidophilus* (Dugan and Apel, 1978; Andrews and Maczuga, 1984).

There are two approaches in which *T. ferrooxidans* can be used to remove pyrite from coal. One approach is to leach pyrite and the second is to allow attachment of *T. ferrooxidans* to pyrite surface selectively to make the surface hydrophilic. The main disadvantage of bioleaching pyrite is that the kinetics are very slow (2 to 3 weeks for greater than 75% removal of sulfur). Murphy et al. (1985) have shown that the kinetics of bioleaching can be substantially increased by using a thermophilic bacteria, such as *Sulfolobus acidocaldarius*, which removes greater than 75% of sulfur in 3 to 6 days. But even this is too long when the overall economics of coal preparation is considered.



Faster kinetics can be realized in removing pyrite if lithotrophs can be used simply for modifying the surface properties of coal pyrite, so that it can be more efficiently separated from coal in a physical separation process. Capes et al. (1973) and Kempton et al. (1980) used *T. ferroxidans* to increase the hydrophilicity of coal-pyrite and, hence, improve its rejection during oil agglomeration. Other microorganisms such as *T. thiooxidans* and *S. acidocaldarius* could be used for modification of pyrite surface chemistry. It has been shown that biomodification requires only a few minutes (5-30 min) of conditioning time. Using *T. ferroxidans*, Isbister et al. (1985) improved ash rejection by 10 to 20% and sulfur rejection in excess of 20% during flotation with a 30 to 120 minutes contact time with coal prior to flotation. On the other hand, El Zeky and Attia (1987) used only 5 to 30 minutes of contact time when the microbes were inoculated into a culture medium containing finely pulverized coal-pyrite and fermented for up to six weeks for adaptation. Results obtained with Upper Freeport coal (using *T. ferroxidans* adapted for 4 weeks at pH 2) showed that both ash and sulfur rejection increased substantially with increasing contact time. Also, there was improvement in pyritic sulfur rejection with increasing adaptation time. These results represent pyritic sulfur contents as low as 0.13%, down from 1.59% in the feed. In another study, Attia et al. (1993) reported that bacterial depression action on pyrite seems to be unaffected by the oxidation state of the pyrite surface.

However, the mechanism of adhesion of *T. ferroxidans* is not clear at this time. Whether it was the direct adsorption of the hydrophilic bacterial cells on pyrite, the adsorption of extracellular compounds, biooxidation of surface layer, or a combination of these mechanisms is yet to be determined. The adsorption of the biomass (bacterial cells and extracellular compounds) is the most likely mechanism for the depression of pyrite floatability. It also produces phospholipids which cling to pyrite and other mineral particles, rendering them more hydrophilic (Dixon, 1985). But recently, Ohmura and Saiki (1993) have shown that increasing the cell density of *T. ferroxidans* increases the rejection of pyrite in column flotation but decreases the coal recovery. At low cell density, the bacteria selectively attaches to pyrite to render the surface hydrophilic. At higher cell concentrations, *T. ferroxidans* also attaches to coal particles by physical adhesion thus decreasing the floatability of coal.

Although a lot of work has been done regarding the use of *T. ferroxidans* as possible depressants for pyrite in coal flotation, it is still in the developmental stage. No research relating to the biomodification of coal to enhance the recovery of fine coal has been carried out so far.

## 2.4 Biofloculation

### 2.4.1 *Mycobacterium phlei*

*Mycobacterium phlei* (*M. phlei*) is a procaryotic microorganism commonly found in soils and on the leaves of plants, particularly grasses (Buchanan and Gibbons, 1974). It is pleomorphic and its shape depends on the culturing conditions. The cellular structure of a typical procaryotic microorganism is shown in Figure 2.1 (Chapelle, 1992). The chromosome of the bacteria is arranged into a closed circle and consists of a single molecule of DNA. Ribosomes are protein assembly structures and provide a surface upon which amino acids can be brought together and covalently bonded in the proper sequence. The cytoplasmic membrane or the cell membrane acts as a boundary between the interior of the cell and the outside environment. A schematic of the cell membrane is shown in Figure 2.2. It consists of approximately 60% protein and 40% phospholipids. The phospholipids are arranged in a bilayer, in which the hydrophobic portion points outward. The purpose of the cell membrane is to regulate the transport of chemicals into and out of the cell.

The cell membrane is enclosed within the cell wall which gives the cell rigidity. A substance called peptidoglycan, which is unique to procaryotic organisms, provides much of the cell wall's structural strength. Peptidoglycan

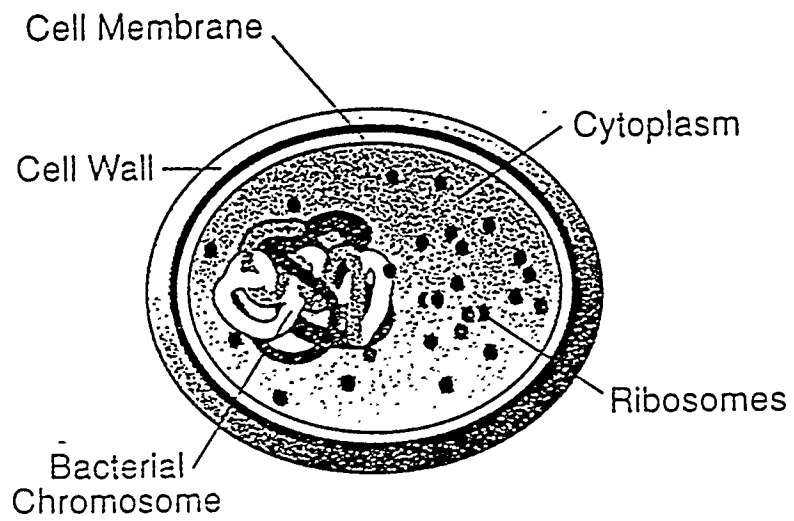


Figure 2.1 Cellular structure of prokaryotic microorganism (from Chapelle, 1992)

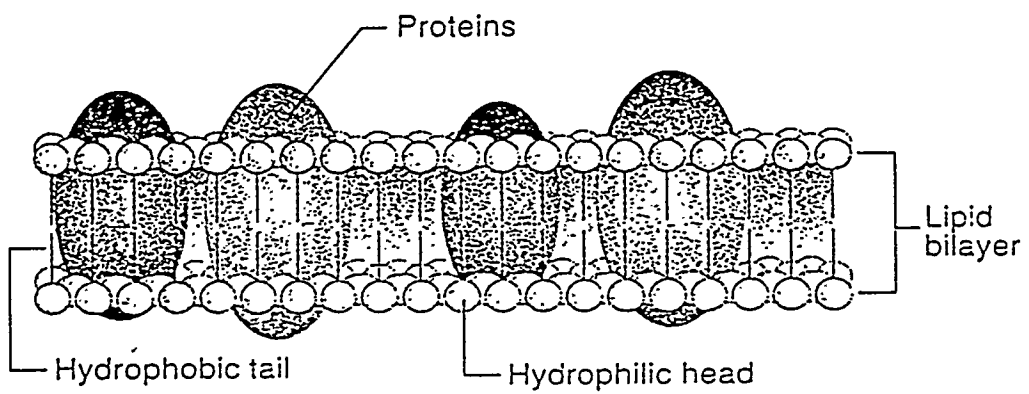


Figure 2.2 Schematic diagram of cell membrane showing the arrangement of proteins and phospholipids (from Chapelle, 1992)

is a three-dimensional polymer of sugars and amino acids that are cross-linked with short peptide bridges. There are two major types of cell walls, the gram-positive and the gram-negative cell wall. The gram-positive cell wall consists of an inner membrane with a relatively thick layer of peptidoglycan covering it. There are varying amounts of teichoic acids, polymers of sugar, alcohols and phosphates present in the cell walls. The gram-negative cell wall has a layer of phospholipids and lipoproteins outside a thinner peptidoglycan layer. Also, there is a space between the cell membrane and the peptidoglycan layer known as periplasmic space.

Various factors such as temperature and culture medium can affect the surface cell composition of *M. phlei*. For example, Reddy et al. (1991) have shown that *M. phlei* grown on glucose not only had a higher amount of phospholipids but improved the yield also. Suutari and Laakso (1993) studied the effect of growth temperature on the fatty acid composition of *M. phlei* and found that the percentage of fatty acids varied with growth temperature. As the temperature was increased from 10 to 35°C, the amount of oleic acid and 10-hexadecanoic acid in the cell wall decreased while the amount of palmitic acid increased. Further, it was shown that the degree of fatty acid unsaturation and branching varied with temperature. With increasing temperature up to 35°C, the degree of unsaturation decreased, which is mainly due to the decrease in 10-hexadecanoic acid and oleic acid. However, the degree of branching increased

with temperature.

van Loosdrecht (1988) studied the hydrophobicity and surface charge of various organisms (shown in Table 2.1). It was reported that *M. phlei* was highly hydrophobic with a contact angle of 70° and had a negative surface charge. These properties may be attributed primarily to the fatty acid surface of *M. phlei* and suggest that these are similar to those of conventional surfactants used in mineral processing. Based on this, the potential of using *M. phlei* as a flotation collector and flocculating agent for various minerals has been studied at the University of Nevada, Reno and some results will be discussed in the following section.

#### *2.4.2 Mycobacterium phlei in Mineral Processing*

Over the past few years, extensive work has been done with regards to the potential application of the hydrophobic bacteria, *M. phlei*, as a flotation and flocculating agent in mineral processing. Chen (1992) has studied the use of *M. phlei* as a flotation collector for hematite and found that maximum flotation recovery could be obtained at pH values of <3.0 at *M. phlei* concentrations of about 15-20 ppm. At higher concentrations of *M. phlei*, hematite formed large flocs. Flocculation experiments showed that at concentrations greater than 120

Table 2.1 Contact angles and Electrophoretic mobilities (EM) of various microorganisms (from van Loosdrecht et al., 1988)

Microorganism	EM (mm/sec/V/cm)	Contact Angle (deg)
<i>Pseudomonas fluorescens</i>	-2.36	21.1 ± 1.5
<i>Pseudomonas putida</i>	-1.60	38.5 ± 1.0
<i>Pseudomonas</i> sp. strain 52	-2.67	19.0 ± 1.0
<i>Escherichia coli</i> NCTC 9002	-0.42	15.7 ± 1.2
<i>Arthrobacter simplex</i>	-1.08	37.0 ± 0.9
<i>Micrococcus luteus</i>	-1.62	44.7 ± 0.9
<i>Thiobacillus versutus</i>	-2.97	26.8 ± 0.8
<i>Agrobacterium radiobacter</i>	-1.48	44.1 ± 0.5
<i>Mycobacterium phlei</i>	-3.09	70.0 ± 5.0



ppm, about 97% flocculation efficiency was obtained. Also, as the pH was increased, the flocculation efficiency was reduced. Maximum efficiency was observed in the pH range of 2-3. This phenomena was attributed to the columbic attraction arising from opposite charges of *M. phlei* and hematite in the pH range of 2-3. Interaction energy calculations obtained using the extended DLVO theory showed that a minimum in interaction energy occurs in the pH range of 2-3, which facilitates the adsorption and hence flocculation of hematite.

Also, *M. phlei* was used as a flocculant for flocculation and dewatering of Florida phosphate waste and kerogen samples. In the absence of bacteria, about 50% of the solids are settled in 45 minutes. However, in the presence of *M. phlei*, nearly 85% of the solids are settled in just 5-6 minutes, indicating that flocculation takes place very rapidly. It was also shown that the flocs formed with *M. phlei* had a lower amount of moisture, which in turn resulted in better dewatering. Therefore, *M. phlei* not only functions as a flocculant, but also as an effective dewatering agent.

## CHAPTER 3

### EXPERIMENTAL MATERIALS AND METHODS

#### 3.1 Materials

Coal and pyrite samples from different sources have been used in this investigation. A list of the samples used are listed in Table 3.1. The coal samples were obtained from different organizations i.e., Illinois No. 6 coal from Illinois State Geological Survey, Champaign, IL and Kentucky No. 9 coal sample from the Center for Applied Energy Research, Lexington, KY. Coal-pyrite (Illinois coal seam), mineral pyrite (Zacatecas, Mexico) and milky quartz samples were obtained from Wards Natural Science Establishment Inc., Rochester, New York. Large pieces were hand picked for contact angle measurements. Coal, pyrite and quartz samples were crushed, ground and sieved under air to obtain different size fractions. The samples were stored in a refrigerator to minimize oxidation.

The microorganism, *Mycobacterium phlei*, was obtained as a freeze-dried culture from Carolina Biological Supply Company, Burlington, North Carolina.

Table 3.1 List of different samples used in this study

Sample	Sample ID	Source
Illinois No.6 Coal Kentucky No.9 Coal	IL Coal KY Coal	Herrin Seam, St. Clair Co., IL Springfield Seam, Muhlenberg Co., KY
Illinois Coal-Pyrite Mineral Pyrite Quartz	ICPY MPY --	Illinois Coal Seam, IL Zacatecas, Mexico Wards Natural Sc. Estb., NY

Table 3.2 List of chemicals used in this study

Chemical Name	Source
Sodium Hydroxide	Fisher Scientific
Nitric Acid	Fisher Scientific
Kerosene	Fisher Scientific
Methyl Isobutyl Carbinol (MIBC)	Sigma Chemical Company
Sodium Nitrate	Fisher Scientific
D-(+)-Glucose	Sigma Chemical Company
Beef Extract	Sigma Chemical Company
Yeast Extract	Sigma Chemical Company
Enzymatic Hydrolysate Casein	Sigma Chemical Company
Polyethylene Oxide	Aldrich Chemical Company
Polyacrylamide	American Cyanamid Company

The microorganism was in the form of a freeze-dried culture containing lyophilized pure strains of viable bacteria and was stored in a refrigerator at 4°C. This freeze-dried culture was incubated and transferred to the culture medium, the details of which will be discussed in the next section.

A list of all the chemicals used in this study are given in Table 3.2. All chemicals used were of analytical grade. Double distilled and deionized water was used throughout this investigation. Unless otherwise stated, all pH adjustments were made with sodium hydroxide and nitric acid.

## 3.2 Techniques and Procedures

Several techniques were used in this investigation for characterization of samples, adhesion of *M. phlei* onto different samples and the effect of *M. phlei* on the surface properties, flocculation behavior of coal and separation of coal flocs. These techniques and procedures are discussed in detail in the following sections.

### 3.2.1 Culture of *M. phlei*

The *M. phlei* culture used in this study was obtained in the form of freeze-dried culture. The freeze-dried culture was first transferred to a rehydration

medium (supplied by Carolina Biological Supply Company) and incubated at 35°C for 48 hours before transferring to a culture medium. A rapid culture medium, suggested by Pratt (1952), was used in the culture of the microorganisms. The culture medium consisted of (per liter of distilled water) 10 g D-(+)-glucose, 2 g enzymatic hydrolysate casein, 1 g beef extract and 1 g yeast extract. The culture medium was sterilized at 124°C for 25 minutes in a Spectroline Model 750 autoclave (Spectronics Corporation, NY). The sterilized culture medium was cooled and the incubated bacteria were inoculated into the medium. Culturing was carried out in 250 ml flasks continuously shaken in a G24 Environmental Incubator Shaker (New Brunswick Scientific Co., NJ) at 35°C. The microorganisms were harvested after 48 hours by filtering through a 0.45µm Millipore filter paper and dried at room temperature for about 30 minutes. The weight of *M. phlei* was noted and was resuspended in distilled water to form suspensions of known concentrations to be used in the experiments. A sample of the suspension was sent to Analytical Services Inc. (Essex Jct., VT) for identification of the microorganism.

The growth of the microorganism was monitored by determining the dry weight of the cells at different time intervals.

### *3.2.2 Sonication of M. phlei cells*

Sonication of the microorganism was performed using a Branson 184V (Branson Sonic Power Co., Dalisbury, CT) ultrasonic probe at 20,000 Hz. Sonication was performed on 100 ml suspension of *M. phlei* of known cell weight. After sonication for a predetermined time, the extracellular surfactant and the sonicated cells were separated by centrifugation. The weight of the cellular debris was determined after drying in the oven for about 30 minutes. The amount of extracellular surfactant released was determined by computing the difference in the weight of the cells before and after sonication. The suspensions of various concentrations of cellular debris and extracellular surfactant were prepared and used in experiments. A sample of the released extracellular surfactant was analyzed in a commercial laboratory (Analytical Services Inc., Essex Jct., VT) for the composition of fatty acids.

### *3.2.3 Zeta Potential Measurements*

The surface charge measurements were carried out with a Lazer Zee Meter - Model 501 (Pen Kem Inc., NY). About 1 g (minus 400 mesh) sample was conditioned in 50 ml 0.01 M sodium nitrate solution for about 5 minutes after pH adjustments were done. The suspension was allowed to stand for 2 minutes and the supernatant was used for measurements. The readings reported in this

study are the average of at least 10 readings. The pH adjustments were made with nitric acid or sodium hydroxide and pH measurements were done using a Accumet Model 5 pH meter.

In the case of *M. phlei* (before and after sonication), the cells were harvested, washed twice and resuspended in distilled water. A few drops of the suspension were then used for surface charge measurements.

#### *3.2.4 Contact Angle Measurements*

The hydrophobic/hydrophilic balance at the surfaces of different samples was measured by using a Ramé-Hart contact angle goniometer Model A-100. The equipment consists of a goniometer with two rotatable cross hairs for measuring the contact angle, a specimen stage and a variable intensity illuminator, all mounted on an optical bench.

Sample Preparation : Coal and pyrite samples of approximately 1 x 1 x 0.5 cm size were selected and then molded in epoxy resin. Freshly polished surfaces were prepared by polishing the surface first with 1000 and 4000 grit SiC paper and then with 0.05  $\mu\text{m}$  alumina suspension. The samples were thoroughly washed with distilled water to remove any adhering alumina and then used for measuring the contact angle. Latex gloves were used throughout

the experiments in order to avoid contamination of the surfaces.

Technique of Measuring Contact Angle : Contact angles of different samples were measured by using the captive bubble technique which involves immersing the freshly polished sample into an optical quartz cell containing water. Then an air bubble is attached to the surface with a calibrated syringe. The angle ( $\theta$ ) formed between the air bubble and the solid surface is measured through the liquid medium and is known as the contact angle. The greater the contact angle, the greater the hydrophobicity of the surface. The contact angles on both sides of the air bubble were measured. An average of at least 4 measurements is reported here. The standard deviation in measuring a single contact angle was about  $\pm 2^\circ$ . All measurements were carried out at  $25 \pm 2^\circ\text{C}$ .

Method of Coating Samples with *M. phlei* : As described earlier, *M. phlei* cells were harvested by filtration and were resuspended in distilled water. Suspensions of different concentrations and pH values were prepared. A few drops of the suspension were placed on the surface of freshly prepared samples and dried at  $45^\circ\text{C}$ . The samples were then rinsed slowly for a few minutes in distilled water to remove any weakly adhering cells from the surface. The samples were again dried and then transferred to the quartz cell containing distilled water. The ionic strength of the water was maintained constant at 0.01 M sodium nitrate. The pH of the water was adjusted to that at which the



*M. phlei* suspension was conditioned.

For estimating the hydrophobicity of *M. phlei* (both whole and sonicated cells), a suspension of the bacteria was first filtered with a 0.45 $\mu$ m Millipore filter paper and dried. Then the contact angle was measured by using the sessile drop technique. These experiments were cursory in nature. No attempt was made to control the ionic strength and measurements were made only at the natural pH of distilled water (pH $\approx$ 6). The contact angle of at least 10 droplets were measured and the averaged readings are reported.

### 3.2.5 Adhesion Experiments

Adhesion of *M. phlei* on different samples was studied with a Spectronic 20 UV Spectrophotometer (Bausch and Lomb, NY). Since the settling velocity of bacteria in water under the influence of gravity is of the order of  $10^{-7}$  to  $10^{-6}$  cm/sec (Kim et al., 1987), the bacterial suspension may be regarded as a colloid. It is well known that the concentration of a colloid is related linearly to the transmittance of light. Based on this, the transmittance as a function of *M. phlei* concentration was measured and a linear plot was constructed. If a transmittance of a particular suspension is known, the concentration of *M. phlei* in that suspension can be determined from the plot. The difference between the

initial and the final concentration gives the amount adhering on the surface of samples. The amount adhering in mg of *M. phlei* per gm of sample ( $\Gamma$ ) is calculated by using the following equation :

$$\Gamma = \frac{(C_1 - C_2) W}{V} \quad (3.1)$$

where  $C_1$  and  $C_2$  represent the initial and final concentrations of *M. phlei* in solution, respectively;  $V$  is the volume of *M. phlei* suspension and  $W$  is the weight of the sample expressed in grams.

Coal (70 x 100 mesh), pyrite and quartz (100 x 200 mesh) samples were prepared by grinding. Coarse size samples were used to avoid the influence of suspended particles on the measurement of transmittance. About 80 ml of *M. phlei* suspension was first taken and the pH was adjusted. To this suspension, about 1 gm of sample was added and conditioned for a predetermined time. After conditioning, the particles were allowed to settle for 2 minutes. The supernatant was used for measuring the transmittance. The concentration of *M. phlei* was determined from the standard plot, and the amount of *M. phlei* adhering on the samples was calculated. This technique was used to study the effect of pH and conditioning time on the amount of *M. phlei* adhering to coal, pyrite and quartz.

### *3.2.6 Scanning Electron Microscopy Studies*

Scanning electron microscopy (SEM) analysis was performed using a JEOL JSM-810A electron microscope. Qualitative analysis of coal and pyrite, the structure and shape of *M. phlei* before and after sonication, and the nature of adhesion of *M. phlei* onto coal and pyrite were performed by SEM.

For qualitative analysis of coal and pyrite, the samples prepared for adhesion tests were used and Energy Dispersive X-ray Analysis (EDX) was carried out. In the case of *M. phlei*, a small amount of the dried sample was used. For studying the nature of *M. phlei* adhesion, the same samples used in adhesion measurements were used here. About 1 gm of sample was conditioned in a *M. phlei* suspension of certain concentration at a particular pH for 10 minutes. The sample was then filtered and dried. All samples were mounted on aluminum substrates (coated with graphite) which were then coated with gold and used for SEM studies.

### *3.2.7 Sedimentation and Flocculation Experiments*

Sedimentation and flocculation experiments were performed in a 11.5" tall graduated cylinder (Figure 3.1). A 500 ml slurry consisting of 10 g coal of

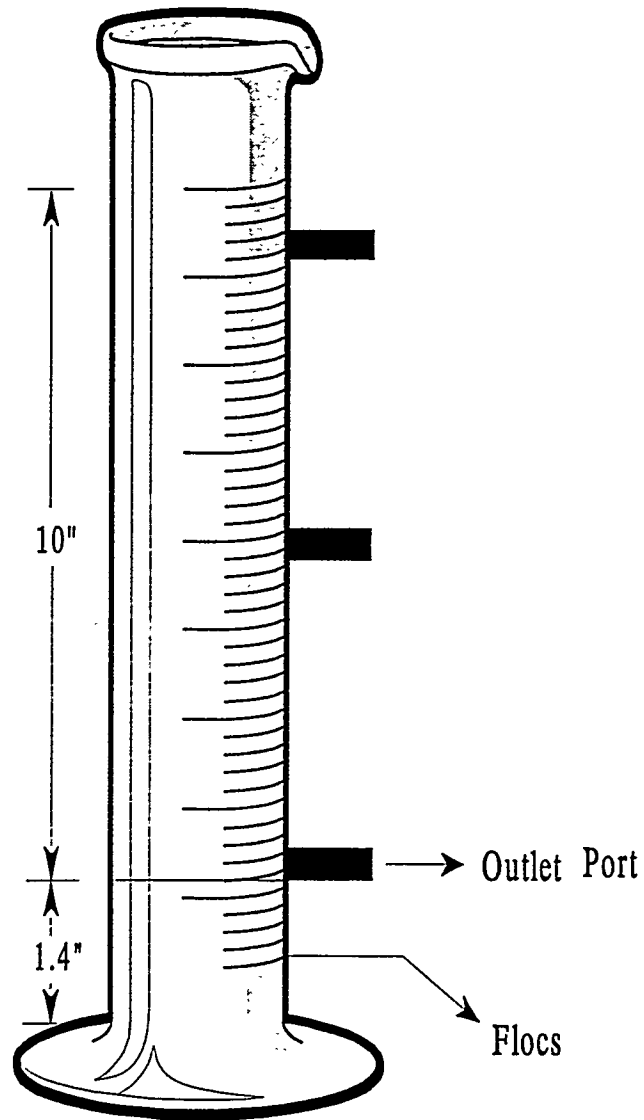


Figure 3.1 Schematic of the graduated cylinder used in sedimentation and flocculation experiments

minus 325 mesh size was conditioned and pH adjusted. After the pH was stabilized, flocculant was slowly added with a pipette. The suspension was stirred by using a Phipps and Bird (Richmond, VA) paddle stirrer at 250 rpm for 1 minute. Further conditioning was done for 2 minutes at 50 rpm to allow for initial floc growth to take place. Then the suspension was transferred to the graduated cylinder. Samples were taken from the bottom outlet after predetermined time intervals. The suspensions were filtered, dried and weighed.

For sedimentation tests, the amount of material settling through the top 10" of the cylinder was used as the criteria for determining the settling rates. For flocculation tests, the flocculation efficiency ( $E_f$ ) was calculated and is defined as:

$$E_f = \frac{(W_{so} - W_{sf})}{W_{so}} \quad (3.2)$$

where  $W_{so}$  represents the weight of the solids in a given volume of the suspension before the addition of flocculant and  $W_{sf}$  represents the same after addition of flocculant. When  $W_{sf} = W_{so}$ , no flocculation occurs and  $E_f = 0$ . When  $W_{sf} = 0$ ,  $E_f = 1$ , maximum flocculation occurs.  $E_f$  can also be negative, in which case dispersion takes place instead of flocculation.

### *3.2.8 Floc Separation*

One of the problems noticed during conventional settling tests of the flocculated material was that the massive coal-flocs settled at a same terminal velocity as that of liberated pyrite and ash due to higher density of materials as compared to coal-flocs. As a result, two alternative separation approaches were undertaken. The first approach was to separate the materials (flocculated and unflocculated) by using different mesh size screens. However, limited success was achieved by this process due to entrapment of fines within the flocs and/or due to the breakdown of loosely bound flocs. The second approach was the flotation of flocs with a laboratory scale column flotation cell. The details of the experimental setup are described below.

The laboratory scale column flotation setup consisted of a small column with a working volume of 320 ml, a nitrogen gas source and a Gilmont No.13 flow meter. Nitrogen gas was passed from the bottom of the column at the required flow rate. After flocculation, the entire slurry was transferred to the flotation column. No pH adjustments were made for flotation. The required amount of methyl isobutyl carbinol (MIBC) as frother was added and flotation was carried out for 5 minutes at the required flow rate. The float and tailings were filtered, dried, weighed and analyzed.

Baseline experiments were performed using kerosene as collector and MIBC as frother. In this case, pH adjustments were carried out before addition of frother and promoter. After 4 minutes of conditioning, the slurry was transferred to the column and flotation was carried out for 5 minutes. These experiments were performed for comparison with the floc-flotation results.

### *3.2.9 Analysis of Coal*

Coal was analyzed for sulfur and ash before and after each flocculation and flotation experiment. For ash analysis, about 1 gm of coal was taken in a porcelain crucible and placed in a muffle furnace for about 2-3 hours at 700-750°C. After all the combustible material has been removed, the crucible is taken out of the furnace and allowed to cool. The weight of the residue i.e., ash, is noted and calculated as a percentage of total coal. Percent ash rejected is calculated based on the difference in ash content of the feed and the float.

Analysis of coal for sulfur content was done by using the PE 2400 Series II CHNS Analyzer (Perkin Elmer Corp., Norwalk, CT). About 1.5 mg of homogenized sample was used for analysis. This analysis gave the total amount of sulfur present in coal (i.e. sulfatic, organic and pyritic). Since most of the sulfatic and organic sulfur reports to the concentrate, it can safely be assumed that the total sulfur in the reject or tailings is from the pyrite. In the case of

concentrate, the amount of pyritic sulfur was estimated by subtracting the organic and sulfatic sulfur from total sulfur. Based on the pyritic sulfur values of the feed coal and float, percent pyritic sulfur rejection was estimated.

The amount of combustibles was calculated by using the amount of concentrate and tail (in percent) and the amount of ash in concentrate and tail (in percent). The procedure for calculating combustible recovery is shown below.

Table 3.3 Procedure for calculating combustible recovery

	Wt%	% Ash	% Combustibles	Combustible Units	Combustible recovery (%)
Conc.	x	a	100-a	$x(100-a) = p$	$p/p+q$
Tailing	y	b	100-b	$y(100-b) = q$	$q/p+q$

### 3.3 Bulk Physical and Chemical Properties of Samples

As mentioned earlier, two coal samples were used in this investigation and the proximate and ultimate analysis of these coal samples are shown in Tables 3.4 and 3.5. As can be seen, both the coal samples have high sulfur content (> 4%). However, the ash content of KY No.9 coal is higher than IL No.6 coal. Also, the carbon content of IL No.6 coal is higher than KY No.9, which explains the higher heating value of IL No.6 coal.



Energy Dispersive X-ray (EDX) analysis was conducted and typical results for coal and coal-pyrite are shown in Figures 3.2 and 3.3 respectively. Both the coal samples showed the presence of Si and Al which are mainly responsible for formation of ash. While the spectra of coal-pyrite (Figure 3.3) showed the presence of some impurities such as Si and Al, mineral pyrite and quartz were found to be relatively pure. Chemical analysis of coal-pyrite revealed the presence of about 0.86% of carbon, which is probably the main difference between coal-pyrite and mineral pyrite.

Table 3.4 Proximate and Ultimate Analysis of Illinois No. 6 Coal

<u>Proximate Analysis</u>	<u>As-Received</u>
% Moisture	9.47
% Ash	16.70
% Volatiles	31.13
% Fixed Carbon	<u>42.70</u>
	100.00
<u>Ultimate Analysis</u>	
% Carbon	63.50
% Hydrogen	4.50
% Nitrogen	1.20
% Total Sulfur	4.34
% Ash	16.70
% Oxygen	<u>9.76</u>
	100.00
<u>Sulfur Forms</u>	
Sulfatic	0.34
Pyritic	2.34
Organic	1.66
<u>Heating Value</u>	
Btu/lb	11533
<u>Major Elements in Ash (%)</u>	
SiO <sub>2</sub>	8.2
Al <sub>2</sub> O <sub>3</sub>	2.9
Fe <sub>2</sub> O <sub>3</sub>	3.4
MgO	0.2
CaO	1.2
Na <sub>2</sub> O	0.2
K <sub>2</sub> O	0.3
P <sub>2</sub> O <sub>5</sub>	trace
TiO <sub>2</sub>	0.2

Table 3.5 Proximate and Ultimate Analysis of Kentucky No. 9 Coal

<u>Proximate Analysis</u>	<u>As-Received</u>
% Moisture	8.27
% Ash	28.20
% Volatiles	40.06
% Fixed Carbon	<u>23.47</u>
	100.00
<u>Ultimate Analysis</u>	
% Carbon	55.30
% Hydrogen	4.68
% Nitrogen	1.24
% Total Sulfur	4.06
% Ash	23.47
% Oxygen	<u>11.25</u>
	100.00
<u>Sulfur Forms</u>	
Sulfatic	0.14
Pyritic	2.10
Organic	1.82
<u>Heating Value</u>	
Btu/lb	9890
<u>Major Elements in Ash (%)</u>	
SiO <sub>2</sub>	5.78
Al <sub>2</sub> O <sub>3</sub>	2.32
Fe <sub>2</sub> O <sub>3</sub>	3.33
MgO	0.17
CaO	0.86
Na <sub>2</sub> O	0.07
K <sub>2</sub> O	0.64
P <sub>2</sub> O <sub>5</sub>	0.04
TiO <sub>2</sub>	0.13

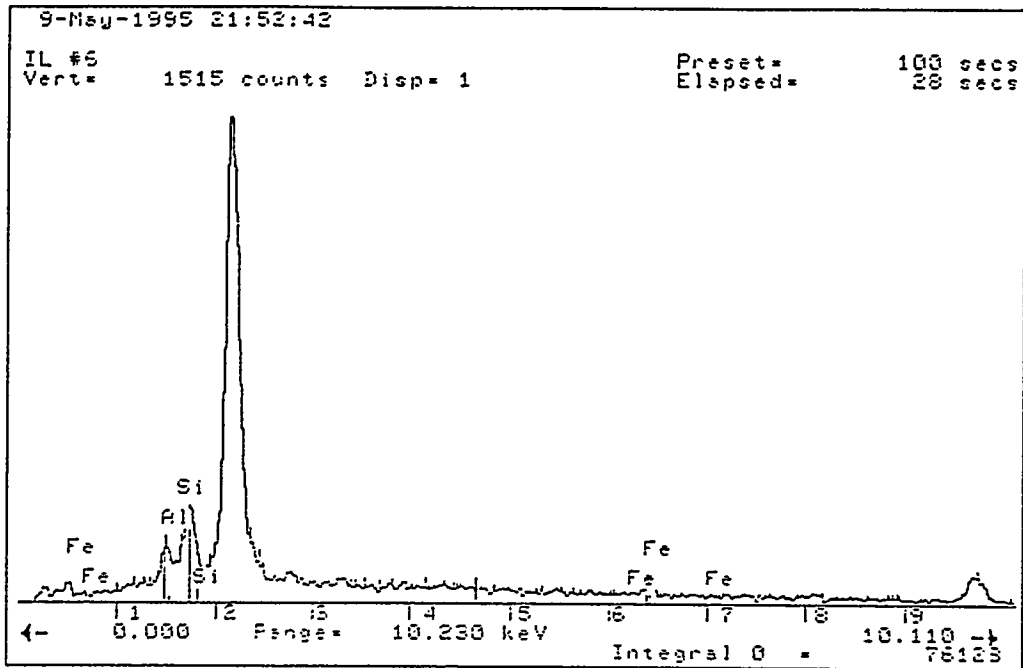


Figure 3.2 SEM-EDX analysis of Illinois No.6 coal

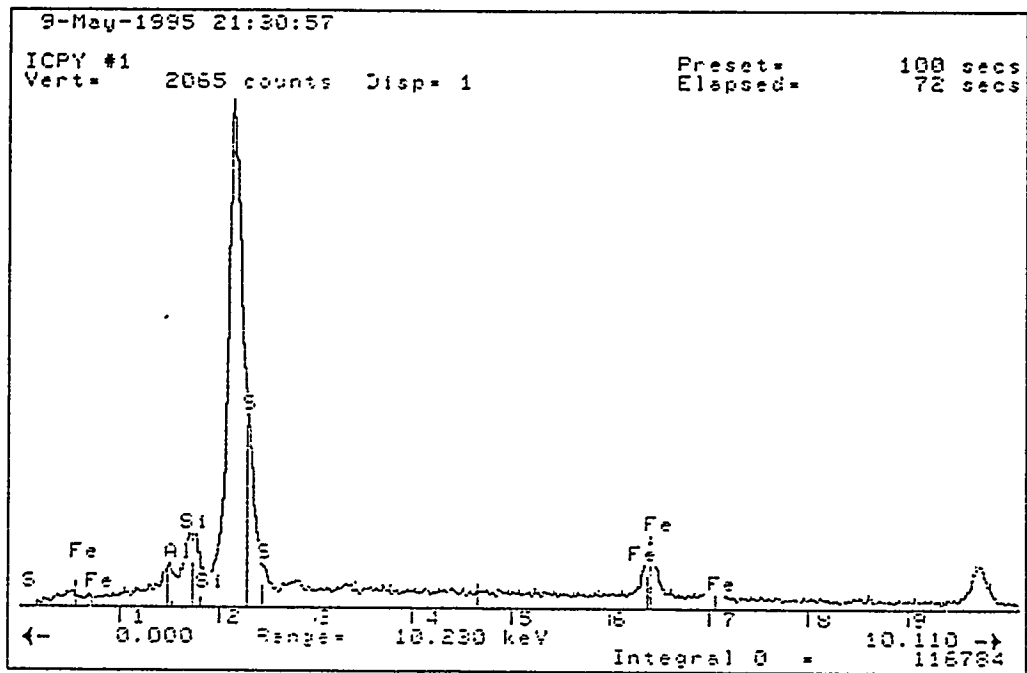


Figure 3.3 SEM-EDX analysis of coal-pyrite

## CHAPTER 4

### RESULTS AND DISCUSSION

#### 4.1 Characterization of *Mycobacterium phlei*

As described in Chapter 2, *M. phlei* is a hydrophobic and negatively charged microorganism. However, the composition of the cell wall, the surface properties and the growth characteristics can change depending on the culture medium and conditions. Therefore, the bacterium cultured in our laboratory was characterized in terms of surface hydrophobicity, surface charge, cell wall composition, size and shape. Also, the effect of sonication of the microorganism on the surface properties were evaluated.

##### 4.1.1 Growth Kinetics

The growth characteristics of *M. phlei* were studied by determining the dry cell mass as a function of culture time and the results are presented in Figure 4.1. Like most other bacteria, the growth of *M. phlei* goes through a

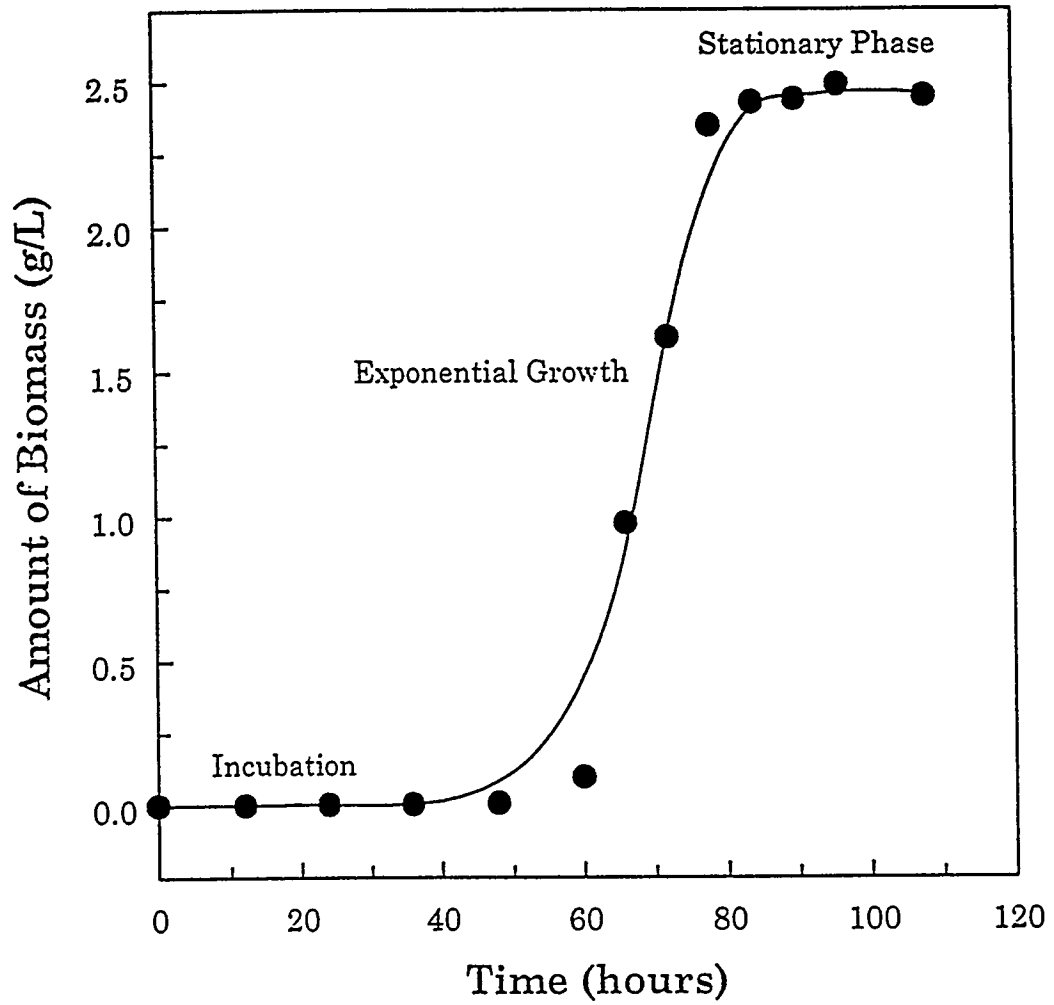


Figure 4.1 Growth curve for *Mycobacterium phlei* as a function of time

series of phases. During the first 48 hours, the freeze-dried bacteria was incubated in the rehydration medium which allowed it to adapt to the environment. After 48 hours, the incubated bacteria was transferred to the culture medium. As can be seen from Figure 4.1, it takes about 12 hours in the culture medium before the bacteria starts growing. This growth takes place very rapidly and is represented by the exponential growth phase. The growth quickly reaches a stationary phase during which the death rate balances the rate at which new bacteria are produced. The time point when exponential growth ends and the stationary phase begins is when the bacteria were harvested from the culture medium for experiments. At this stage, the amount of biomass produced was at a maximum (2.5 g/L) and the amount of viable bacteria was maximal. A rough bacterial cell count after 80 hours (with a Petroff-Hausser Counter) showed that the number of cells was in the range of  $9.9 \times 10^{10}$  cells/ml. These results indicate that the bacterium, *M. phlei*, grows very rapidly and the number of cells produced is very high.

#### 4.1.2 Morphology of *M. phlei*

The morphology of the microorganism was studied by using a Scanning Electron Microscope. The microphotograph of *M. phlei* cells harvested after the exponential growth phase is shown in Figure 4.2. As can be seen, the bacterium



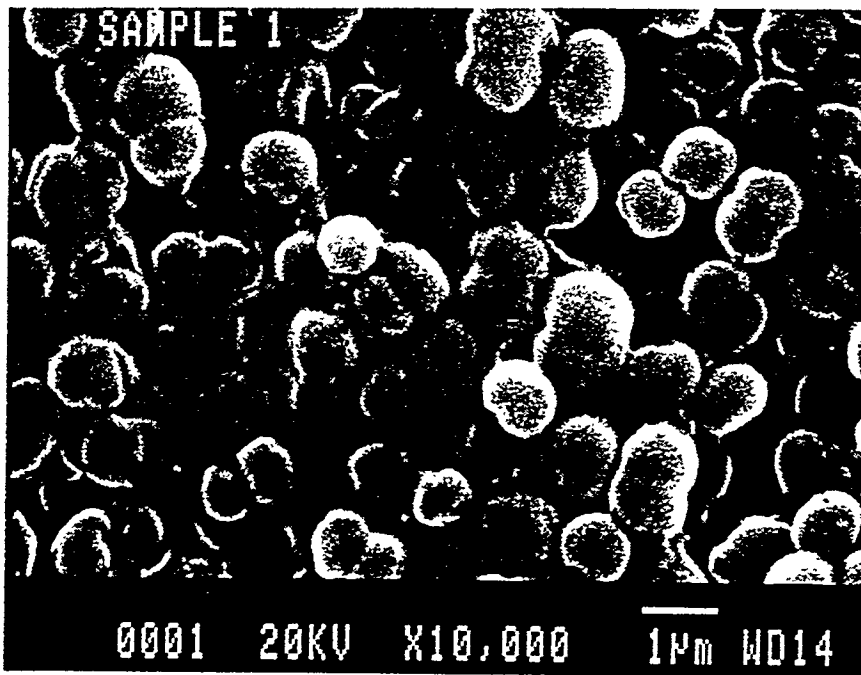


Figure 4.2 Scanning electron microphotograph of *M. phlei* whole cells

is spherical or coccal in shape with a diameter of about 1  $\mu\text{m}$ . Also, it is evident from the microphotograph that the extracellular surfactants that are produced during the growth of the bacteria or that are secreted by the bacteria hold the bacteria together. This was also observed under the microscope during bacterial counting. However, after sonication of the cells by sonication, the cells were less attached to one another and this is shown in Figure 4.3. This is due to the release of the extracellular surfactants during sonication. Also, sonication did not seem to affect the shape of the cells, as the cells were still spherical and about the same size as before sonication. It should be noted that cells before sonication will be referred to as whole cells and cells after sonication will be referred to as sonicated cells throughout this discussion.

#### 4.1.3 Cell Wall Composition of *M. phlei*

The surface functional groups present in the cell wall of whole cells were determined by FTIR analysis. Cell wall composition was studied by determining the weight of the extracellular surfactant released during sonication and by fatty acid analysis of the extracellular surfactant. Figure 4.4 shows the FTIR spectra of whole cells. It can be seen that the surface of *M. phlei* cells consists of carboxylic, hydroxyl and phosphate groups. The presence of these groups renders the surface of *M. phlei* negatively charged. The amount of extracellular

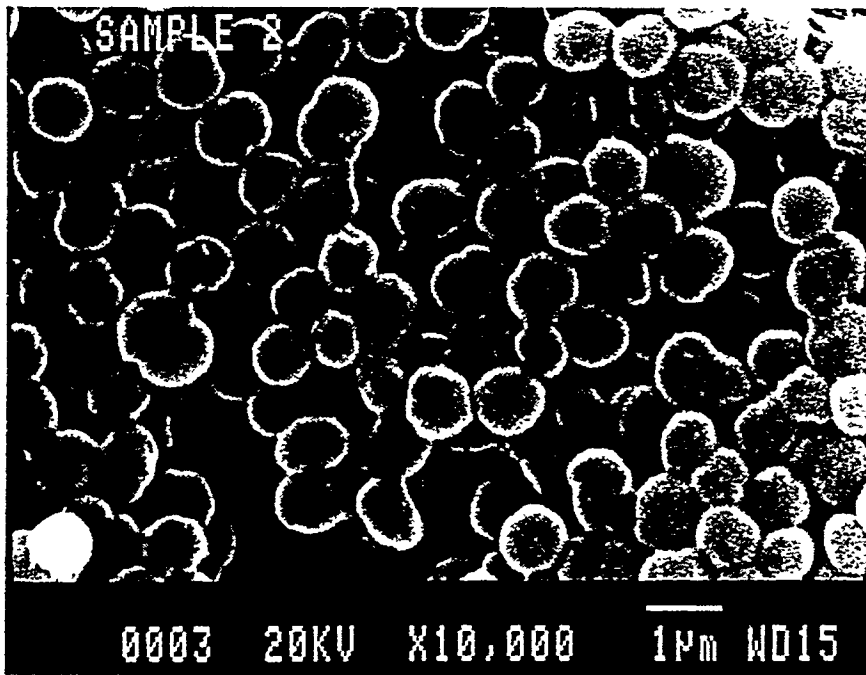


Figure 4.3 Scanning electron microphotograph of *M. phlei* ruptured cells

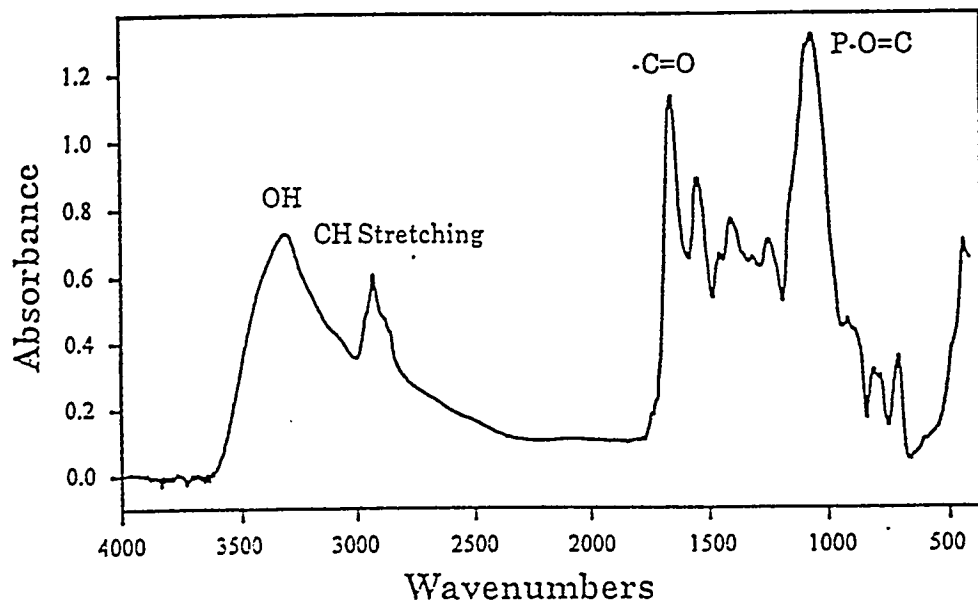


Figure 4.4 FTIR spectra of *M. phlei* whole cells

surfactant released during sonication was studied as a function of sonication time and the results are shown in Figure 4.5. As the sonication time increased, the amount of extracellular surfactant released also increased and reached a plateau after about 18 minutes. Increasing the sonication time after this did not affect the amount of extracellular surfactant released indicating that all of it had been released. The amount of extracellular surfactant released in 18 minutes corresponds to approximately 40% of the total cell mass. This value is consistent with those reported in literature (Minniken, 1982). Based on this result a sonication time was fixed at 20 minutes for future experiments.

The extracellular surfactant consists mainly of lipids, glycolipids, proteins and fatty acids that are present in the cell wall of *M. phlei*. The extracellular surfactant released was analyzed for its fatty acid composition by fatty acid analysis and the results are shown in Table 4.1. The released fraction consisted of straight chain fatty acids with carbon chain lengths varying from 14 to 20. It was observed that the fatty acids of carbon chain length  $C_{18}$  and  $C_{20}$  were more predominant than that of  $C_{14}$  and  $C_{16}$ .

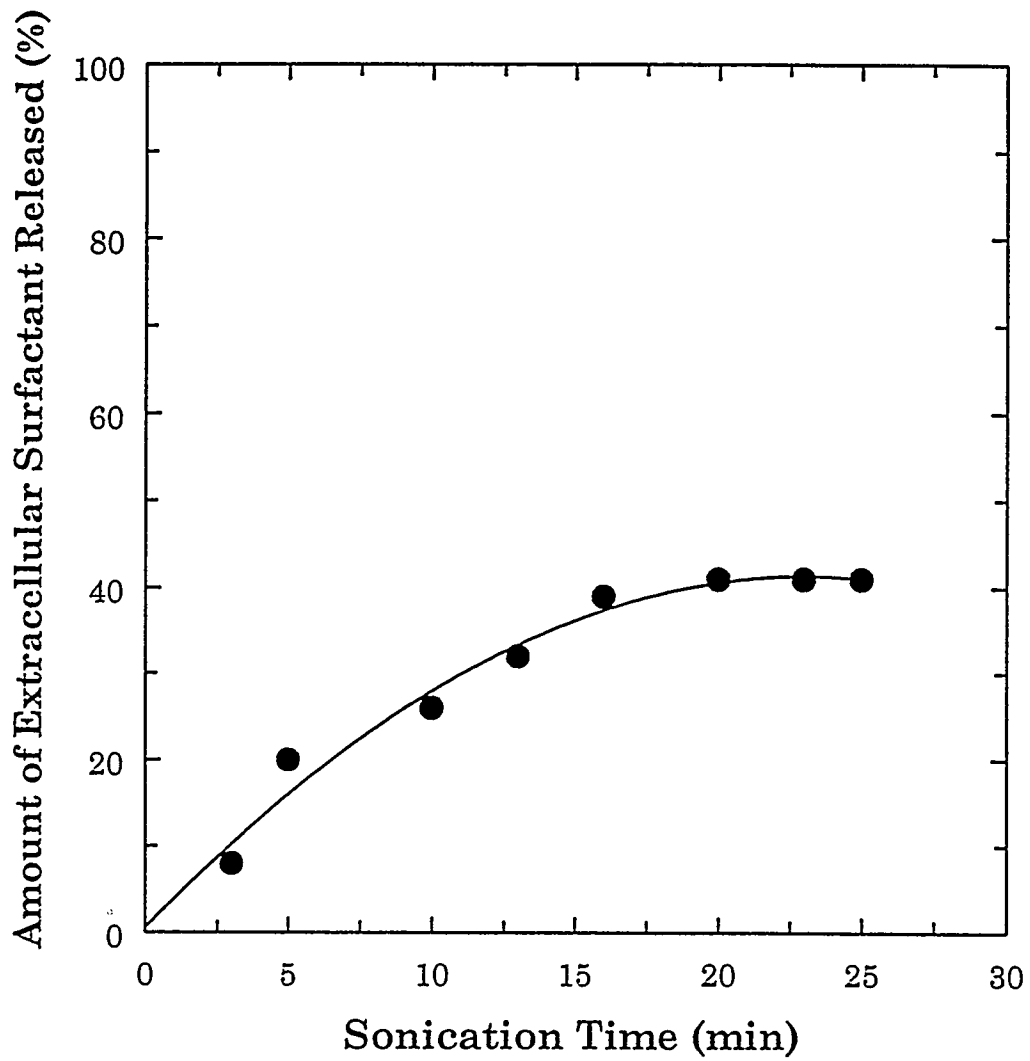


Figure 4.5 Amount of extracellular surfactant released as a function of sonication time

Table 4.1. The fatty acid composition of the extracellular surfactant

Fatty Acid	Composition (%)
14-C	4.01
16-C	13.61
18-C	43.53
20-C	38.85

#### 4.1.4 Surface properties of *M. phlei*

The surface properties of *M. phlei*, i.e., the surface hydrophobicity and the surface electrical properties, were studied by measuring the contact angle and zeta potential of the bacterium. The results of the hydrophobicity measurements are shown in Table 4.2. It should be noted that these measurements were conducted at natural pH of distilled water (ca. pH 6). The contact angle of the whole cell is about 68° which indicates that the surface is very hydrophobic. This value is very close to that reported by van Loosdrecht (1988). The presence of lipids, proteins and fatty acids makes the surface of the bacterium very hydrophobic. On the other hand, after sonication, the contact angle decreased substantially to 43° and this may be attributed to the loss of lipids and fatty acids present in the cell wall.

Table 4.2 The contact angle of *M. phlei* before and after sonication

<i>M. phlei</i> cells	Contact Angle (deg)
Whole	68°
Sonicated	43°

The zeta potential measurements of whole and sonicated cells are presented in Figure 4.6. As can be seen, the whole cells have an IEP around pH 2. Above pH 2, the surface of whole cells is negatively charged. Below pH 2, it was very difficult to measure the zeta potential. The surface charge of a bacterium is determined by the charging of anionic and cationic acid/base groups on the cell surface, together with some specific adsorption of some ions. The following acid/base couples could be the most probable ones involved in the charging of microbial surfaces (James, 1991): phosphate either in phosphodiester bridges ( $R-O-HPO_2-O-R/R-O-PO_2^-O-R$ ) as in teichoic acids, or at the end of a polymer ( $R-H_2PO_4/R-HPO_4^-$ ) as in phospholipids; protein- or peptidoglycan-associated ( $COOH/COO^-$ ); polysaccharide-associated ( $COOH/COO^-$ ); protonated phosphate ( $R-HPO_4^-/R-PO_4^{2-}$ ); and peptidoglycan or protein associated ammonium ( $R-NH_3^+/R-NH_2$ ). An IEP  $\leq 2.8$  for *M. phlei* indicates the predominance of a specific type of polymer, namely anionic polysaccharides containing phosphate and/or carboxylic acid groups which have a  $pK_a \leq 2.8$ . This was confirmed by FTIR analysis. However, after sonication the IEP shifted to higher



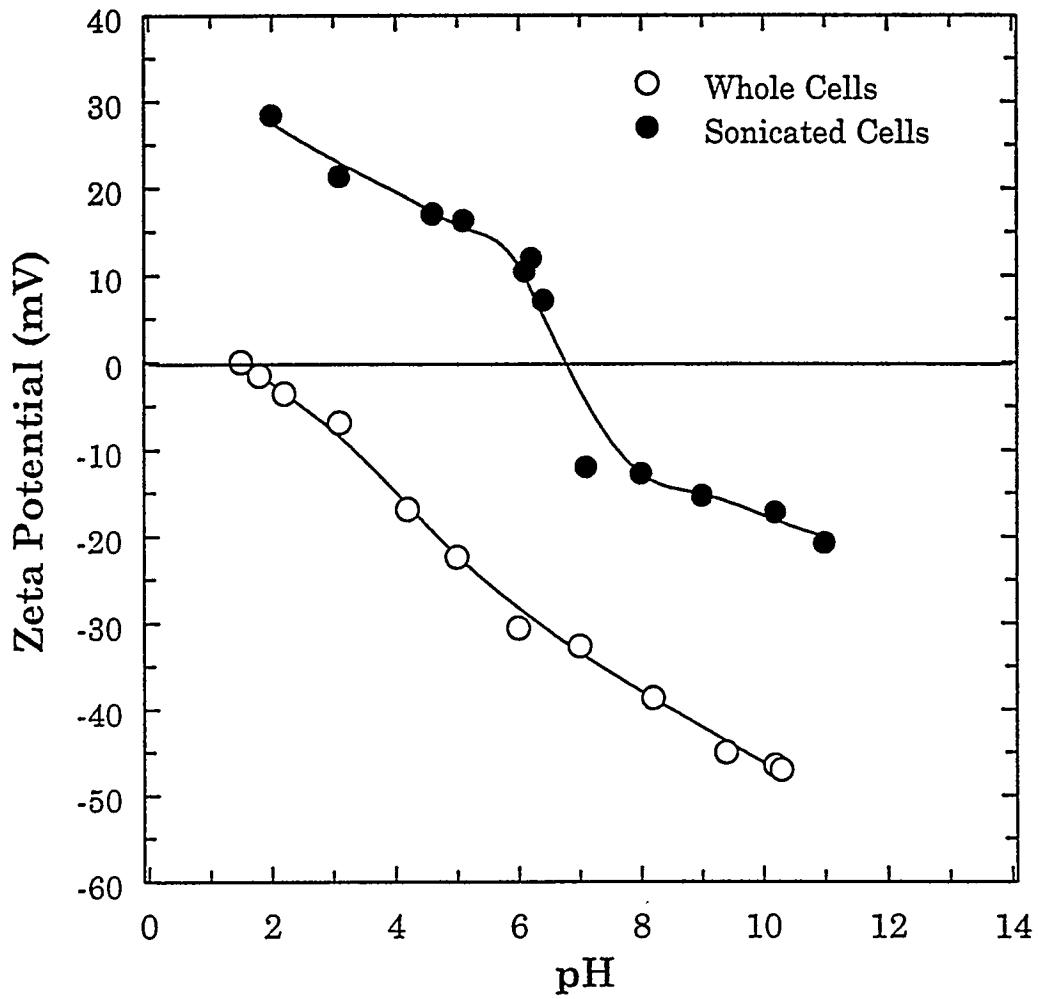


Figure 4.6 Zeta potential measurements of whole and sonicated cells of *M. phlei*

pH values (ca. pH 7). The drastic change in the surface electrical properties can be attributed to the loss of the surface functional groups such as carboxylic and phosphatic groups during sonication.

The above results suggest that the cell wall composition of *M. phlei* plays a major role in determining the surface properties of the bacterium. This in turn determines the behavior of the bacterium as a flocculation and flotation agent.

#### 4.2 Characterization of Coal and Mineral Samples

The coal and mineral samples were characterized in terms of their surface charge and hydrophobicities in the presence and absence of *M. phlei*. The surface charge measurements for the two coal samples, coal-pyrite, mineral pyrite and quartz are shown in Figure 4.7. The zeta potential of IL No.6 coal is positive up to pH 6 and beyond that pH it is negative. KY No.9 coal had an IEP around pH 5.2. The lower IEP of KY No.9 coal as compared to IL No.6 might be due to the presence of higher amount of ash in KY No.9 coal. Interestingly, coal-pyrite also exhibited a zeta potential similar to the coal samples with a IEP close to pH 6. This similar behavior may be due to the presence of coal/carbonaceous matter in the matrix of coal-pyrite and/or due to the higher reactivity of coal-pyrite as compared to mineral pyrite. However, mineral pyrite exhibited a different zeta potential profile with an IEP around pH 7. As expected, the IEP of quartz was

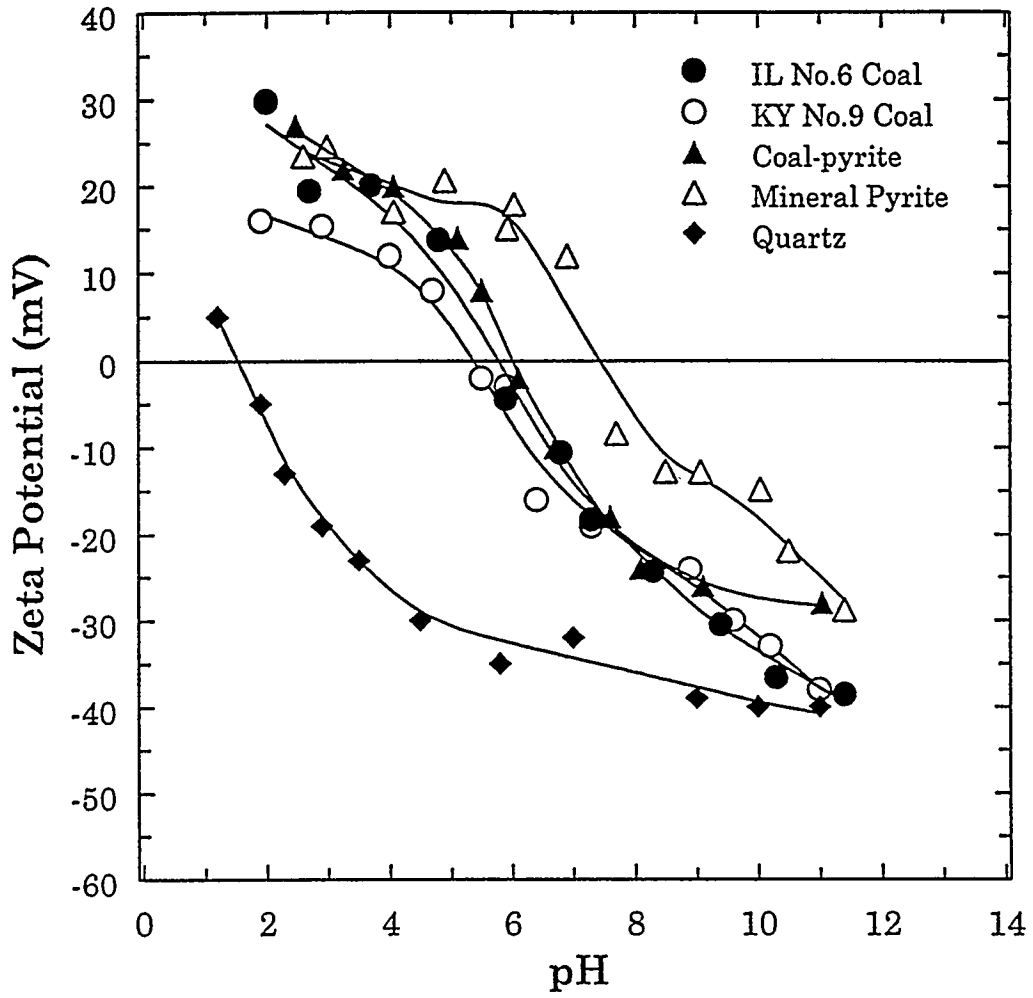


Figure 4.7 Zeta potential measurements of coal, coal-pyrite, mineral pyrite and quartz as a function of pH

found to be around pH 2 and beyond that pH the surface is negatively charged. The zeta potential measurements indicate that *M. phlei*, which is negatively charged, will adhere to coal particles in the pH range of 4-6 and to some extent to pyrite but not onto quartz.

The intrinsic hydrophobicities of the coal and mineral samples were studied by measuring the advancing contact angle as a function of pH and the results are presented in Figure 4.8. The variation in contact angle as a function of pH was found to be similar in all the cases with a maximum near neutral pH. This maximum coincides with the IEP of the coal samples and pyrite samples. However, the magnitude of contact angle measured was different for all the samples. In the case of coal samples, IL No.6 coal exhibited a higher contact angle than KY No.9 over the whole pH range, indicating that it was more hydrophobic. The lower hydrophobicity of KY No.9 coal may be due to its higher ash content and lower carbon content than IL No.6 coal. Ash forming minerals consist mainly of silica and clay minerals which are hydrophilic in nature and hence decrease the hydrophobicity of the coal. In the case of pyrites, coal-pyrite exhibited a significantly higher contact angle than mineral pyrite. As mentioned earlier, coal-pyrite has some coal/carbonaceous matter present in its matrix which could be responsible for its higher hydrophobicity than mineral pyrite. Mineral pyrite, on the other hand, was relatively pure. It is interesting to see that the hydrophobicities exhibited by coal and coal-pyrite are very similar. This

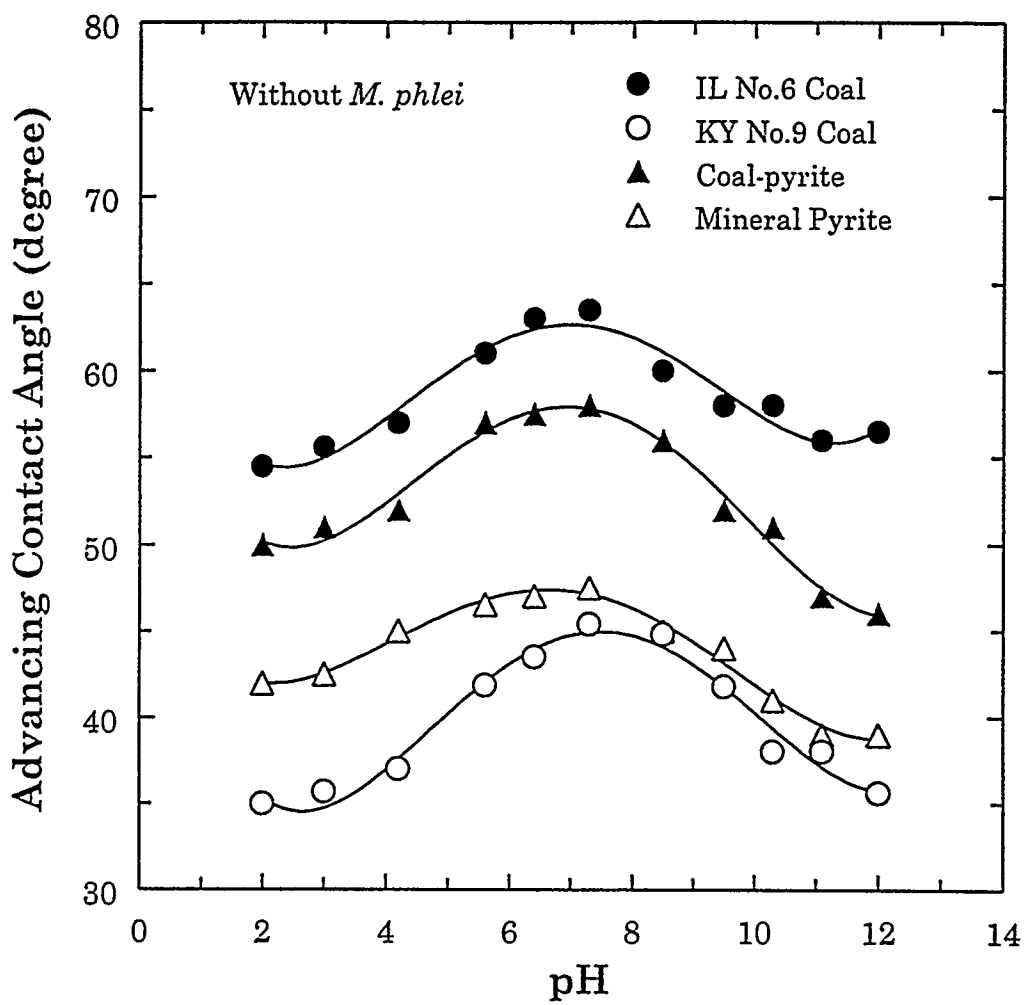


Figure 4.8. Advancing contact angle measurements of coal and pyrite as a function of pH in the absence of *M. phlei*

could be one of the reasons for the difficulty in separating coal-pyrite from coal by using surface chemistry based methods such as flotation.

### 4.3 Adhesion Experiments

As described in the previous chapter, the adhesion of *M. phlei* whole and sonicated cells onto coal, pyrite and quartz were studied by using a UV spectrophotometer. A calibration plot was first developed for whole and sonicated cells to determine the relationship between transmittance and concentration of *M. phlei* in suspension and the results are shown in Figures 4.9 and 4.10 respectively. In both cases it can be seen that a linear relationship exists between the concentration of the microorganism in suspension and the transmittance. However, the linear relationships for whole and sonicated cells were different. This could be due to the presence of extracellular surfactants in the case of whole cells. Also, mutual attachment of cells in the case of whole cells could be responsible for the lower transmittance compared to sonicated cells. The equations shown in the figures were used for determining the concentration of cells in the suspension after adhesion. The concentration determined is then used to calculate the amount adhering to the surface.

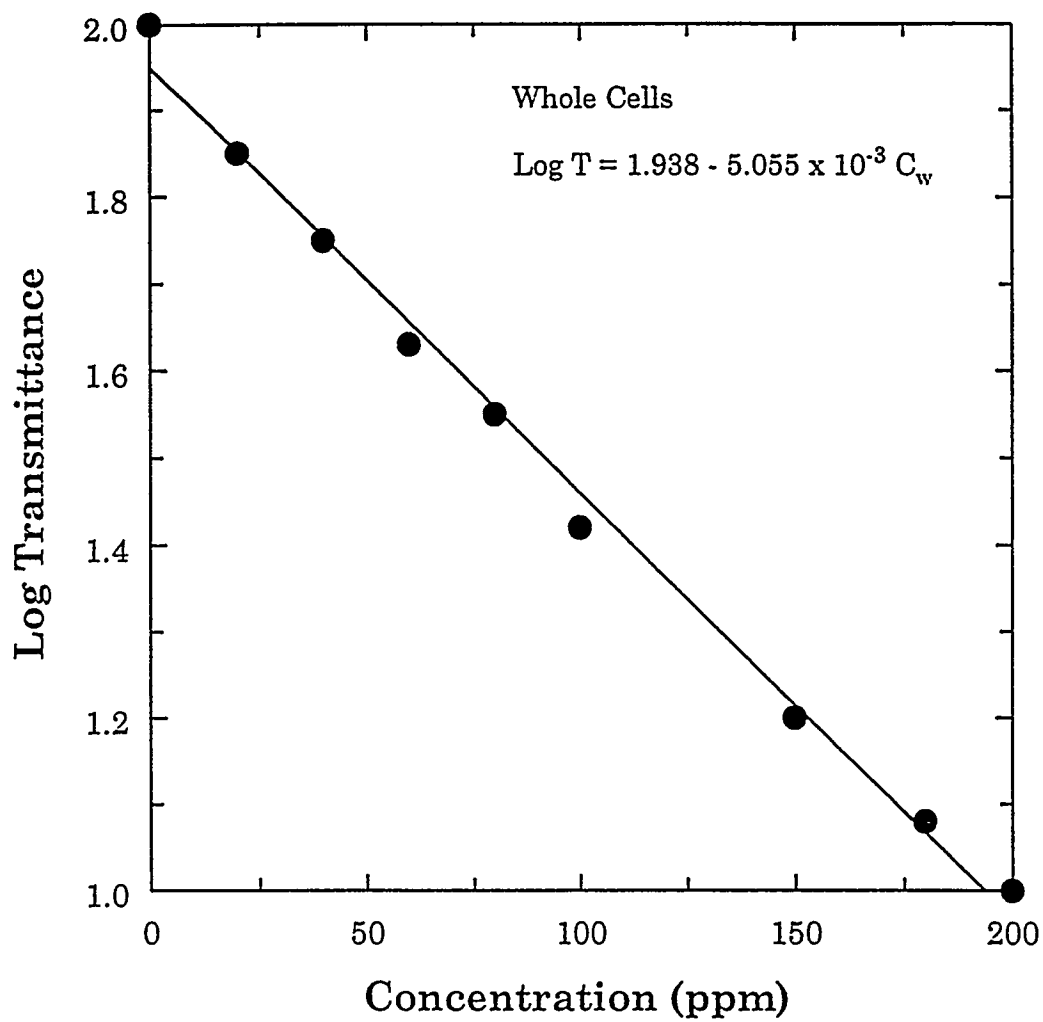


Figure 4.9 Calibration plot for *M. phlei* whole cells

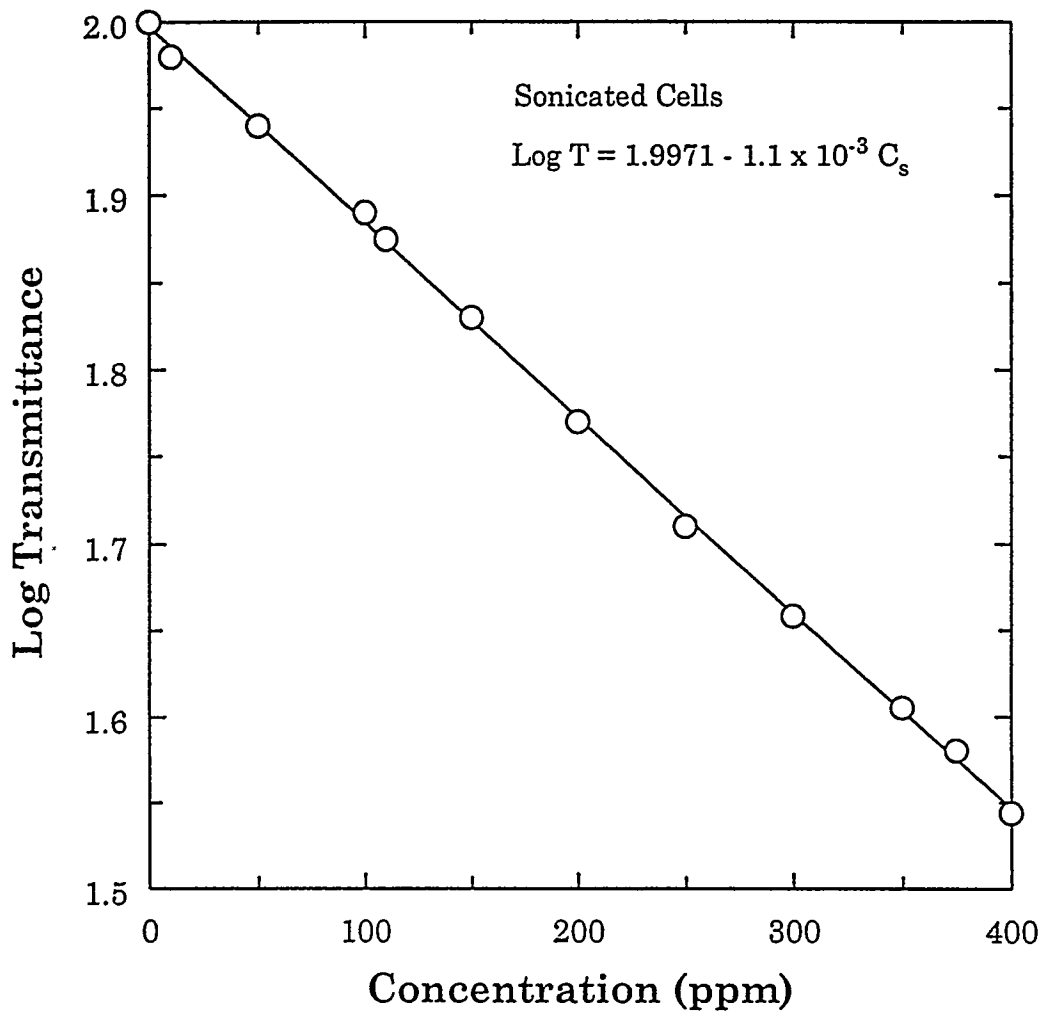


Figure 4.10 Calibration plot for sonicated cells of *M. phlei*



#### 4.3.1 Adhesion of *M. phlei* whole cells

The effect of various parameters such as conditioning time, concentration of microorganism and pH on the adhesion behavior of *M. phlei* was investigated. Figure 4.11 shows the effect of conditioning time on the amount of whole cells adhering to different mineral surfaces at pH 3. As can be seen, the amount of bacteria adhering to both coal samples increases with conditioning time and a maximum is attained in 5-6 minutes. Further conditioning did not have any effect on the amount adhered; however, the maximum amount adhering on the two coal samples was different and this could be due to the difference in hydrophobicities between the two coal samples. In the case of coal-pyrite, the amount of *M. phlei* adhering to its surface was much less compared to coal and increased only slightly after 10 minutes of conditioning. But in the case of mineral pyrite and quartz, conditioning time did not have any effect on the amount of *M. phlei* adhering to the surface. Based on the above data, a conditioning time of 5 minutes was used in subsequent studies.

The effect of concentration of *M. phlei* on the amount adhering to different mineral surfaces at pH 4 is shown in Figure 4.12. The conditioning time was maintained constant at 5 minutes. In the case of both the coal samples, the amount of *M. phlei* adhering to the surface increased as the concentration was

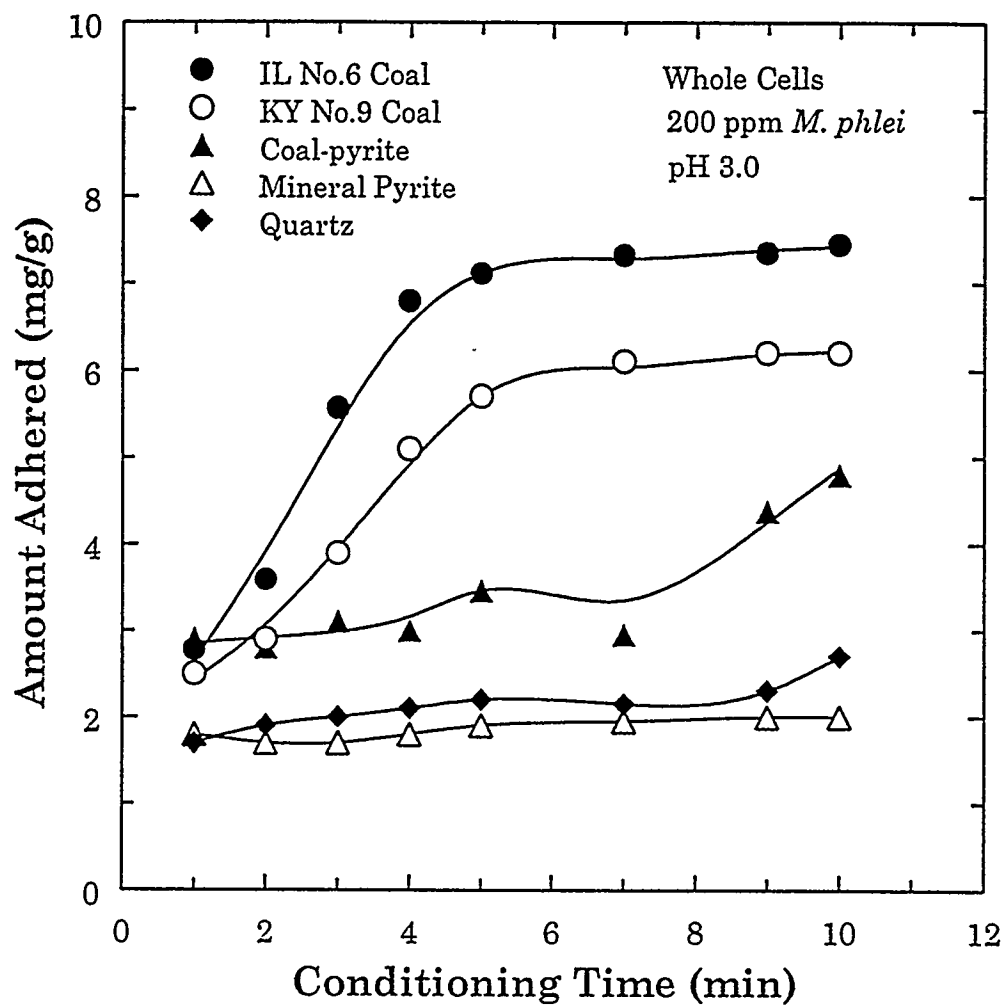


Figure 4.11 Effect of conditioning time on the amount of whole cells adhering onto coal, pyrite and quartz surfaces

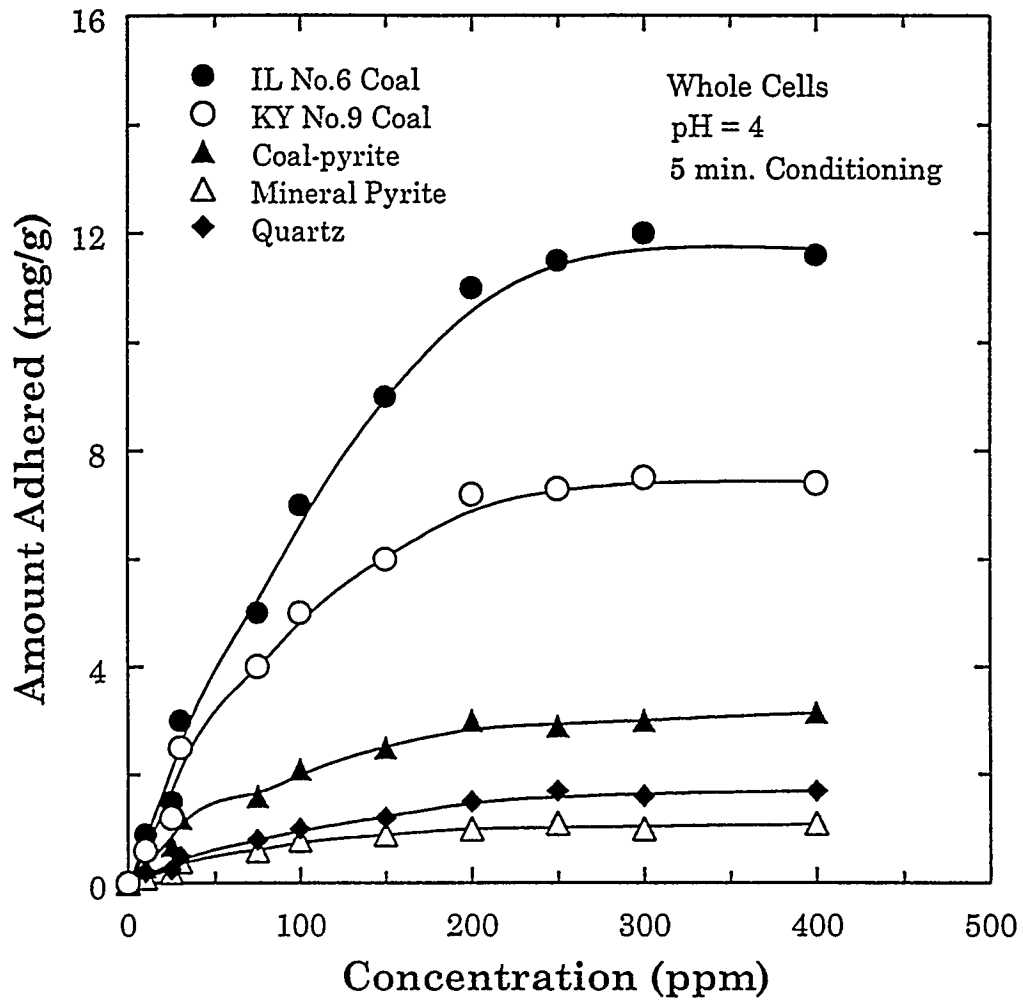


Figure 4.12 Effect of concentration of whole cells of *M. phlei* on the amount adhering onto coal, pyrite and quartz

increased before reaching a maximum at about 200 ppm. Further increase in concentration did not affect the amount adhering to coal surfaces. But the maximum amount of *M. phlei* adhering for both coal samples was significantly different. The maximum in the case of IL No.6 coal was about 12 mg/g, while in the case of KY No.9 it was about 7.5 mg/g. In the case of coal-pyrite, mineral pyrite and quartz, the maximum amount adhering was only about 2-3 mg/g, suggesting that *M. phlei* selectively attaches to coal in comparison with its associated impurities such as pyrite and quartz.

Figure 4.13 presents the results of the effect of pH on the adhesion behavior of *M. phlei* whole cells to coal and its associated impurities. The concentration of *M. phlei* was maintained at 200 ppm and conditioning time at 5 minutes. Adhesion of *M. phlei* onto coal was found to be highly dependent on pH with maximum adhesion in the pH range of 3.5-4.5. Between pH 3.5 and 4.5, the coal surface is positively charged and *M. phlei* is negatively charged, which facilitates columbic attraction. Below pH 2, where *M. phlei* is positively charged, adhesion was relatively low. Similarly, at higher pH values, the adhesion of *M. phlei* onto both coal samples was relatively low, and this could be due to repulsion developed by similar charges on coal surface and *M. phlei* surface. The adhesion of *M. phlei* on pyrite and quartz was low and remained essentially constant over the entire pH range. The increase in adhesion on coal-pyrite at pH

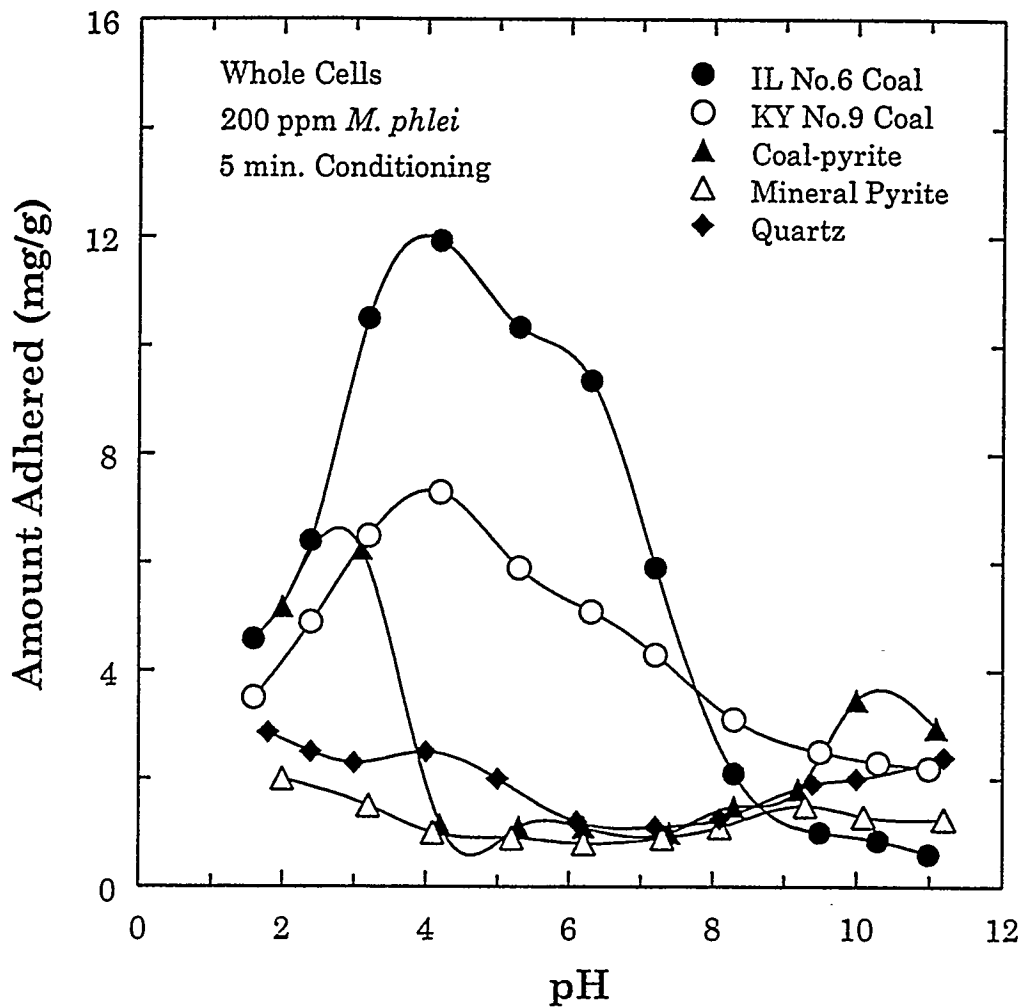


Figure 4.13 Effect of pH on the amount of whole cells of *M. phlei* adhering to coal, pyrite and quartz

values less than 3.5 can probably be attributed to the presence of coal/carbonaceous particles present in the matrix. From the above results it can be concluded that coal can be selectively flocculated in the pH range of 3.5-4.5 by selective adhesion of *M. phlei*.

#### 4.3.2 Adhesion of sonicated cells of *M. phlei*

Adhesion tests also were performed with sonicated cells of *M. phlei* as a function of concentration and pH. Conditioning time had a similar effect as that observed for whole cells and hence the conditioning time was fixed at 5 minutes. The effect of concentration is shown in Figure 4.14. The amount adhered showed a similar trend as the whole cells, but there were two major differences: (i) the amount of sonicated cells adhering as compared to whole cells and (ii) the concentration at which maximum adhesion was obtained. In the case of sonicated cells, maximum adhesion occurred at concentrations greater than 250 ppm, and the maximum amount adhering was almost 50% less when compared with whole cells. This difference in adhesion behavior between whole and sonicated cells might be due to the lower hydrophobicity of sonicated cells. As discussed earlier, sonication of *M. phlei* cells decreases the hydrophobicity of cells in comparison with whole cells.

The effect of pH on the adhesion of sonicated cells was also investigated

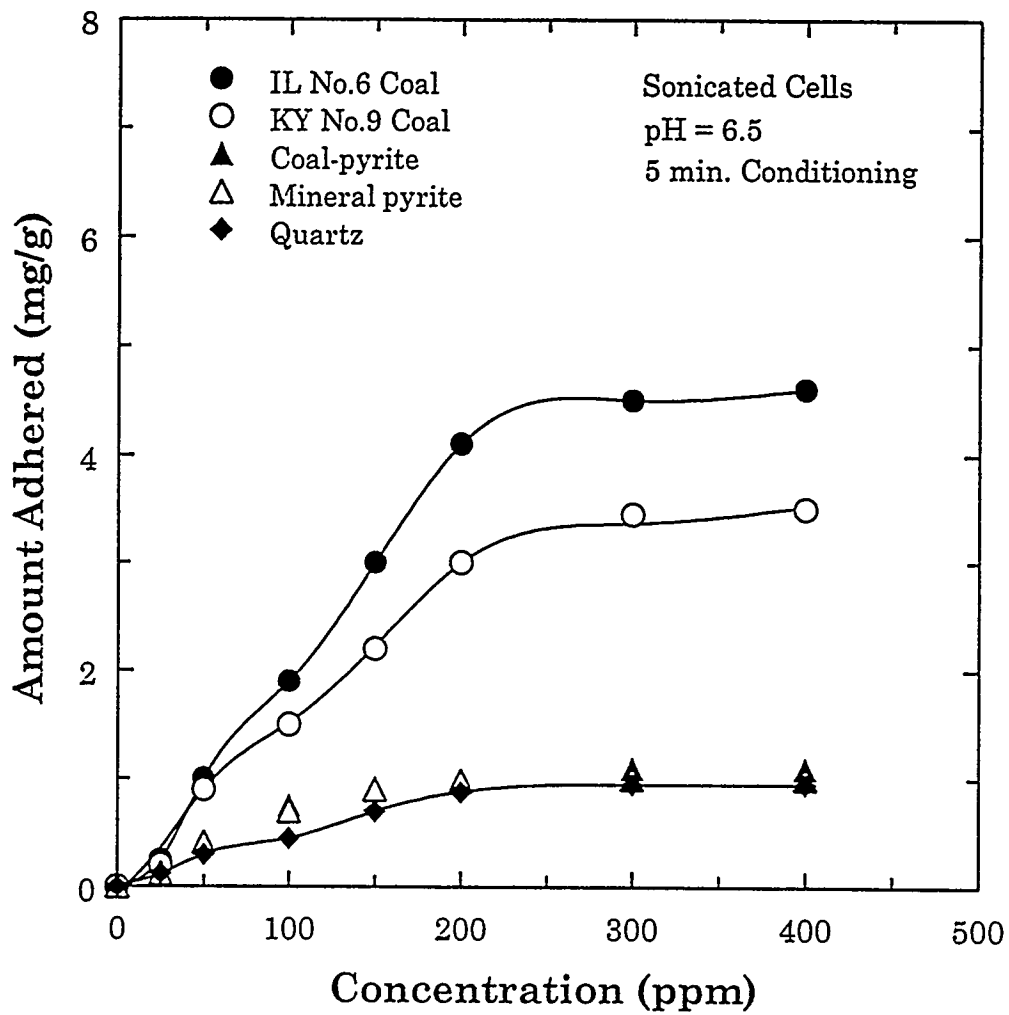


Figure 4.14 Effect of concentration on the amount of sonicated cells of *M. phlei* adhering to coal, pyrite and quartz

and the results are shown in Figure 4.15. It is interesting to see that for coal-pyrite, mineral pyrite and quartz, pH did not influence the adhesion behavior of sonicated cells and the amount adhered was constant at about 1 mg/g. However, for the coal samples, adhesion of sonicated cells varied as a function of pH with a maximum in the pH range of 5-6.5 as opposed to a pH range of 3.5-4.5 in the case of whole cells. Also, the maximum amount adhering was low when compared to whole cells.

#### 4.4 Effect of Adhesion on Hydrophobicity

The variation in contact angle with the adsorption of whole and sonicated cells of *M. phlei* was studied as a function of pH for all the coal and pyrite samples. Figures 4.16 and 4.17 show the variation of contact angle of IL No.6 and KY No.9 coal in the presence of whole and sonicated cells. For both the coal samples, the contact angle at every pH was invariably increased as a result of the adhesion of whole cells of *M. phlei*. The maximum values of contact angles, however, were shifted to lower pH values. Large increases in contact angle occurred in the acidic pH range of 2-6. Beyond this pH range, the increase in contact angle was marginal. The increase in contact angle in the pH region where maximum was observed was about 10-15 degrees. This indicates that as a result of *M. phlei* adhesion, the coal surfaces have become more hydrophobic. However in the case of sonicated cells, although an increase in contact angle was



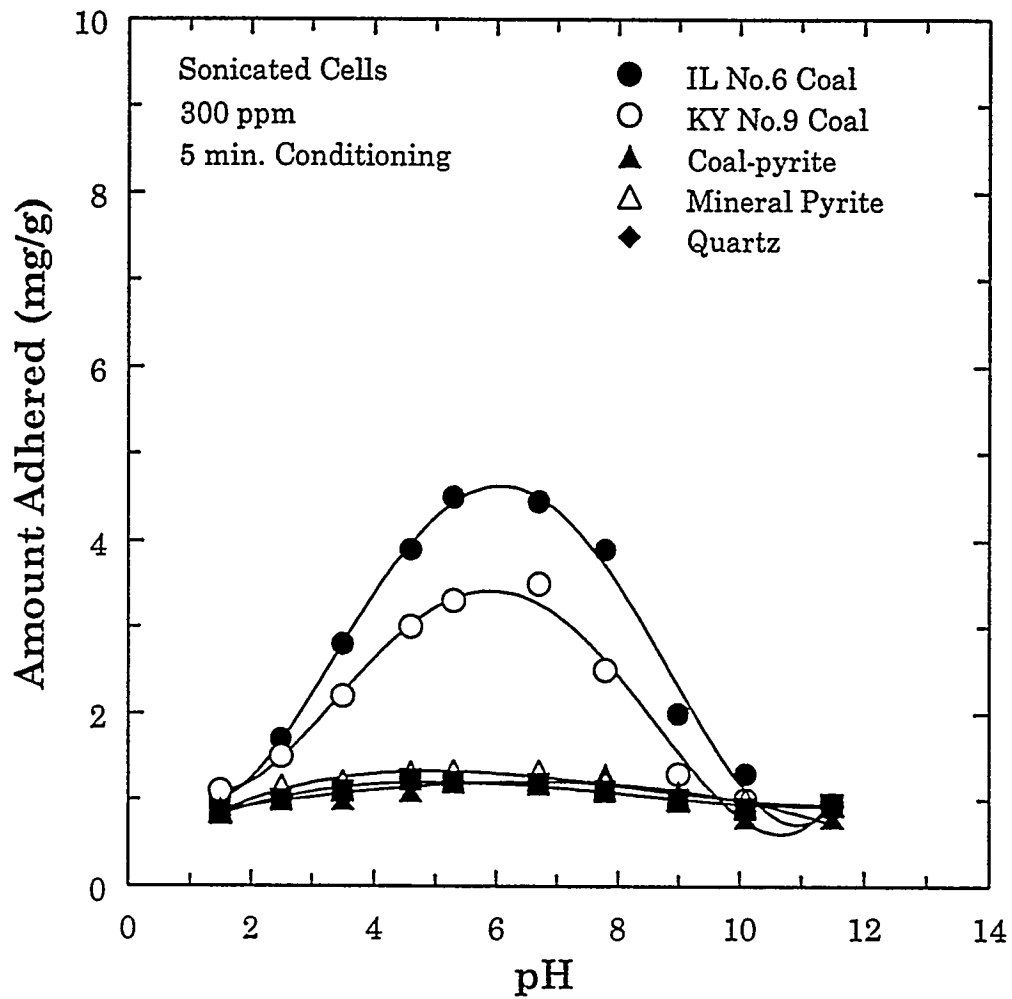


Figure 4.15 Effect of pH on the amount of sonicated cells of *M. phlei* adhering to coal, pyrite and quartz

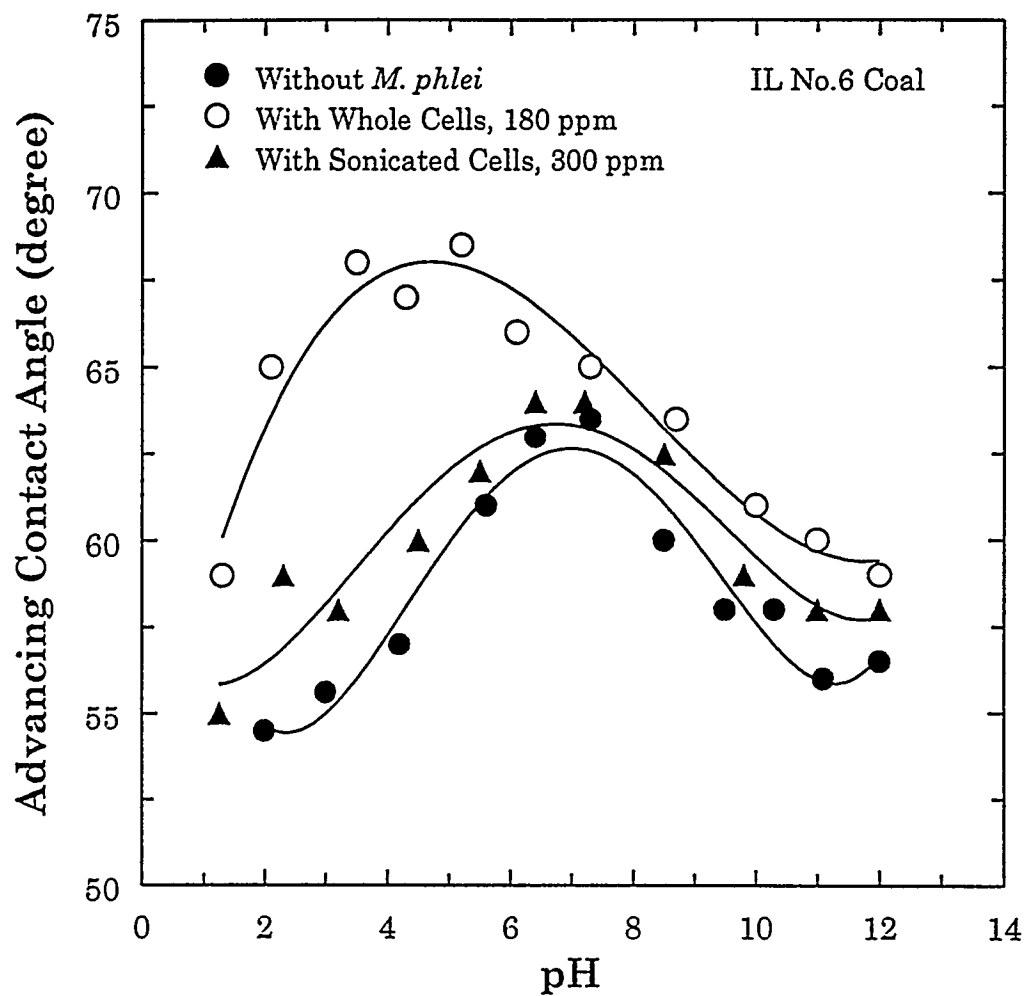


Figure 4.16 Comparison of advancing contact angle measurements for IL No.6 Coal in the presence and absence of *M. phlei*

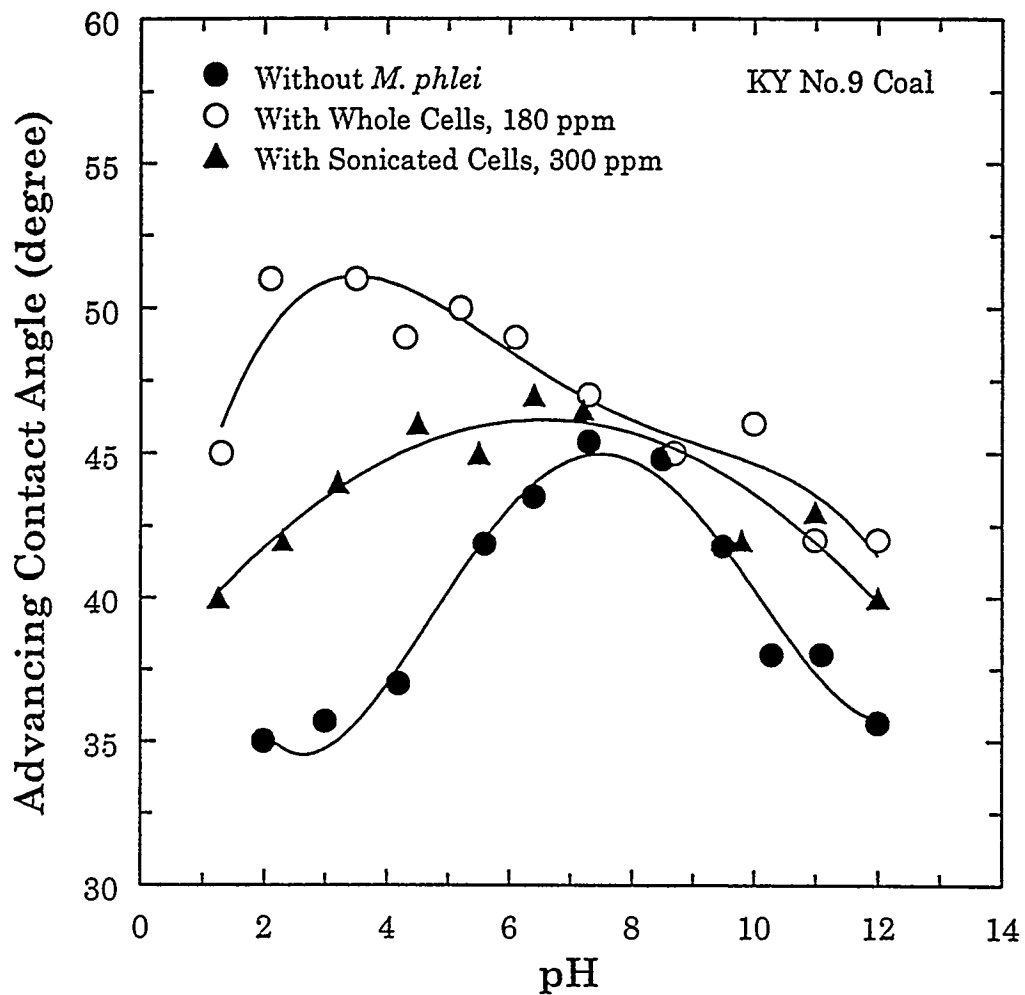


Figure 4.17 Comparison of advancing contact angle measurements for KY No.9 Coal in the presence and absence of *M. phlei*

observed, it was not as significant as that observed with whole cells. The sonicated cell walls of *M. phlei* have a lower hydrophobicity as compared to whole cells and this probably leads to lower adhesion of sonicated cells onto coal. Hence, lower contact angles are observed with sonicated cells when compared with whole cells of *M. phlei*.

In the case of coal-pyrite, the adhesion of whole cells showed a slight increase in contact angle at all pH values studied and the results are shown in Figure 4.18. But the increase in hydrophobicity due to adhesion of *M. phlei* was not as significant as in the case of coal. Mineral pyrite did not exhibit any increase in contact angle indicating that little or no adhesion of *M. phlei* had occurred (Figure 4.19). Further, sonicated cells did not affect the hydrophobicity of both the coal-pyrite and mineral pyrite samples. Quartz, on the other hand, did not exhibit any increase in hydrophobicity with either whole or sonicated cells which indicates that very little *M. phlei* attaches to the surface.

The above results suggest that whole cells of *M. phlei* selectively attach to the surface of coal making it more hydrophobic in relation to coal-pyrite. The increase in hydrophobicity is the principal reason which causes coal to flocculate selectively.

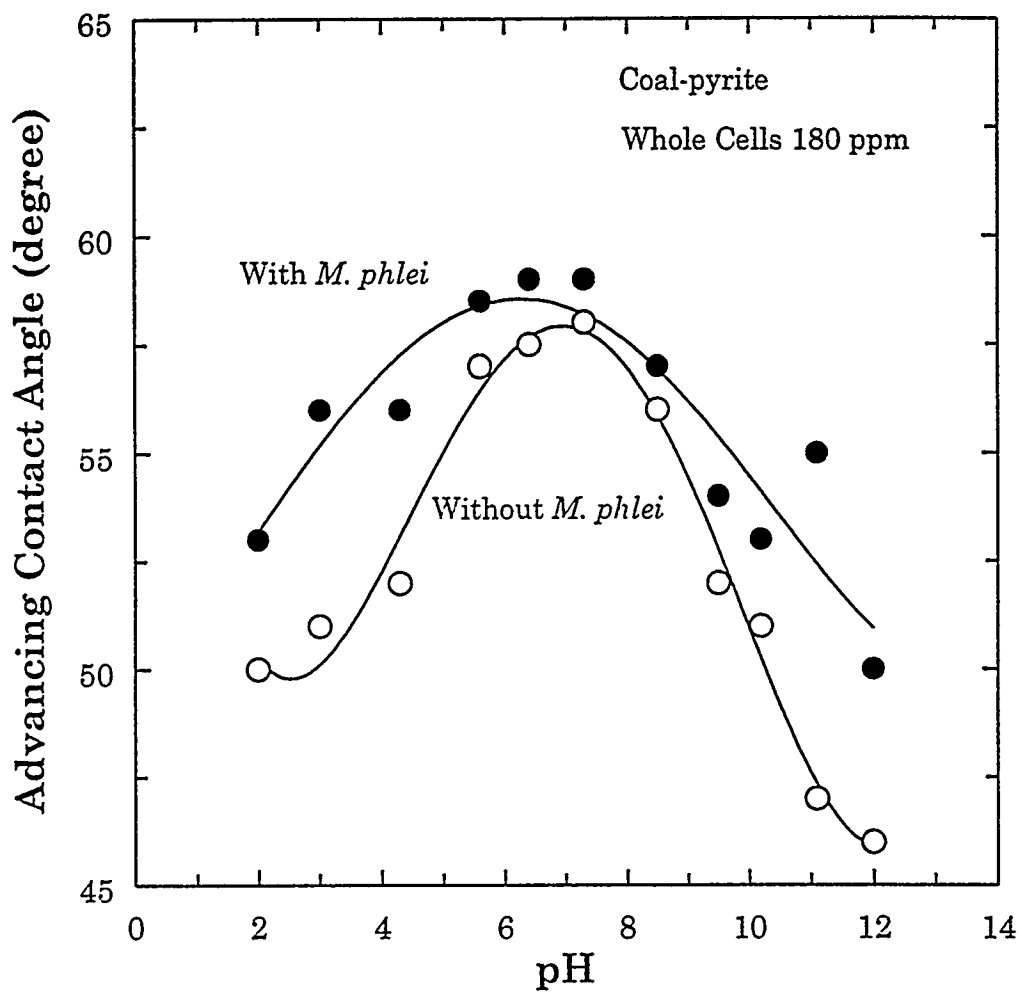


Figure 4.18 Contact angle measurements of coal-pyrite in the presence and absence of whole cells of *M. phlei* as a function of pH

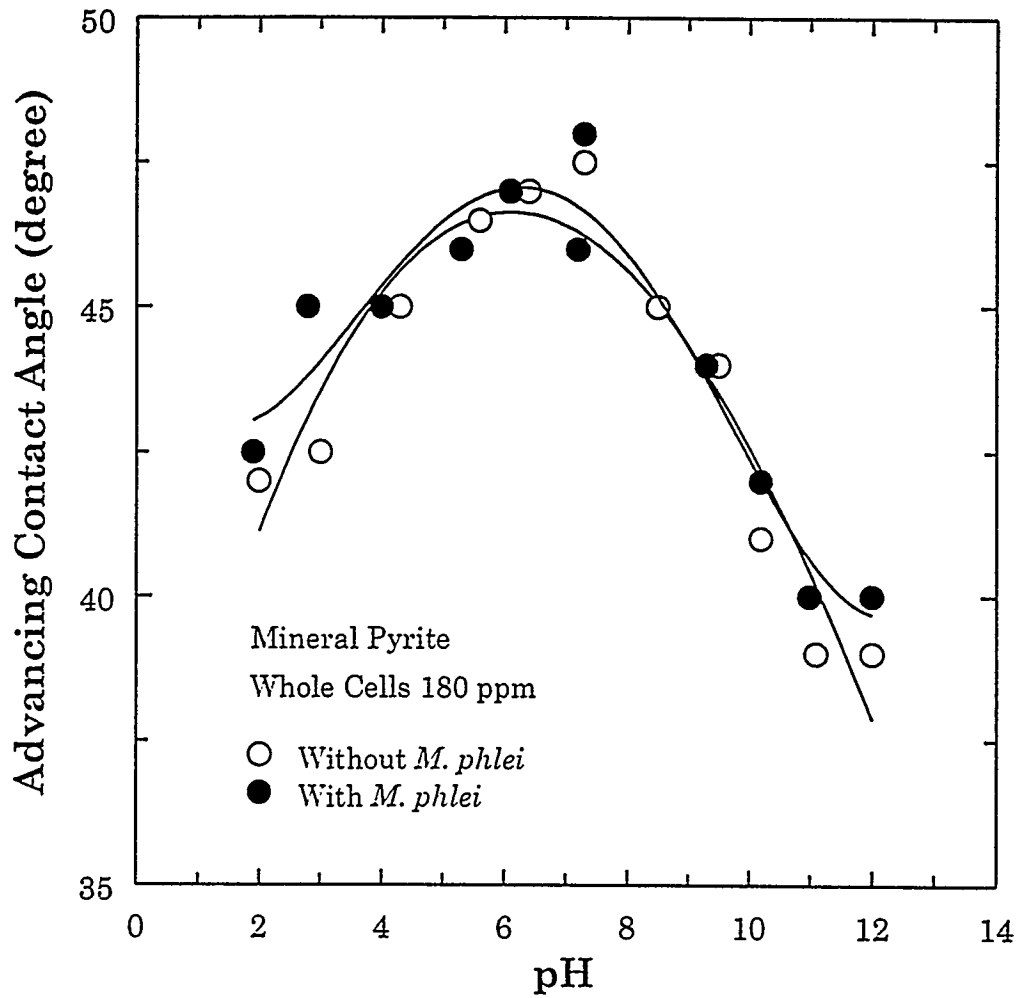


Figure 4.19 Contact angle measurements of mineral pyrite in the presence and absence of whole cells of *M. phlei* as a function of pH

#### 4.5 Scanning Electron Microscopy (SEM) Studies

SEM studies were undertaken to obtain direct evidence regarding the mode and nature of adhesion of *M. phlei* whole cells on the surfaces of coal, pyrite and quartz. All the samples were prepared at a *M. phlei* whole cell concentration of 180 ppm and at pH values of 3.5 and 8.2. In the case of IL No.6 coal at pH 3.5 (Figure 4.20), *M. phlei* formed massive flocs and adhered tenaciously to the coal surface. At pH 8.2 very little adhesion was observed (Figure 4.21). Similar results were observed with KY No.9 coal. These results confirmed the results obtained from adhesion and contact angle experiments. In the case of coal-pyrite (Figure 4.22), although some *M. phlei* attachment was observed, it was not as dense as in the case of coal. It is possible that *M. phlei* might be adhering to some coal/carbonaceous inclusions on the coal-pyrite rather than onto the surface of clean pyrite. Very little attachment was observed at pH 8.2. Microphotographs of mineral pyrite showed that very few cells of *M. phlei* attached at pH 3.4 (Figure 4.23) while at pH 8.2 (Figure 4.24) no attachment was observed. The mineral pyrite does not contain any carbon as opposed to coal-pyrite. Thus it can be concluded that the coal/carbonaceous inclusions in coal-pyrite are probably responsible for greater adhesion as compared to mineral pyrite. Similarly, quartz did not show any adhesion of *M. phlei* cells at pH 3.5 (Figure 4.25) at all thus confirming the findings of adhesion and contact

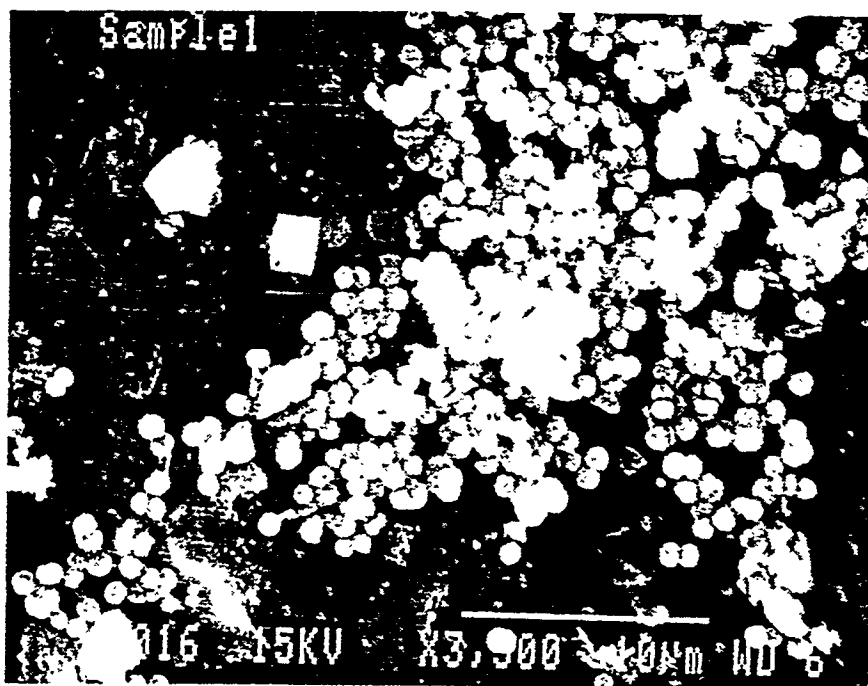


Figure 4.20 Scanning electron microphotograph of *M. phlei* adhering to IL No. 6 coal (pH 3.5; 180 ppm concentration)





Figure 4.21 Scanning electron microphotograph of *M. phlei* adhering to IL No. 6 coal (pH 8.2; 180 ppm concentration)

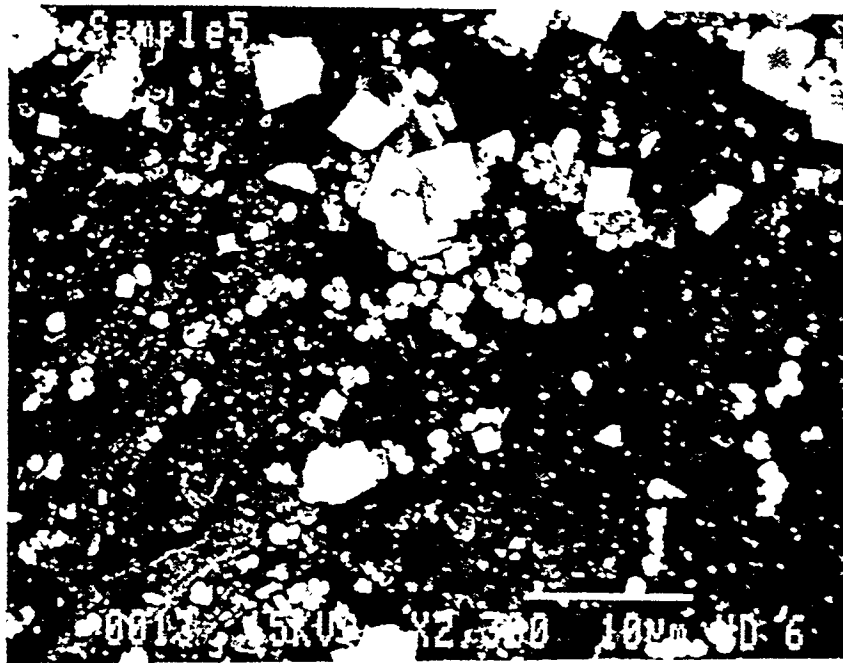


Figure 4.22 Scanning electron microphotograph of *M. phlei* adhering to coal-pyrite (pH 3.5; 180 ppm concentration)

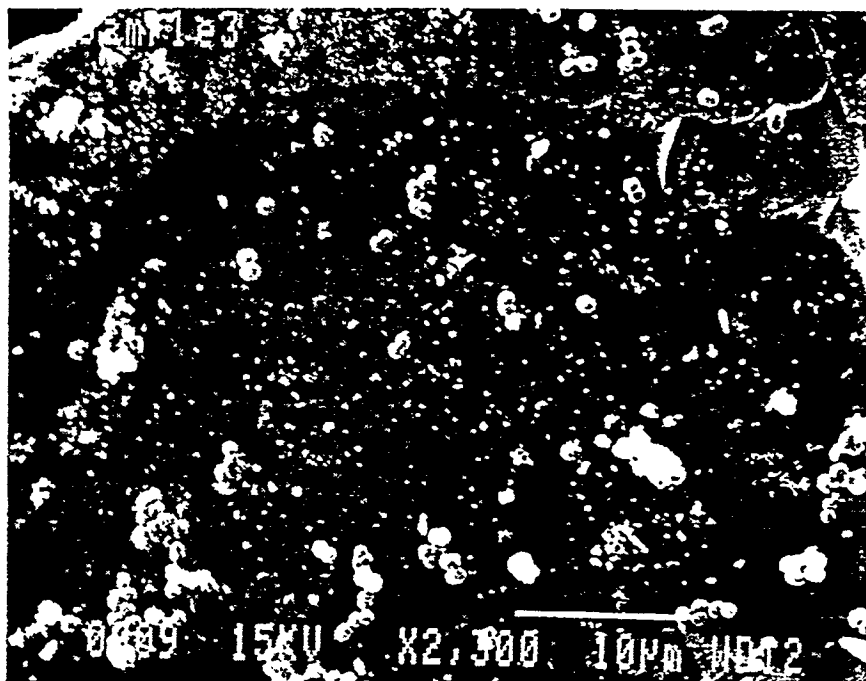


Figure 4.23 Scanning electron microphotograph of *M. phlei* adhering to mineral pyrite (pH 3.5; 180 ppm concentration)

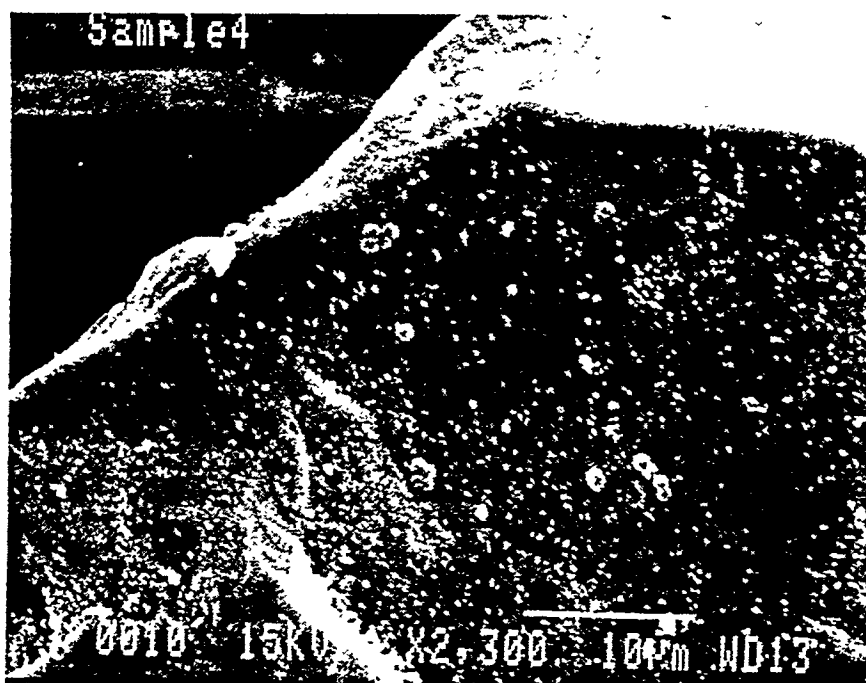


Figure 4.24 Scanning electron microphotograph of *M. phlei* adhering to mineral pyrite (pH 8.2; 180 ppm concentration)

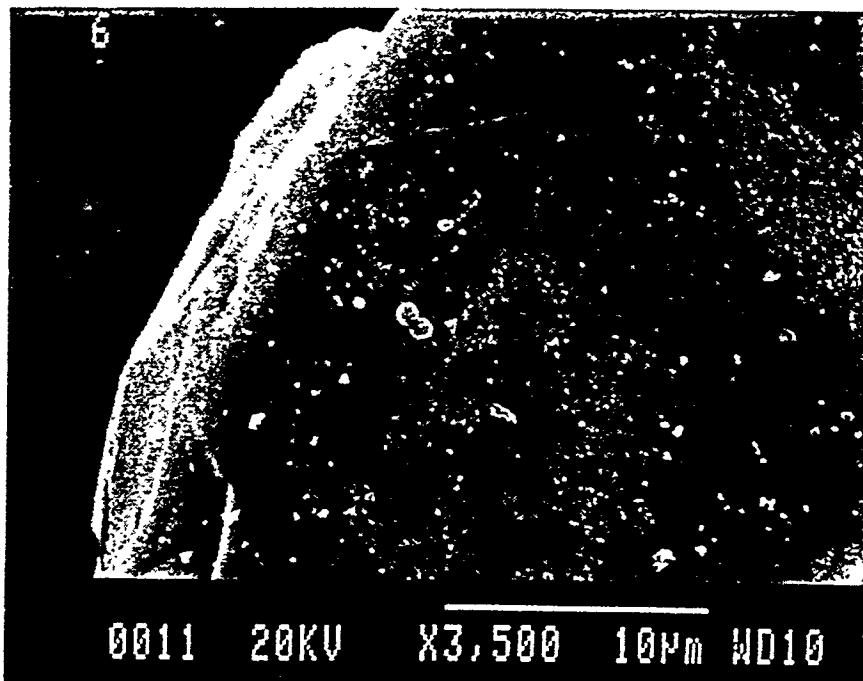


Figure 4.25 Scanning electron microphotograph of *M. phlei* adhering to quartz (pH 8.2; 180 ppm concentration)

angle measurements.

The above studies clearly show that greater quantities of *M. phlei* attached onto coal than coal-pyrite and that the attachment was tenacious. Adhesion and contact angle studies revealed that very little adhesion of sonicated cells took place onto the coal and pyrite samples; therefore, SEM studies were not conducted.

#### 4.6 Sedimentation and Flocculation Experiments

Sedimentation and flocculation tests were performed with IL No.6 and KY No.9 coals. Flocculation tests were performed in the presence of whole cells, sonicated cells and the extracellular surfactant. For comparison purposes, tests were also performed with two synthetic polymeric flocculants, polyethylene oxide (PEO) and polyacrylamide (PAM). PEO is nonionic with an average molecular weight of 600,000 while PAM is anionic and has a molecular weight of 12-15 million.

##### 4.6.1 *Effect of Time*

Figure 4.26 shows the effect of time on the amount of IL No.6 coal settled in the presence of different flocculants. The best results, i.e. maximum amount

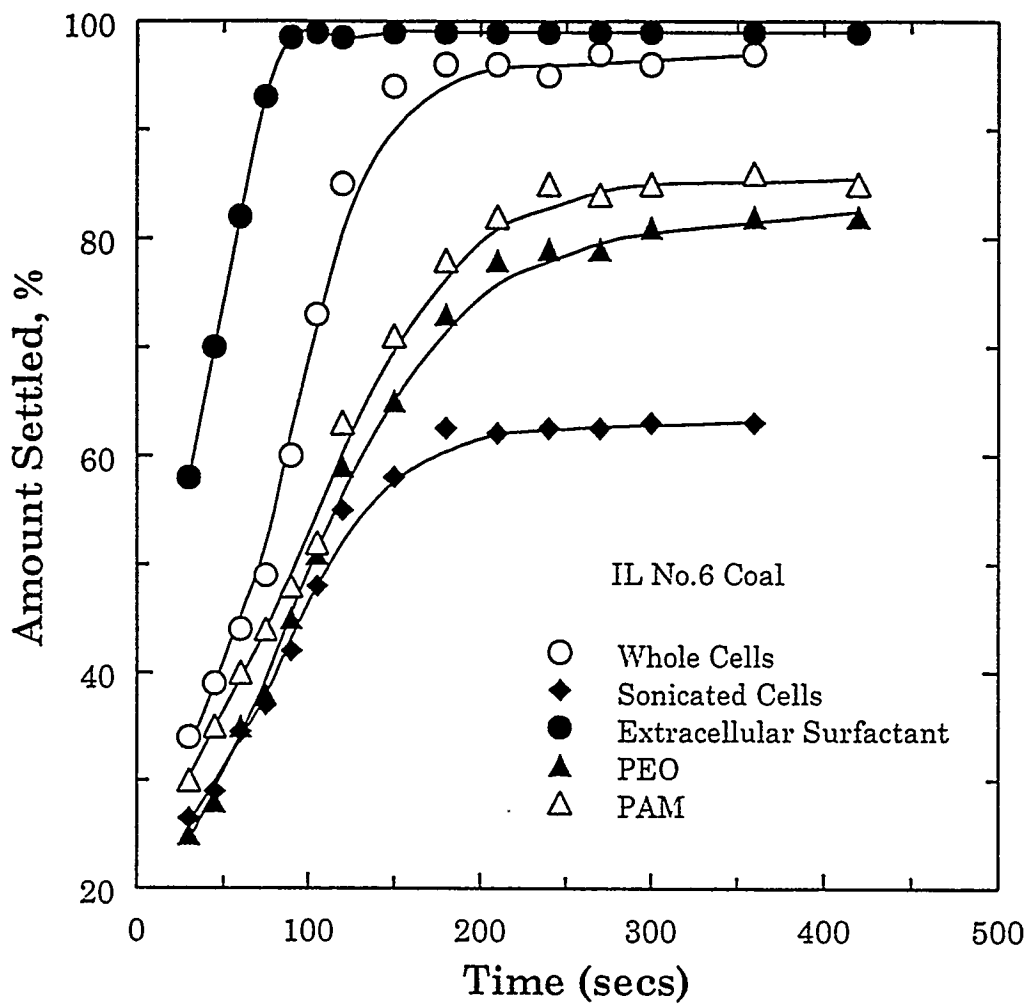


Figure 4.26 Amount of IL No.6 coal settled as a function of time in the presence of different flocculants

of coal settled in minimum time, were obtained in the presence of extracellular surfactant. The amount of coal settled increased with time and reached a maximum value of about 98% in about 2 minutes and remained constant with further increase in time. In the presence of whole cells also, the maximum amount of coal settled was about 95%, but only after 3 minutes. In the case of the two polymeric flocculants, the maximum amount of coal settled was around 80% which was attained after 4 minutes. With sonicated cells, the maximum amount of coal settled was about 60% after 4 minutes. Faster settling rates in the presence of extracellular surfactant and whole cells of *M. phlei* were achieved because the flocs form very rapidly and settle very quickly. But in the case of other flocculants, formation of flocs occurred slowly.

Similar tests were conducted with KY No.9 coal, and the results are presented in Figure 4.27. Once again a settling behavior similar to IL No.6 coal was observed, although the time required was slightly more. With extracellular surfactant, the maximum amount of coal settled was about 95% after 3 minutes. In the presence of whole cells, the maximum amount of coal settled was only about 80% after 4 minutes. With synthetic polymeric flocculants, the maximum amount settled was about 75-77%, while with sonicated cells it was only 58%. These results are very similar to those obtained with IL No.6 coal, although the amount of coal settled was different. This difference can be explained in terms of differential adhesion of the bacterium and the extracellular surfactant on the



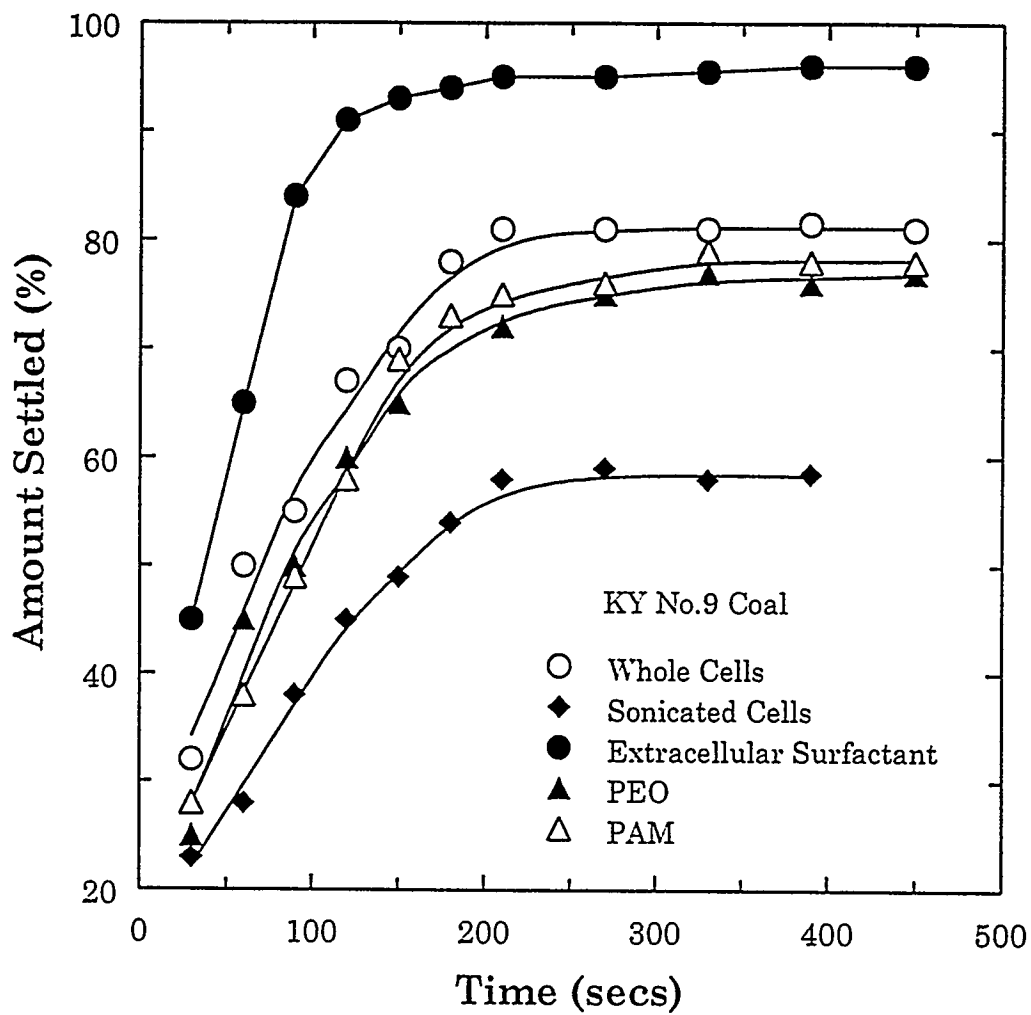


Figure 4.27 Amount of KY No.9 coal settled as a function of time in the presence of different flocculants

two coal samples.

#### 4.6.2 Effect of Concentration on Flocculation Efficiency

The effect of concentration of different flocculants on the flocculation efficiency ( $E_f$ ) of IL No.6 coal is presented in Figure 4.28. The time for flocculation was maintained at 3 minutes while the pH was chosen from the adhesion test results. As the concentration of *M. phlei* whole cells increased, the  $E_f$  increased until it reached a maximum of 0.93 at 200 ppm. Any additional increase in concentration did not affect the  $E_f$ . With the extracellular surfactant, a maximum  $E_f$  of about 0.98 was obtained at 50 ppm and remained constant at higher concentrations. These results clearly indicate that flocculation with the released extracellular surfactant, which contains all the lipids and functional groups, increases the  $E_f$  of coal and that this is obtained at considerably lower concentrations. A similar behavior was observed with sonicated cells, although the  $E_f$  was significantly less and the concentrations required were greater than that of extracellular surfactant or the whole cells. Even though the extracellular surfactants have been removed during sonication, the residual bacterial cell wall may still contain some proteins and lipids which can cause adherence to coal surface and hence flocculation. Since the amount of proteins or lipids remaining in the cell wall after sonication is less, the concentration of sonicated cells required for flocculation is very high (>300 ppm).

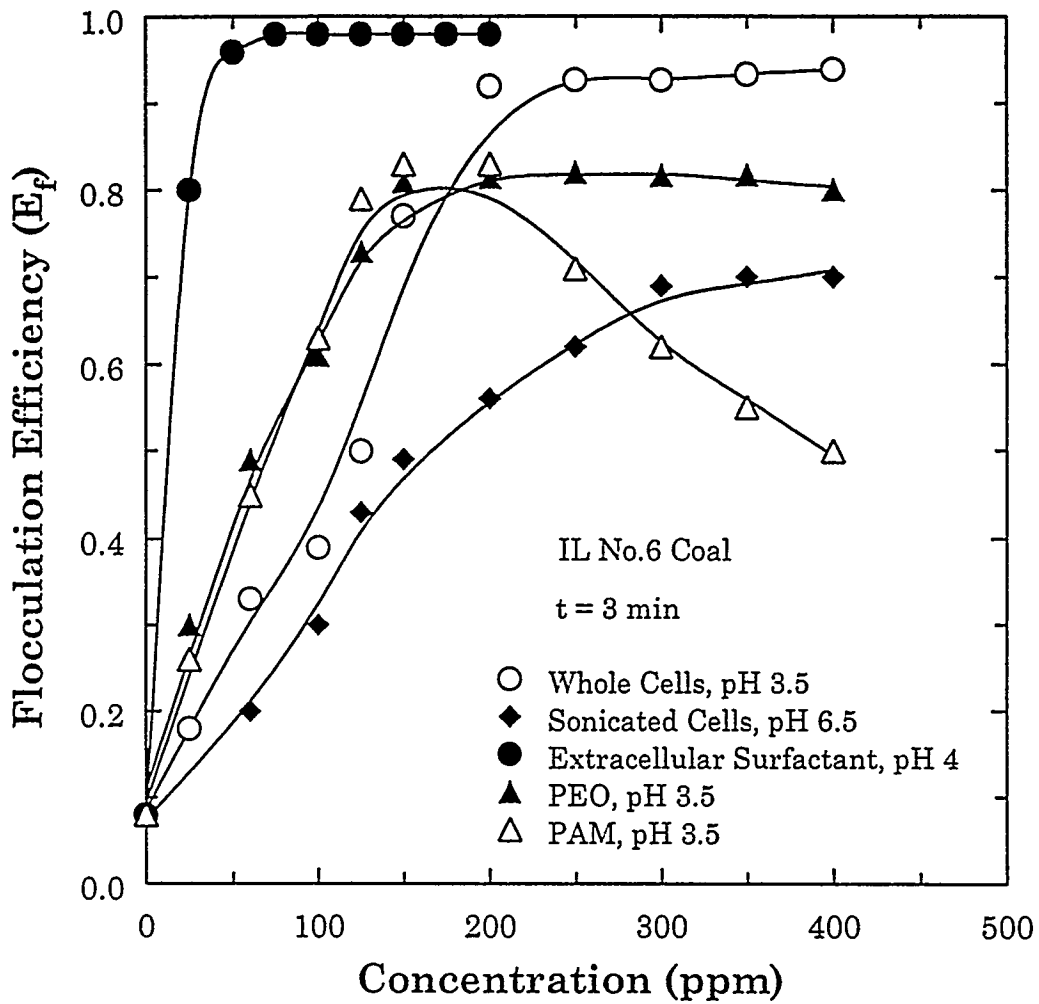


Figure 4.28 The effect of concentration of different flocculants on the flocculation efficiency of IL No.6 coal

Flocculation with PEO and PAM revealed that a maximum  $E_f$  of only about 0.8 was obtained at concentrations of about 150 ppm. Additional increase in concentration of PEO did not affect the flocculation efficiency. However, at higher concentrations of PAM, the flocculation efficiency decreased. This may be attributed to stearic stabilization of particles which leads to the formation of hydrophilic surfaces. On the other hand, flocculation efficiency with the extracellular surfactant and whole cells of *M. phlei* increased and reached a plateau, indicating that the coal surfaces were completely covered with *M. phlei*. These results indicate that there is a fundamental difference in the behavior of synthetic polymeric flocculants when compared to bioflocculants. Unlike the coal flocs obtained with synthetic polymer flocculant (in which coal particles are attached to the back bone of the polymer) the structure of the coal aggregate formed with *M. phlei* is very different. Since the size of coal particle is much larger than the *M. phlei* bacteria cell and each cell is presumed to have multiple sites for attachment with coal particles, coal aggregate formation occurs through *M. phlei* bridges. Thus coal flocs obtained by the bioflocculation using *M. phlei* tend to be spherical. SEM analysis of the coal floc, as presented in Figure 4.29, indicates the spherical nature of the aggregate. Also noteworthy, the dosages of synthetic flocculants used in this study were much higher than that reported in literature. One reason might be that these flocculants work much better in the neutral to slightly alkaline pH range than in the acidic pH range. A pH value of 3.5 was used in this study which might have lead to a higher flocculant

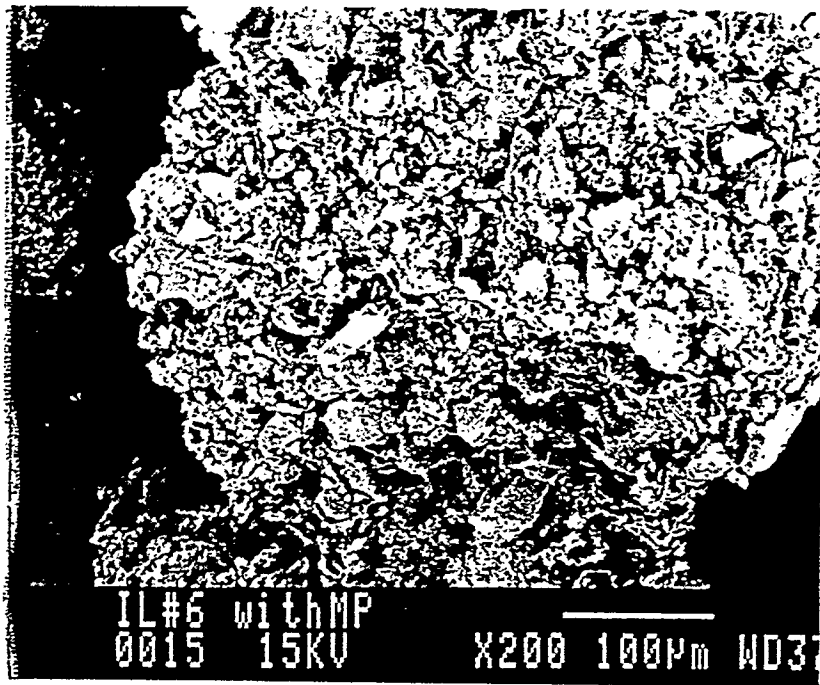


Figure 4.29 Scanning electron microphotograph of coal flocs formed using whole cells of *M. phlei*

requirement.

Figure 4.30 shows the flocculation results of KY No.9 coal. In the presence of extracellular surfactant, a maximum  $E_f$  of about 0.96 was obtained at concentrations greater than 100 ppm, while with whole cells the maximum  $E_f$  obtained was only about 0.8 at concentrations greater than 200 ppm. The flocculation efficiencies remained constant at higher concentration levels. A similar trend was observed with sonicated cells. The maximum  $E_f$  achieved was 0.57 at concentrations greater than 300 ppm. However with PEO and PAM,  $E_f$  increased initially with increase in concentration, but decreased after attaining a maximum. This decrease can again be attributed to stearic stabilization.

#### *4.6.3 Effect of pH on Flocculation Efficiency*

The effect of pH on the flocculation efficiency of coal was studied with whole cells, sonicated cells and extracellular surfactant. The results obtained with IL No.6 coal are presented in Figure 4.31. In all the three cases, flocculation efficiency was found to be highly dependent on pH. In the case of whole cells, a maximum was obtained in the pH range of 3-5. A maximum  $E_f$  of about 0.97 was achieved in this pH range. Also, flocculation efficiencies in the acidic pH range were, in general, higher than those obtained in the alkaline pH range. Sonicated cells also showed a maximum in flocculation efficiency,

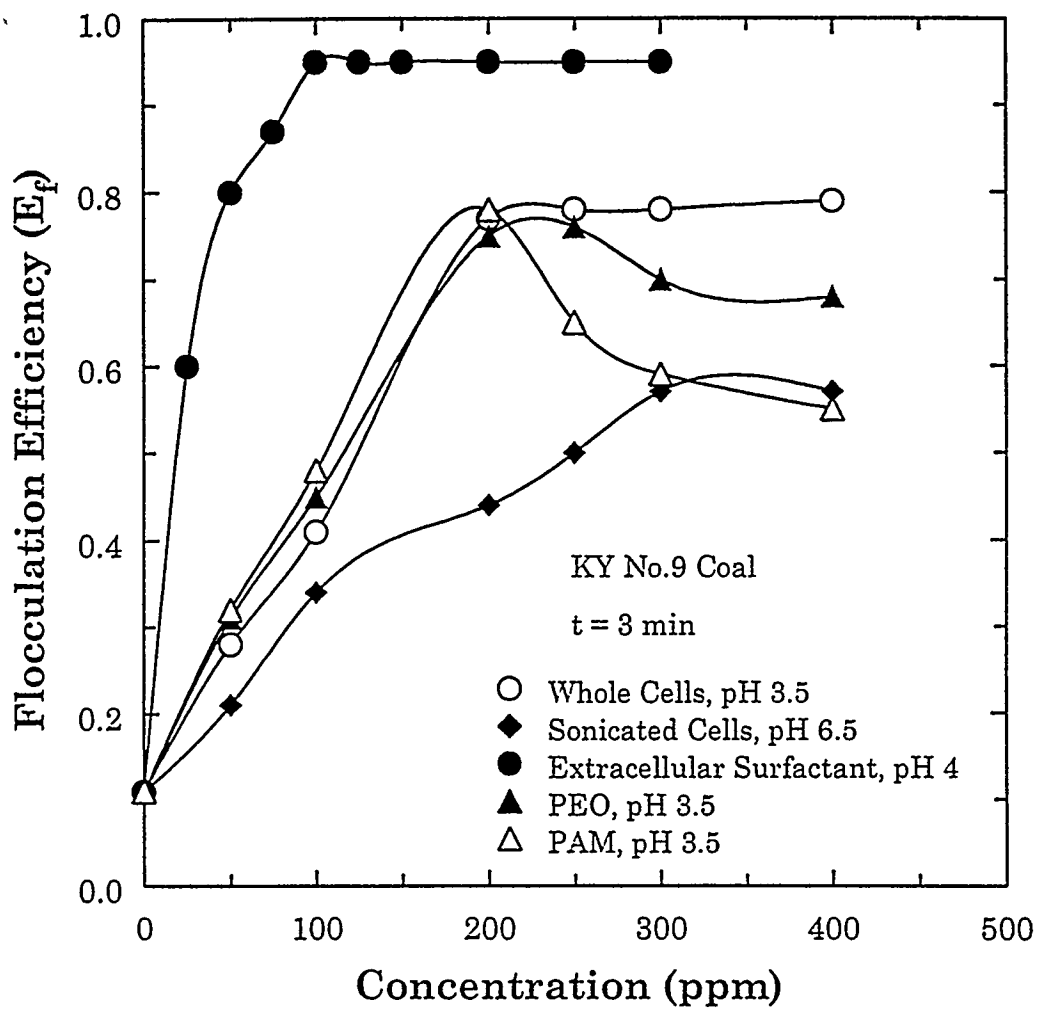


Figure 4.30 Effect of concentration of different flocculants on the flocculation efficiency of KY No.9 coal

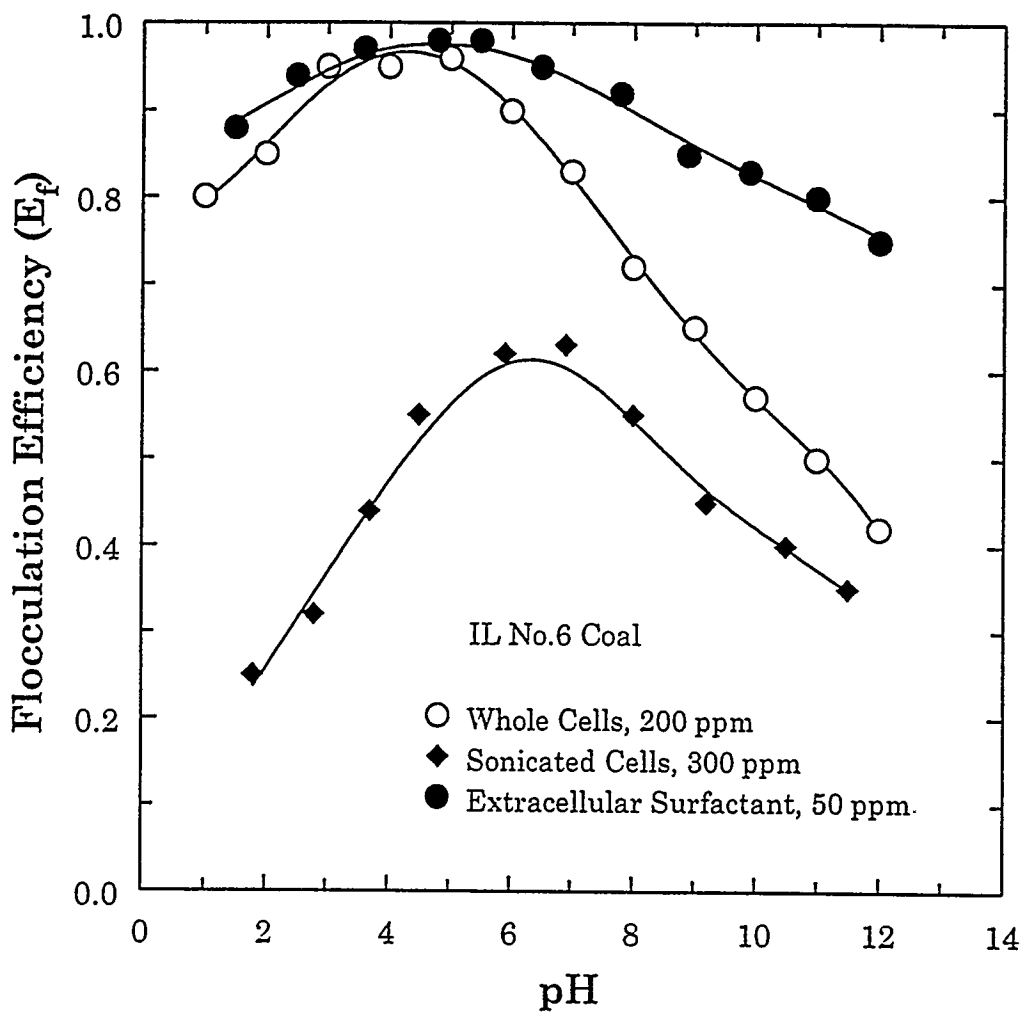


Figure 4.31 The effect of different flocculants on the flocculation efficiency of IL No.6 coal as a function of pH



although the maximum was only about 0.6 and was observed around neutral pH. In this pH range, the surface of sonicated cells has zero charge and this probably facilitates to some extent the adhesion of sonicated cells onto coal surfaces. However, flocculation with extracellular surfactant showed that flocculation efficiencies as high as 0.98 could be obtained at much lower concentrations and over a wider pH range. Also, the efficiencies achieved over the entire pH range studied were superior to those obtained with whole cells or sonicated cells. These results suggest that the extracellular surfactant can be used as an effective flocculant for coal.

Similar studies were also conducted with KY No.9 coal and the results are shown in Figure 4.32. Similar trends to those of IL No.6 coal were noticed with KY No.9 coal also. However the maximum flocculation efficiency with whole cells was considerably less, which might be attributed to the lower hydrophobicity of KY No.9 coal. Extracellular surfactant showed very high flocculation efficiencies on the order of 0.95, but at higher concentrations (100 ppm).

The above results clearly showed that the extracellular surfactant acted as a much better flocculant for coal when compared with whole cells and that this was attainable at lower concentrations. Also, extracellular surfactant showed excellent flocculation efficiencies over a wider pH range as compared to

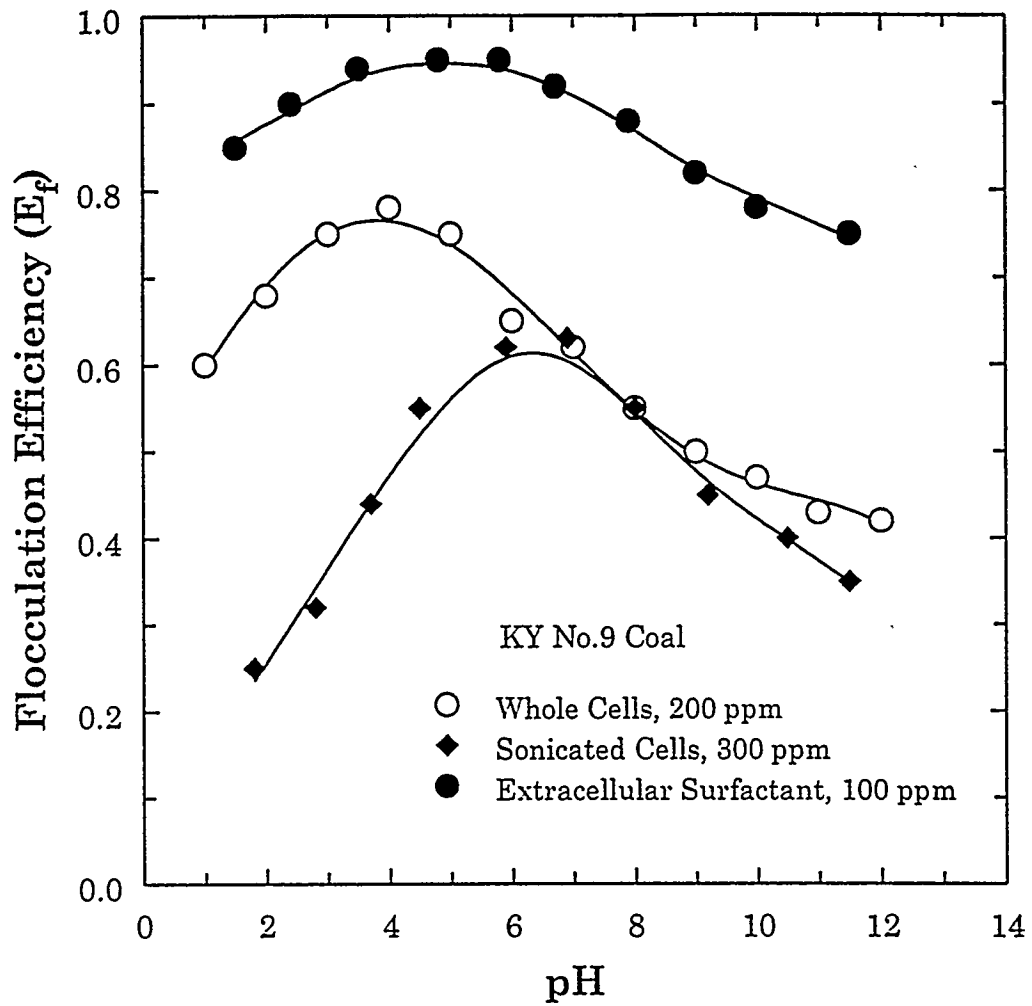


Figure 4.32 The effect of different flocculants on the flocculation efficiency of KY No.9 coal as a function of pH

whole cells. The above results demonstrate that flocculation of coal with *M. phlei* and the extracellular surfactant derived from it occurs through a combination of electrostatic and hydrophobic interactions.

## 4.7 Floc-Separation

### 4.7.1 Settling

Despite successful flocculation of coal particles, it was observed that an efficient separation of the combustibles from the mineral matter was not accomplished neither by whole cells nor by extracellular surfactant. Analysis of the separated flocs showed no significant difference in the amounts of ash and sulfur contents from that of the feed. A typical example is shown in Table 4.3.

Table 4.3 Analysis of IL No.6 Coal Before and After Flocculation with Whole Cells of *M. phlei*

	Ash, %	Total Sulfur, %
Before Flocculation	15.66	4.34
After Flocculation	14.91	3.91

The inefficiency in separation is not due to the lack of specificity on the part of

*M. phlei* or the extracellular surfactant in the flocculation of coal particles. This may be due to the rapid flocculation of coal particles which in turn leads to formation of large flocs. These flocs tend to settle down very quickly and apparently settle at the same velocity as that of the dense pyrite particles of pyrite. Single mineral tests were conducted with IL No.6 coal and coal-pyrite and the results are presented in Figure 4.33. In the absence of *M. phlei*, about 75% of the coal settled in about 5 minutes. However, in the presence of *M. phlei* the weight percent solids settled is about 92% in about 2 minutes. On the other hand, the amount of coal-pyrite settled was much higher due to the higher density of pyrite. The addition of *M. phlei* enhanced the settling rate of pyrite, although no massive flocs were observed. Similar settling velocities of coal-flocs and coal-pyrite could be one reason for the inefficient separation of pyrite and ash from coal. In addition, it is also quite possible that pyrite particles are entrapped in the coal flocs and settle down with them. To overcome this problem and to separate the combustibles from the pyrite and other minerals, the flocculated coal aggregates were subjected to a column flotation process.

#### 4.7.2 Column Flotation

After flocculation with various flocculants, the flocs were transferred to the column flotation cell. No pH adjustments were made and only MIBC as frother was added. Nitrogen gas was used for flotation, which was carried out

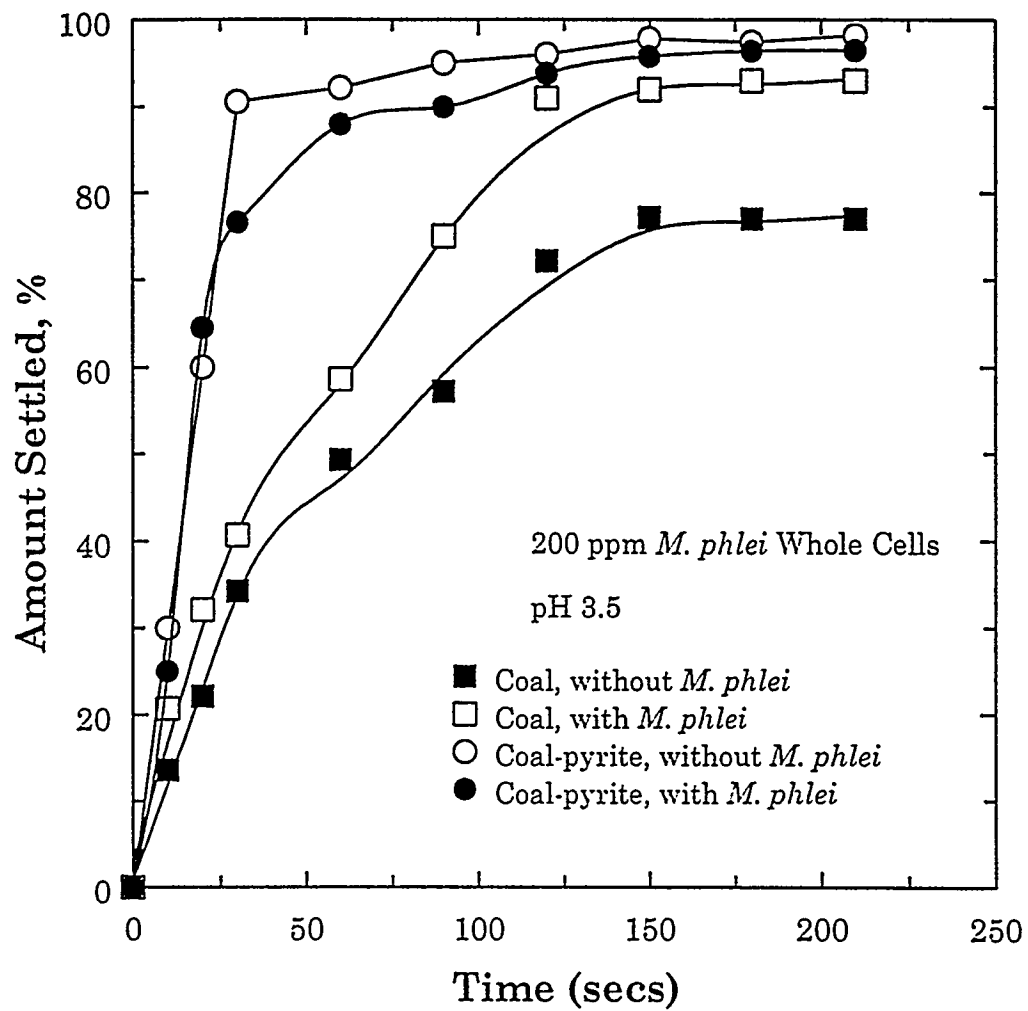


Figure 4.33 The amount of coal and coal-pyrite settled in the presence and absence of *M. phlei* whole cells as a function of time

for 5 minutes. Frother dosage and gas flow rate are the two major parameters that influence the flotation characteristics of coal. Thus the effect of these two parameters on the combustible recovery and pyrite and ash rejection were investigated to determine the optimum value. The effect of flow rate of nitrogen on the recovery and pyrite and ash rejection is shown in Figure 4.34. It can be seen that initially recovery increased with gas flow rate. However, ash and pyritic sulfur rejection decreased at flow rates greater than 0.6 L/min. Maximum pyritic sulfur rejection (ca. 70%) and ash rejection (ca. 45%) and combustible recovery of about 80% were obtained at a gas flow rate of 0.6 L/min. Although a higher recovery of coal was obtained at higher flow rates, more ash and pyritic sulfur started collecting in the concentrate thus decreasing the quality of coal.

The effect of frother (MIBC) dosage on the flotation characteristics of flocculated coal was also studied and the results are presented in Figure 4.35. The gas flow rate was maintained at 0.6 L/min. The combustible recovery increased with an increase in dosage of MIBC. However, pyritic sulfur and ash rejection increased first and then decreased after attaining a maximum. The best combination of maximum combustible recovery, pyritic sulfur rejection and ash rejection were obtained at a frother dosage of 0.7 kg/ton. Based on these studies, a gas flow rate of 0.6 L/min and a frother dosage of 0.7 kg/ton were used for further experiments.

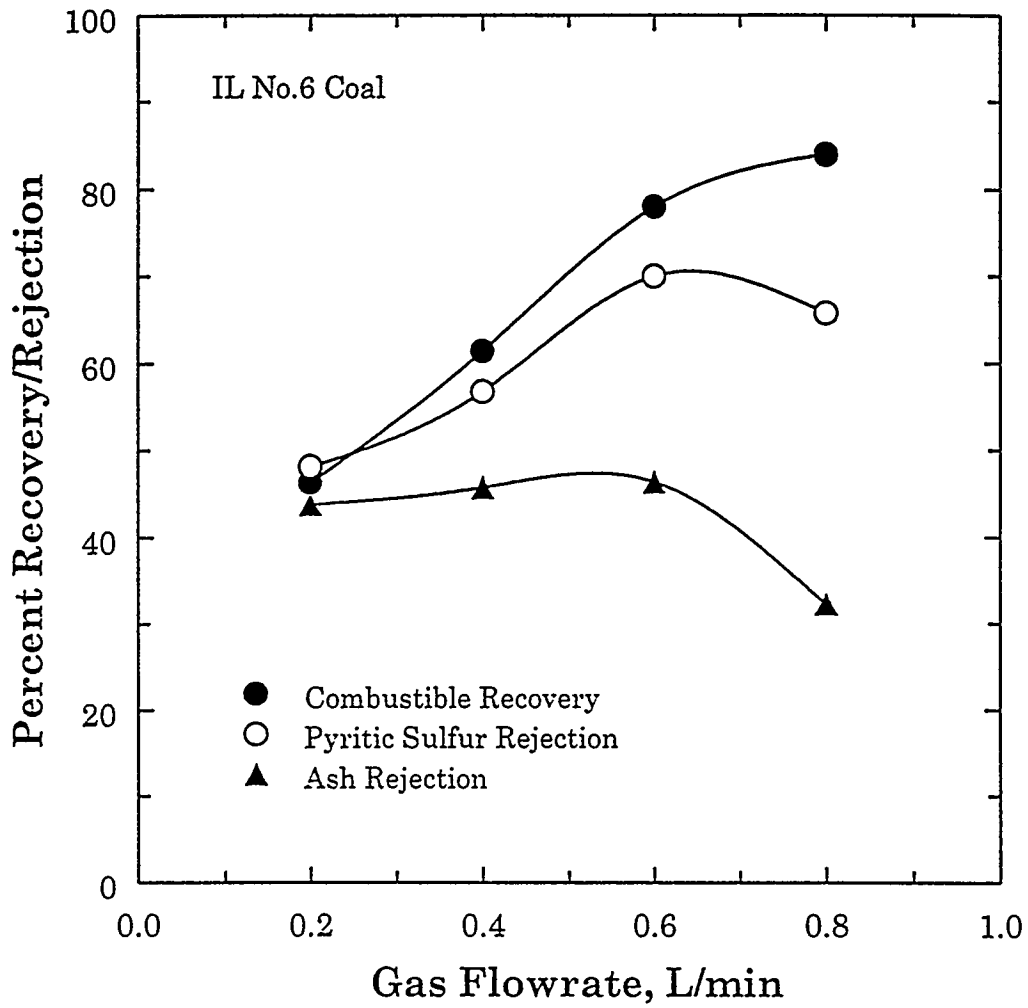


Figure 4.34 The effect of gas (nitrogen) flow rate on the combustible recovery and pyritic sulfur/ash rejection for IL No.6 Coal

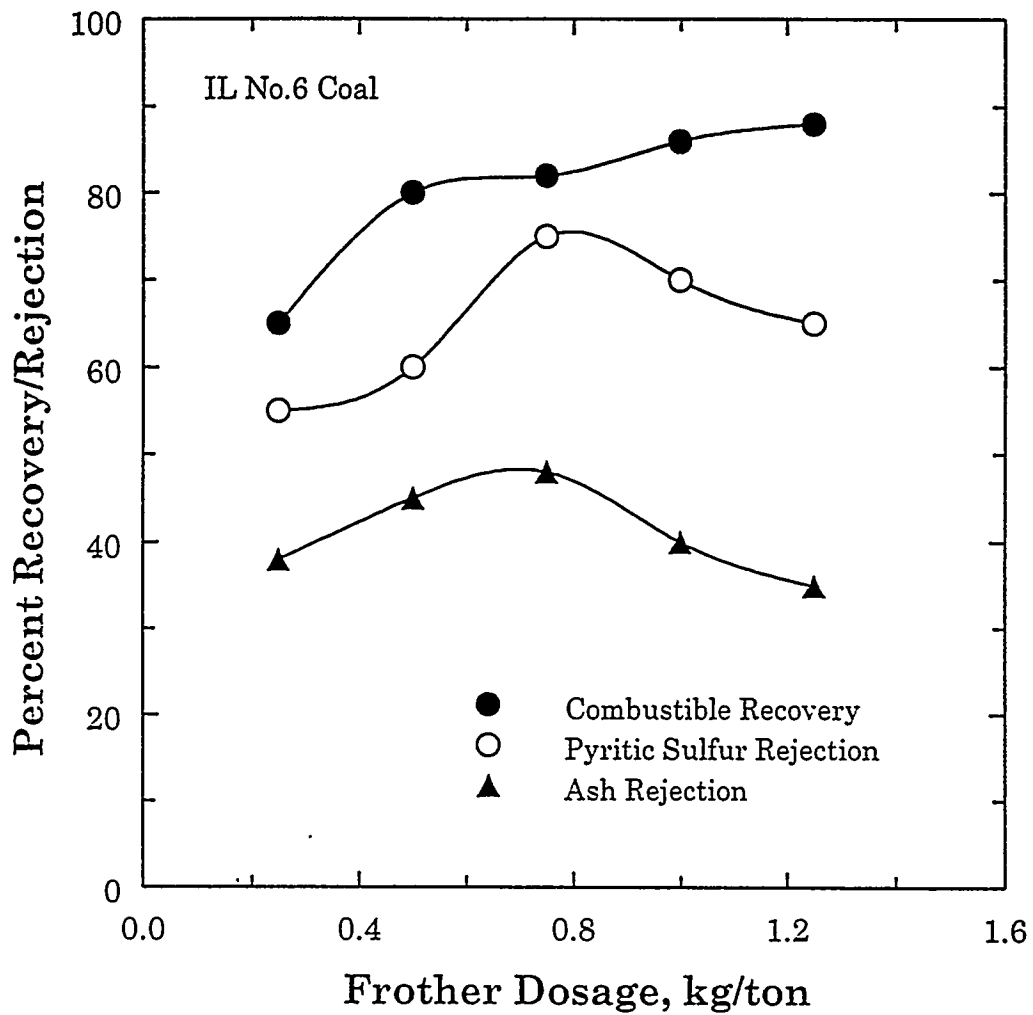


Figure 4.35 The effect of frother (MIBC) dosage on the combustible recovery and pyritic sulfur/ash rejection for IL No.6 Coal



Initial experiments were conducted with coal flocculated with different flocculants. Both *M. phlei* and synthetic polymeric flocculants were used. Also, for comparison purposes, the effect of kerosene and frother on the floatability of coal was evaluated. The flotation results for IL No.6 coal at pH 3.6 with different reagents is shown in Table 4.4. With frother alone, the combustible recovery of coal is about 50% and the pyritic sulfur rejection is 45%. In the presence of an oily promoter like kerosene, the combustible recovery and pyritic sulfur rejected increased substantially to 76% and 56% respectively. When coal flocculated with extracellular surfactant of *M. phlei* was floated, the amount of combustibles increased to 91% while the pyritic sulfur rejection increased to 78%. A similar trend was noticed with whole cells. Adhesion of *M. phlei* and extracellular surfactant increased the surface hydrophobicity of coal which probably enhanced the floatability of coal. While the combustible recovery increased by 15% when compared with kerosene, the pyritic sulfur rejection increased by 22%. This meant that the flocculation of coal with *M. phlei* followed by flotation produced a substantially higher quality product than flotation with kerosene alone.

When coal flocculated with sonicated cells of *M. phlei* was floated, only 60% of the combustibles were recovered along with a sulfur rejection of 50%, which is due to the decreased hydrophobicity of *M. phlei* cells after sonication.

Table 4.4. Flotation results of IL No.6 Coal at pH 3.6 (Gas flowrate 0.6 l/min and frother dosage 0.7 kg/ton)

Reagents Used	Combustible Recovery (%)	Pyritic Sulfur Rejection (%)	Ash Rejection (%)
Frother Only	50	45	44
Frother + Kerosene	76	56	46
Frother + Extracellular Surfactant	91	78	59
Frother + Whole Cells	82	68	48
Frother + Sonicated Cells	60	50	45
Frother + PEO	28	35	40
Frother + PAM	25	33	42

However, when flotation was carried out after flocculation with synthetic flocculants such as PEO and PAM, the combustible recovery was only about 25-28% with a sulfur rejection of 33-35%. This is because of the hydrophilic nature of synthetic polymeric flocculants which also render the coal surface hydrophilic when adsorbed.

Similar studies were conducted with KY No.9 coal, which is less hydrophobic compared to IL No.6 coal, and the results are shown in Table 4.5. As can be seen, the flotation results are very similar to those of IL No.6 coal in the presence of various flocculants and kerosene. The best results were obtained through flocculation followed by flotation with extracellular surfactant and *M. phlei* whole cells. However, the combustible recovery is lower compared to that of IL No.6 coal. This might be due to KY No.9 coal being less hydrophobic compared to IL No.6 coal. These tests clearly indicate that *M. phlei* not only acts as an effective flocculant, but also acts as a good flotation collector for coal. It should however be noted that pH can influence the flotation recovery and pyrite and ash rejection.

The effect of pH on flotation recovery in the presence of different flocculants was investigated for both coal samples. Only whole cells and extracellular surfactant were used for studying the effect of pH on the flotation of flocs. Kerosene was used for comparison purposes.

Table 4.5. Flotation results of KY No.9 Coal at pH 3.9 (Gas flowrate 0.6 l/min and frother dosage 0.7 kg/ton)

Reagents Used	Combustible Recovery (%)	Pyritic Sulfur Rejection (%)	Ash Rejection (%)
Frother Only	45	38	42
Frother + Kerosene	60	50	44
Frother + Extracellular Surfactant	80	70	61
Frother + Whole Cells	70	63	55
Frother + Sonicated Cells	48	40	40
Frother + PEO	20	30	35
Frother + PAM	18	31	38

The effect of pH on the combustible recovery, pyritic sulfur rejection and ash rejection for IL No.6 coal are shown in Figures 4.36 to 4.38 respectively. In the case of kerosene, combustible recovery varied with pH exhibiting a maximum in the neutral pH range. This is consistent with values reported in literature (Groppo, 1986). A maximum combustible recovery of about 72% was obtained at pH 6.1. In the presence of whole cells, combustible recovery increased in the acidic pH range, and a maximum of 80% recovery was observed at pH 4. Further increase in pH decreased the recovery to values comparable with those obtained with kerosene. However, in the case of extracellular surfactant, the combustible recovery increased over the entire pH range. Recoveries on the order of 85-92% were obtained in the pH range of 2-6. At pH values greater than 6, a slight decrease in recovery was obtained. One of the reasons for the higher recoveries in the presence of extracellular surfactant over the entire pH range might be due to increased hydrophobicity. Also, better flotation kinetics in the presence of extracellular surfactant could be partially responsible for the greater recoveries.

In the case of pyritic sulfur rejection, the best results were obtained with the extracellular surfactant. A maximum rejection of about 75% was observed at pH 4. At higher pH values, the pyritic sulfur rejection dropped in all three cases. However, ash rejection remained constant with change in pH. In the case of extracellular surfactant, ash rejection remained essentially

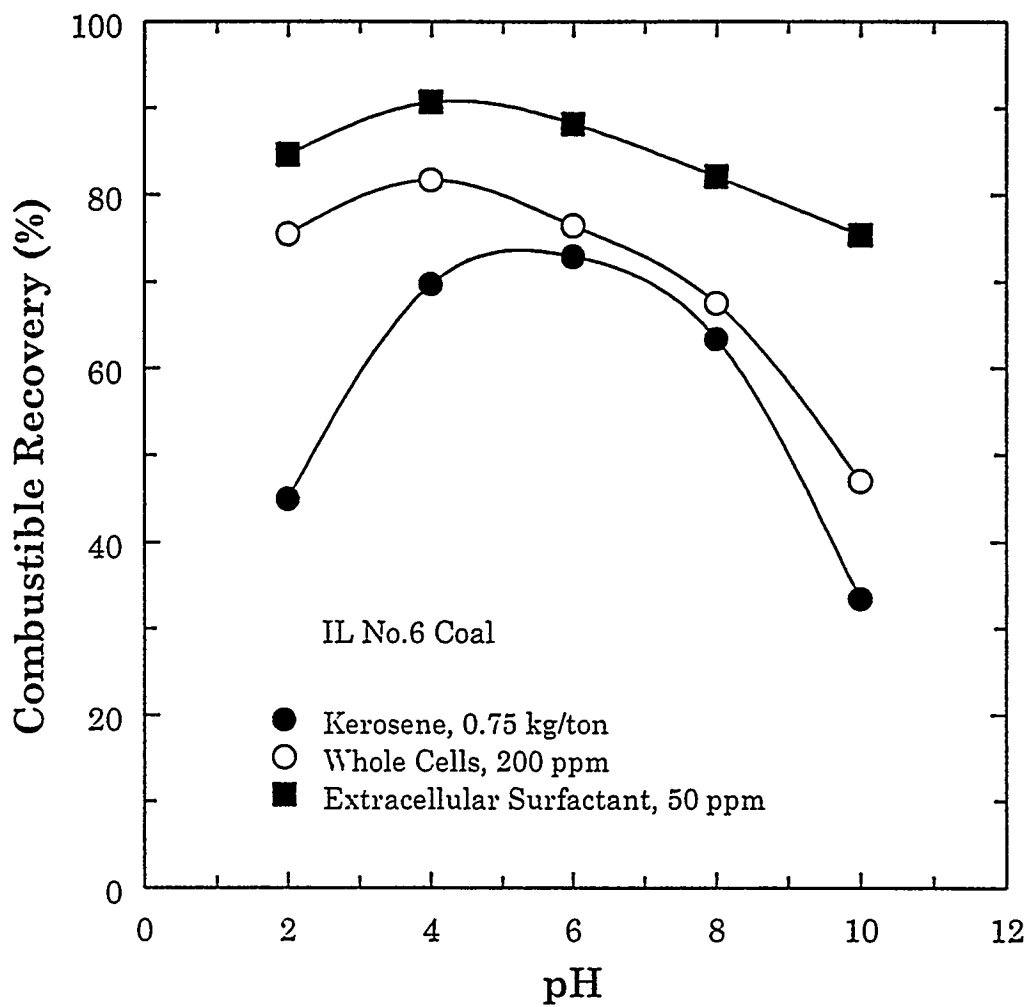


Figure 4.36 Combustible recovery for IL No.6 Coal in the presence of different reagents as a function of pH

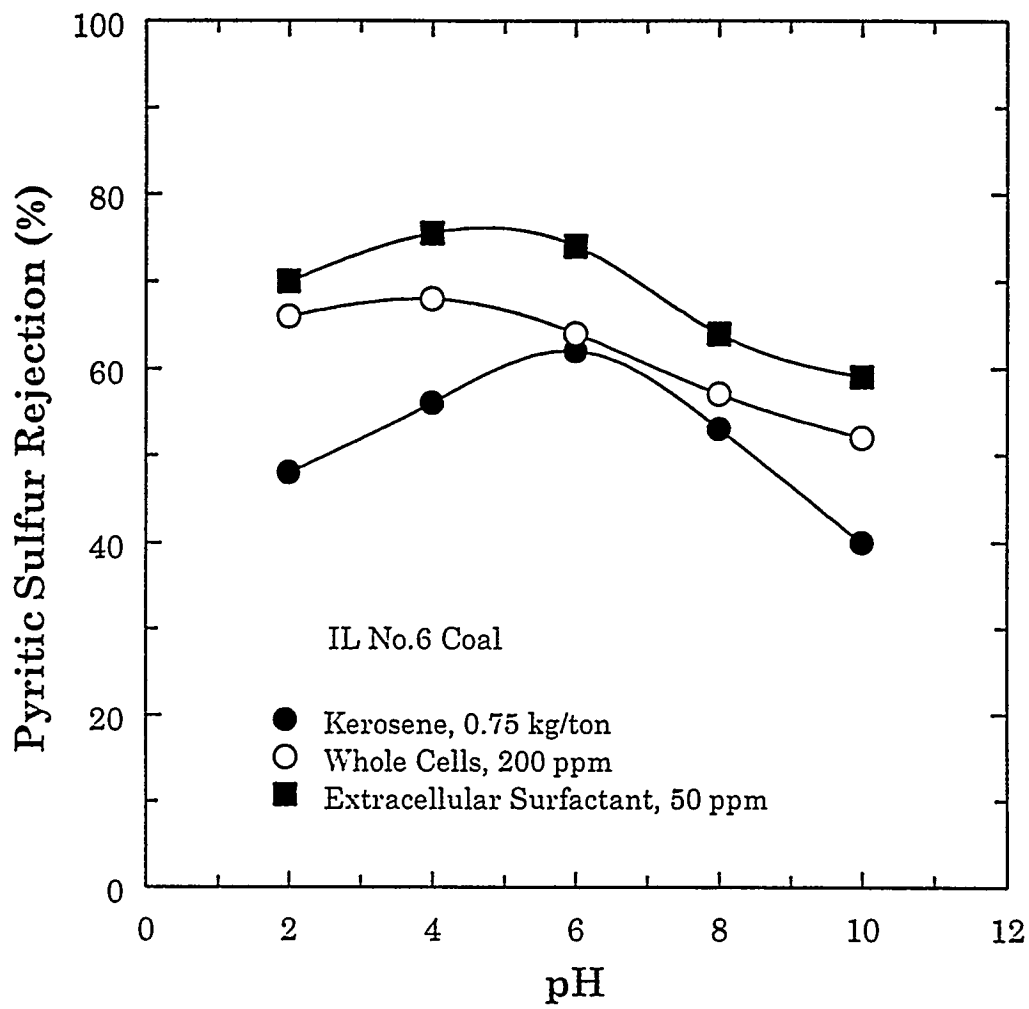


Figure 4.37 Pyritic sulfur rejection for IL No.6 Coal in the presence of different reagents as a function of pH

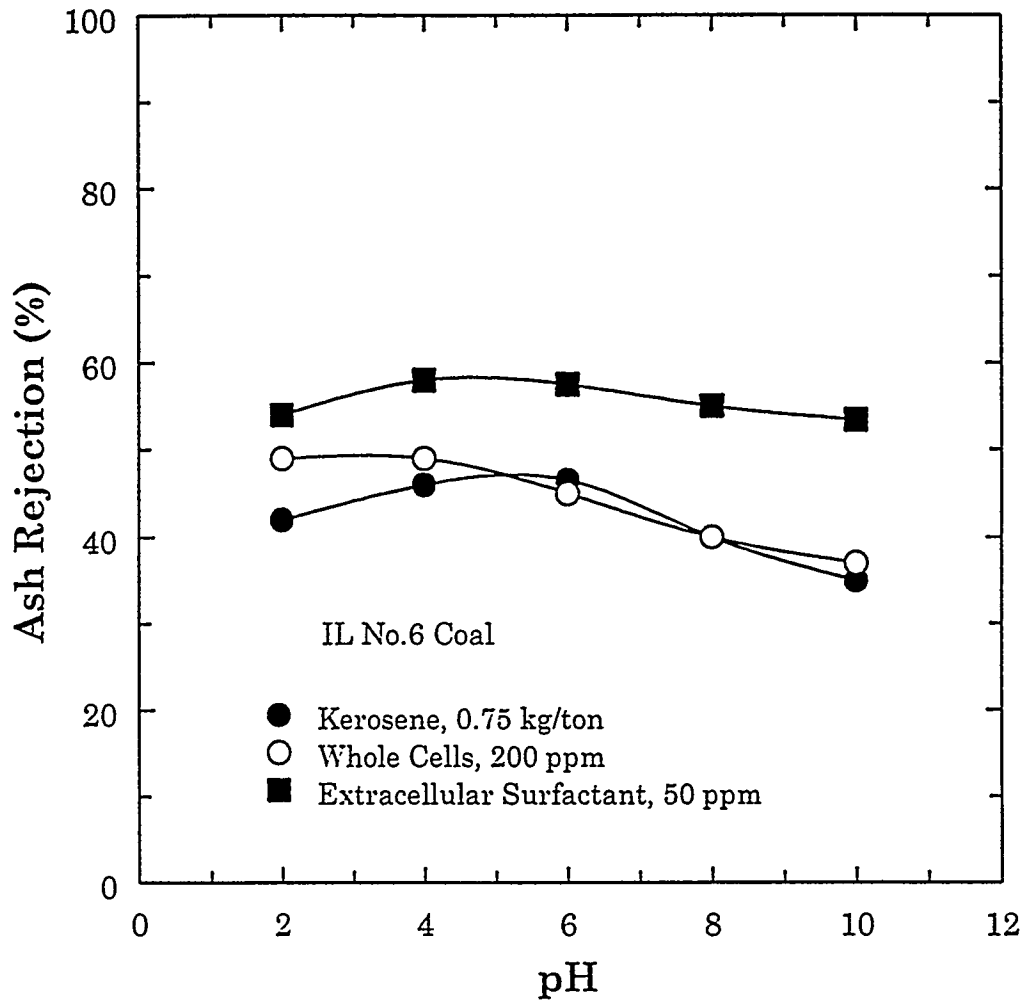


Figure 4.38 Ash rejection for IL No.6 Coal in the presence of different reagents as a function of pH



constant at around 56%. With whole cells and kerosene, ash rejection varied in the range of 40 - 50%.

The effect of pH on the combustible recovery and rejection of pyrite and ash were conducted with KY No.9 coal, and the results are presented in Figures 4.39-4.41. The results showed a trend similar to that of IL No.6 coal although the magnitudes were different. The recoveries in the case of KY No.9 coal were slightly less compared to IL No.6 coal, and this could be due to the lower hydrophobicity of the coal. Also, it was shown in the adhesion experiments that less bacteria adheres to the surface of KY No.9 coal than onto IL No.6 coal which could lead to lower recoveries. The pyritic sulfur and ash rejection were also similar in comparison with IL No.6 coal.

## 4.8 Interaction Energy Calculations

### 4.8.1 *Columbic Interaction Energy*

From the above studies, it can be seen that flocculation and flotation by *M. phlei* and the extracellular surfactant yielded better results with IL No.6 when compared to KY No.9 coal. Also, *M. phlei* showed a preference for coal in comparison with other associated minerals. The surface charge and the surface hydrophobicity of both the bacterium and the solid surface seem to play an

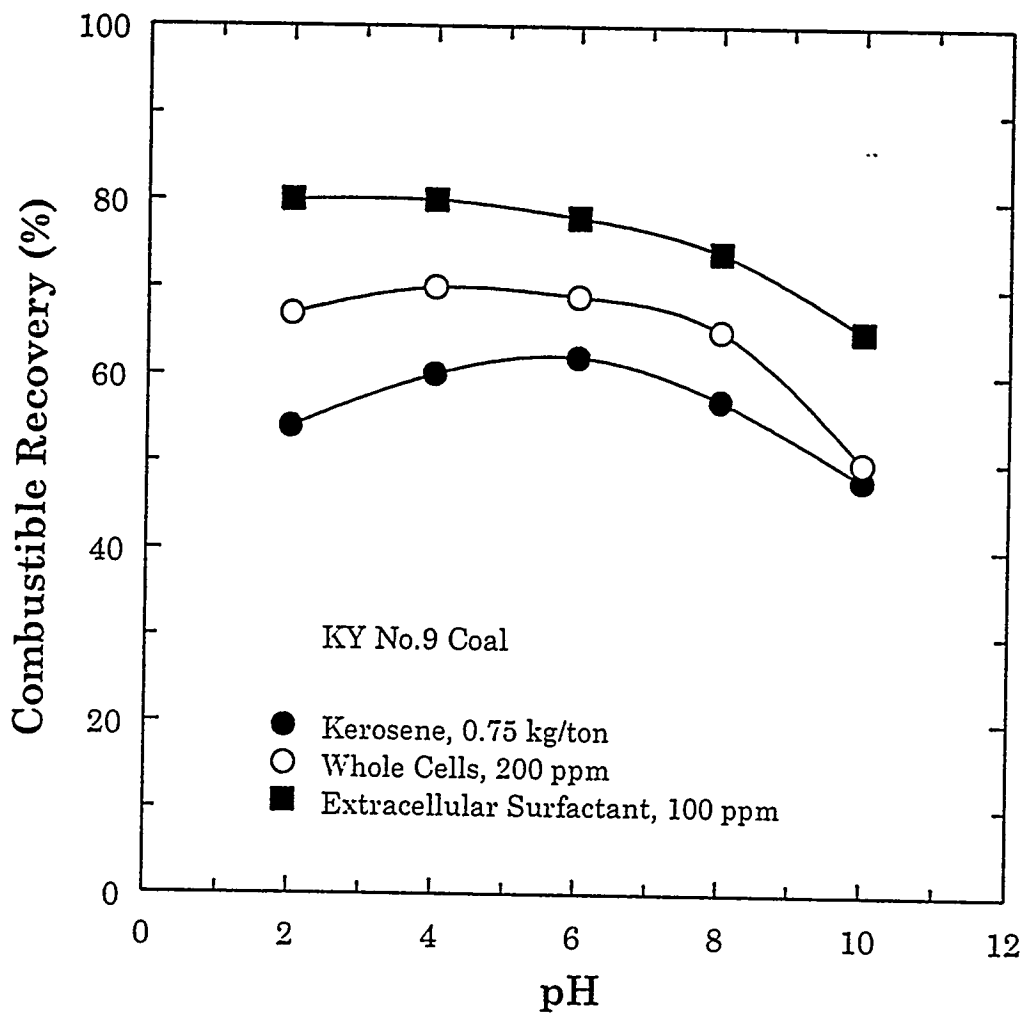


Figure 4.39 Combustible recovery for KY No.9 Coal in the presence of different reagents as a function of pH

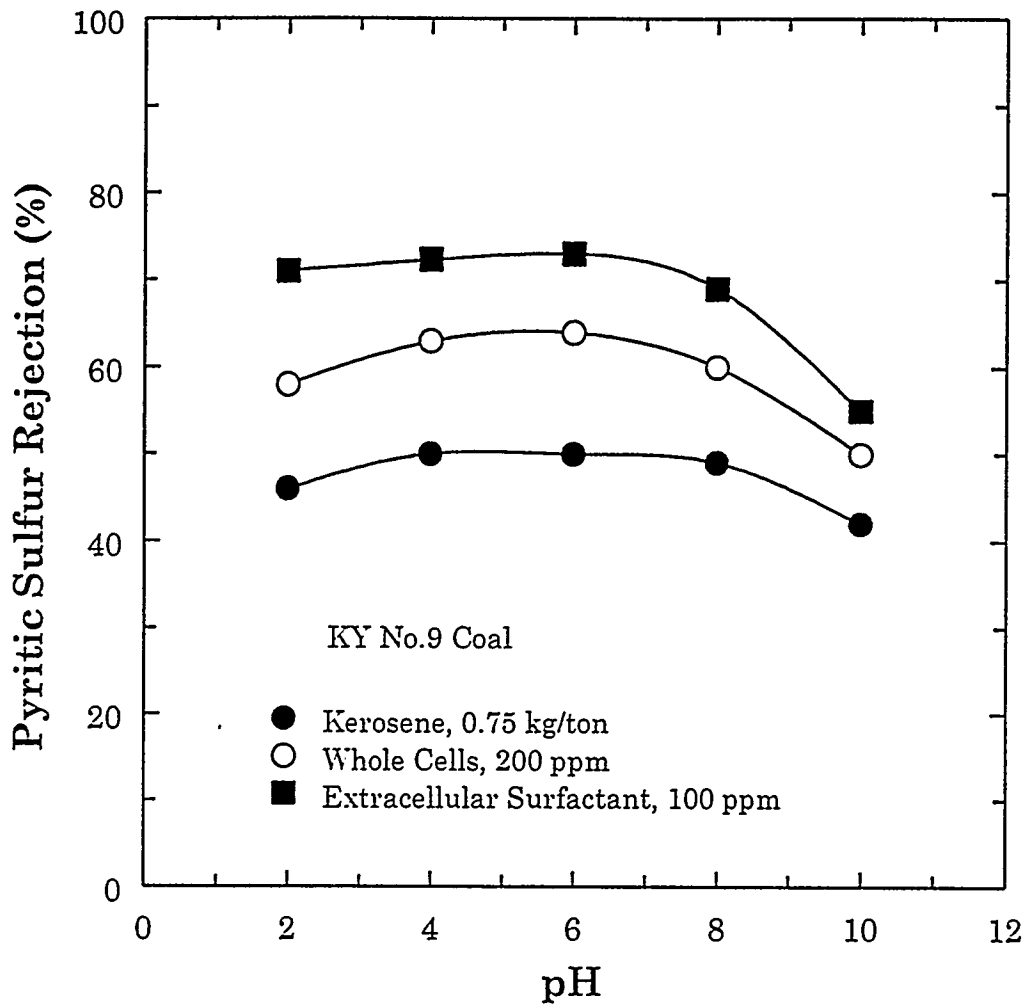


Figure 4.40 Pyritic sulfur rejection for KY No.9 Coal in the presence of different reagents as a function of pH

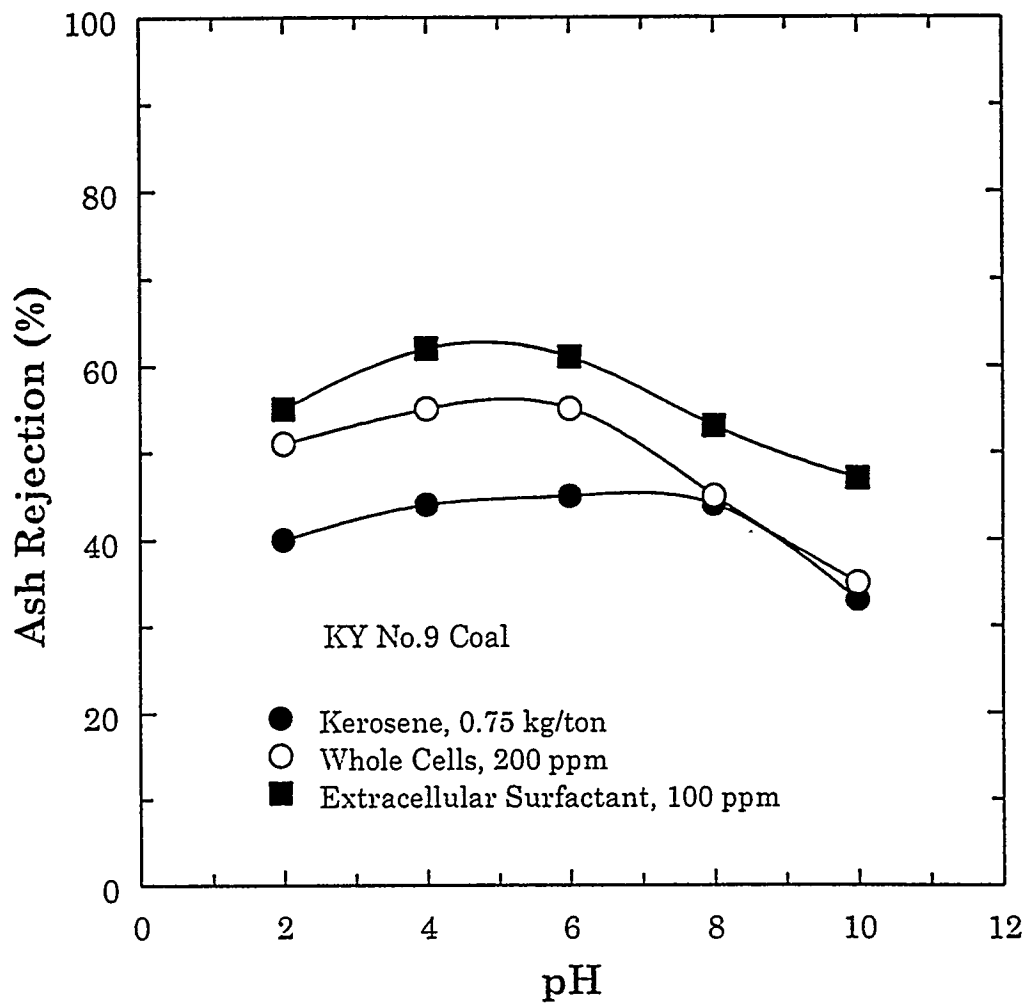


Figure 4.41 Ash rejection for KY No.9 Coal in the presence of different reagents as a function of pH

important role in controlling the adhesion of bacterium. To understand this behavior and to find an explanation for the same, DLVO calculations were performed using the extended DLVO theory.

The theoretical analysis of the interactions between colloidal particles was originally developed by Derjaguin and Landau (1941) and Verwey and Overbeek (1946) in terms of repulsive and attractive potential energies of interaction (more commonly known as the DLVO theory).

The total interaction energy ( $V_T$ ) is calculated from the following equation:

$$V_T = V_R + V_A \quad (4.1)$$

where,

$V_R$  = repulsive potential energy due to the formation of electrical double layer around particles and

$V_A$  = van der Waals attractive potential energy

The electrostatic repulsive force between mineral and *M. phlei* particles can be expressed by the following equation :

$$V_R = \frac{(\epsilon a_1 a_2)}{4(a_1 + a_2)} (\psi_1^2 + \psi_2^2) \left[ \frac{2\psi_1\psi_2}{(\psi_1^2 + \psi_2^2)} \ln \frac{(1 + \exp(-\kappa H_0))}{(1 - \exp(-\kappa H_0))} + \ln(1 - \exp(-2\kappa H_0)) \right] \quad (4.2)$$

where,

$\epsilon$  is the dielectric constant of the aqueous medium =  $8.84 \times 10^{-10}$  ergs/mV<sup>2</sup>.cm

$a_1$  is the diameter of coal/mineral particle = 30  $\mu$ m

$a_2$  is the diameter of *M. phlei* = 1  $\mu$ m

$\psi_1$  and  $\psi_2$  are surface potentials of coal/mineral and *M. phlei* respectively

$H_0$  is the minimum separation distance between particle and *M. phlei* surface

$\kappa$  is the Debye-Huckel double layer thickness

Considering  $a_1 \gg a_2$ ,  $a_1 a_2 / a_1 + a_2$  can be approximated as  $a_2$  and Equation 4.2 can be reduced to

$$V_R = \frac{\epsilon a_2}{4} (\psi_1^2 + \psi_2^2) \left[ \frac{2\psi_1\psi_2}{(\psi_1^2 + \psi_2^2)} \ln \frac{(1 + \exp(-\kappa H_0))}{(1 - \exp(-\kappa H_0))} \right] + \ln(1 - \exp(-2\kappa H_0)) \quad (4.3)$$

The London - van der Waals attractive force  $V_A$  is given by :

$$V_A = - \frac{(a_1 a_2) A}{6 (a_1 + a_2) H_0} \quad (4.4)$$

where  $A$  is the composite Hamaker constant.

Considering the diameter of a coal/mineral particle to be much greater

than that of *M. phlei*, Equation 4.4 is simplified to :

$$V_A = - \frac{\alpha_2 A}{6 H_0} \quad (4.5)$$

The most important parameters determining the van der Waals interaction are the Hamaker constant ( $A$ ), which is a material property, the distance ( $H_0$ ) between the bacterium and coal/mineral, and the geometry of the particles.

The composite Hamaker constant,  $A_{132}$ , for coal/mineral-water-*M. phlei* system was evaluated using the following approximations:

$$A_{32} = [\sqrt{A_{33}} - \sqrt{A_{22}}]^2 \quad (4.6)$$

$$A_{31} = [\sqrt{A_{33}} - \sqrt{A_{11}}]^2 \quad (4.7)$$

$$A_{21} = [\sqrt{A_{22}} - \sqrt{A_{11}}]^2 \quad (4.8)$$

$$A_{132} = A_{21} + A_{33} - A_{31} - A_{32} \quad (4.9)$$

where 1 represents coal/mineral, 2 represents *M. phlei* and 3 represents water. The Hamaker constant for water ( $A_{33}$ ) was selected from Viser (1972) as  $4.38 \times 10^{-13}$  ergs. The Hamaker constant for *M. phlei* has been estimated using the Fowkes equation (1967) as given below.

$$A_{22} = 6 \pi r_{..}^2 \gamma_s^d \quad (4.10)$$

where  $r_{..}$  represents the intermolecular distance and  $\gamma_s^d$  the dispersion component of surface free energy of a solid. According to Fowkes, for water and systems with volume elements such as oxide ions, metal atoms,  $\text{CH}_2$  and  $\text{CH}$  groups which have nearly the same size, the value of  $6\pi r_{..}^2 = 1.44 \times 10^{-14}$  can be used. The  $\gamma_s^d$  value for *M. phlei* has been estimated by Chen (1992) to be 43.6 dyne/cm. Using these values, the Hamaker constant for *M. phlei* was estimated to be about  $6.26 \times 10^{-13}$  ergs. The value for  $6\pi r_{..}^2$  can be assumed to be valid even in the case of sonicated cells, since the cell wall is made up of mainly lipids and proteins and contains  $\text{CH}_2$  and  $\text{CH}$  groups. However, since the contact angle of sonicated cells was about  $43^\circ$ , the  $\gamma_s^d$  value was estimated to be 62.5 dyne/cm, and the Hamaker constant for sonicated cells was found to be  $9 \times 10^{-13}$  ergs.

The values of  $\gamma_s^d$  for coal and coal-pyrite were taken from Good et al. (1990) and Raichur (1992). It has been very well established that the value of  $\gamma_s^d$  for coal is independent of coal rank. Therefore, the same value has been used for both coal samples. The value for quartz was taken from Fowkes (1967). Based on these values the following values of  $A_{11}$  were determined and are shown in Table 4.6.

For the above calculations, the separation distance,  $H_0$  was varied from 1



to 100 Å and the various surface potentials at different pH values are listed below in Table 4.7. Values of zeta potential were used in place of surface potentials for the total interaction energy calculations. This procedure is justified if it is considered that the plane of shear approximately coincides with the stern plane and that this layer is tightly bound to, and may be considered a part of, the surface.

The value of  $\kappa$  was calculated using the well known expression

$$\frac{1}{\kappa} = \frac{4.3}{\sqrt{2 I}} \text{ \AA} \quad (4.11)$$

where  $I$  is the ionic strength of the solution. This equation is valid when water is used as solvent at 25°C. The ionic strength was calculated using the equation

$$I = \frac{1}{2} \sum [ C_i Z_i^2 ] \quad (4.12)$$

where  $C_i$  is the concentration of ionic species and  $Z_i$  is the charge of the ionic species. In this case 0.01M NaNO<sub>3</sub> was used as electrolyte. Using this value, the value of  $I$  and the value of  $\kappa$  were calculated and found to be 0.01 and 0.03289/Å respectively.

The total interaction energy was calculated as a function of separation distance  $H_0$  and as a function of pH. The separation distance was varied from

Table 4.6. The  $\gamma_s^d$  values and Hamaker constants ( $A_{11}$ ) for different minerals

Mineral	$\gamma_s^d$ (dyne/cm)	$A_{11}$ (ergs)
IL No.6 Coal	36	$5.18 \times 10^{-13}$
KY No.9 Coal	36	$5.18 \times 10^{-13}$
Coal pyrite	58.5	$8.35 \times 10^{-13}$
Quartz	123	$1.77 \times 10^{-13}$

Table 4.7 Zeta potential values of different samples (in mV) used for DLVO calculations

pH	Whole Cells	Ruptured Cells	IL No.6 Coal	KY No.9 Coal	ICPY	Quartz
2	-2	28	28	16	31	-6
3	-8	23	23	13	24	-20
4	-16	19	17	10	20	-26
6	-28	12	-4	-7	1	-33
8	-38	-13	-22	-21	-21	-36
10	-46	-17	-34	-31	-28	-39

1 to 100 Å, while the pH was varied from 2 to 10. The interaction energy between mineral particles/whole cells and mineral particles/sonicated cells was calculated.

The total interaction energy for IL No.6 coal as a function of separation distance is shown in Figure 4.42. As can be seen with an increase in separation distance, the interaction energy becomes less negative and approaches zero at distances greater than 40 Å. Also, as the pH increases, the interaction energy becomes positive, implying that repulsion becomes predominant. A similar behavior was observed with other minerals. Figure 4.43 shows the effect of pH on the total interaction energy for IL No.6 coal. As pH is increased, the total interaction energy becomes more negative up to pH 4. Above pH 4, the interaction energy becomes less negative. At pH 4, a minimum in interaction energy is observed and this corresponds to the maximum in adhesion and flocculation efficiency. Also, it is clear from Figure 4.43 that as  $H_0$  increases, the interaction energy increases, thereby decreasing adhesion. Similar calculations were also performed for KY No.9 coal, coal-pyrite, and quartz.

Figure 4.44 compares the interaction energies of all the samples with whole cells of *M. phlei* as a function of pH. KY No.9 coal exhibited a trend similar to IL No.6 coal. However, coal-pyrite also had a minimum at pH 4 and

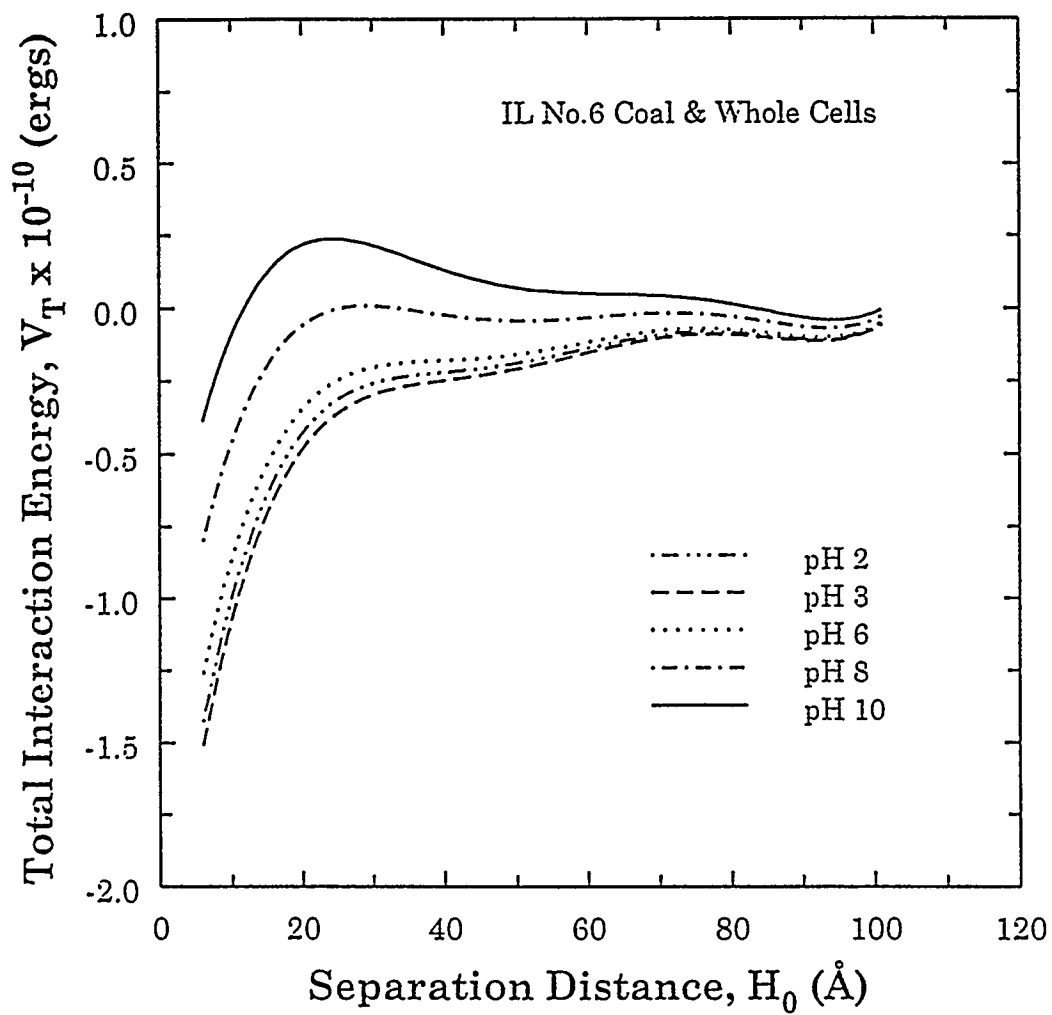


Figure 4.42 The variation of total interaction energy as a function of separation distance at different pH values for IL No.6 coal and whole cells

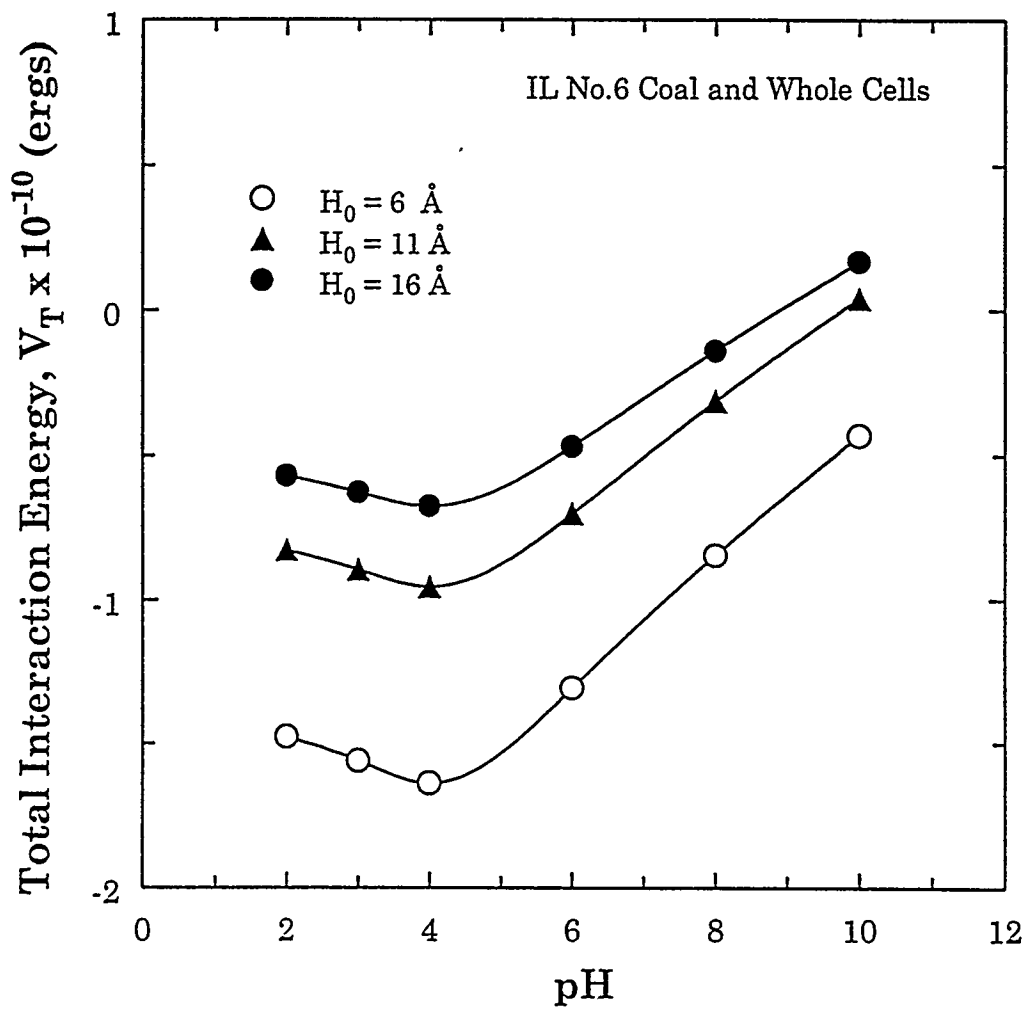


Figure 4.43 Effect of pH on the total interaction energy for IL No.6 coal and whole cells of *M. phlei*

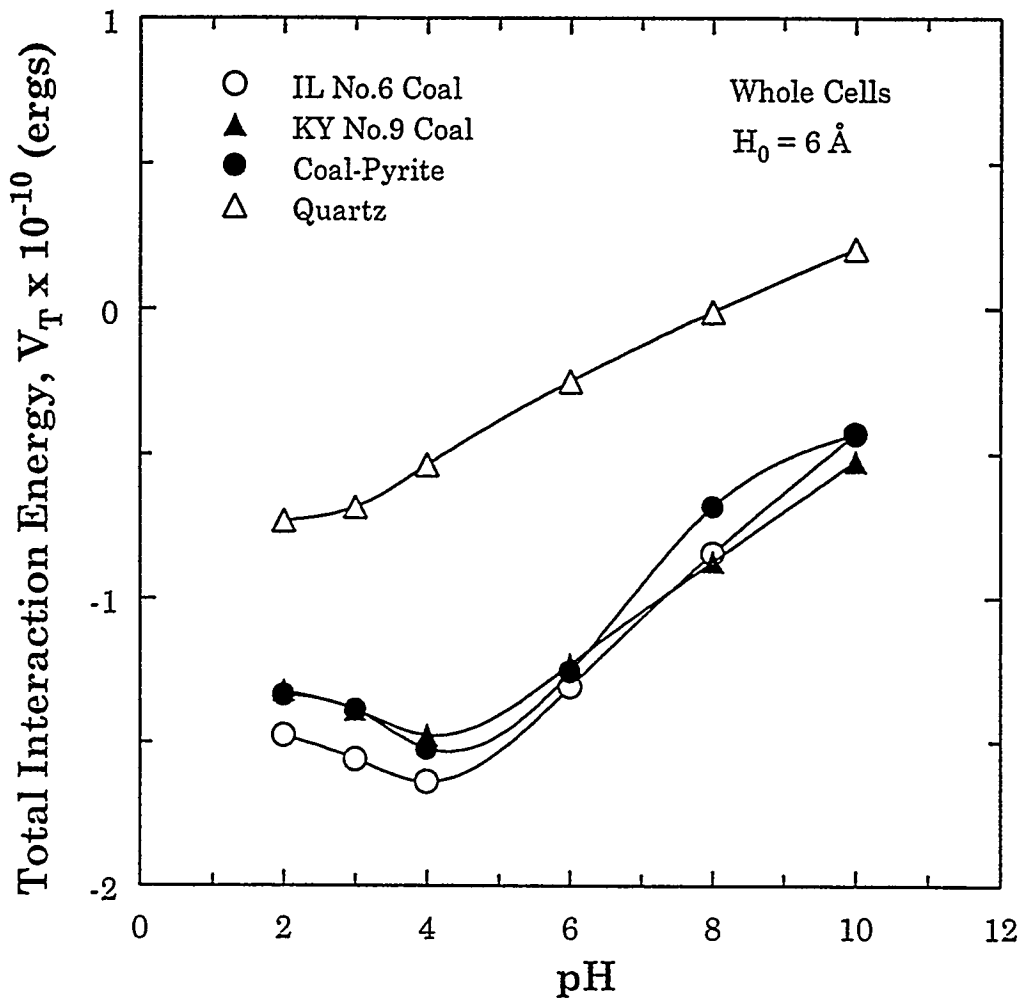


Figure 4.44 Comparison of total interaction energies for coal, coal-pyrite and quartz with whole cells of *M. phlei* as a function of pH

the interaction energies were very similar to that of coal. This means that *M. phlei* would adhere to coal-pyrite as strongly as it does to coal which is, however, not the case. One of the reasons could be that the values of zeta potential of coal-pyrite measured may not be the true values. Since the surface of coal-pyrite is covered with coal/carbonaceous matter, the zeta potentials may be of the coal particles rather than of the pyrite particles. Also, the dielectric constant of water is used for calculations; but the dielectric constant of bound water is different from that of the bulk water and is dependent on the surface property of the mineral.

Further, the interaction energy calculations for the sonicated cell/mineral interface were also calculated. Figure 4.45 compares the interaction energies of different samples with sonicated cells as a function of pH. A minimum in interaction energy occurred in all cases studied. This corroborates well with the adhesion and flocculation results with sonicated cells where a maximum was observed at around pH 6. It is also interesting to note that the magnitude of interaction energy with sonicated cells is less negative when compared with whole cells.

Figure 4.46 compares the interaction energies for whole cell/coal and sonicated cell/coal interface for IL No.6 coal. It is clear that upon sonication the

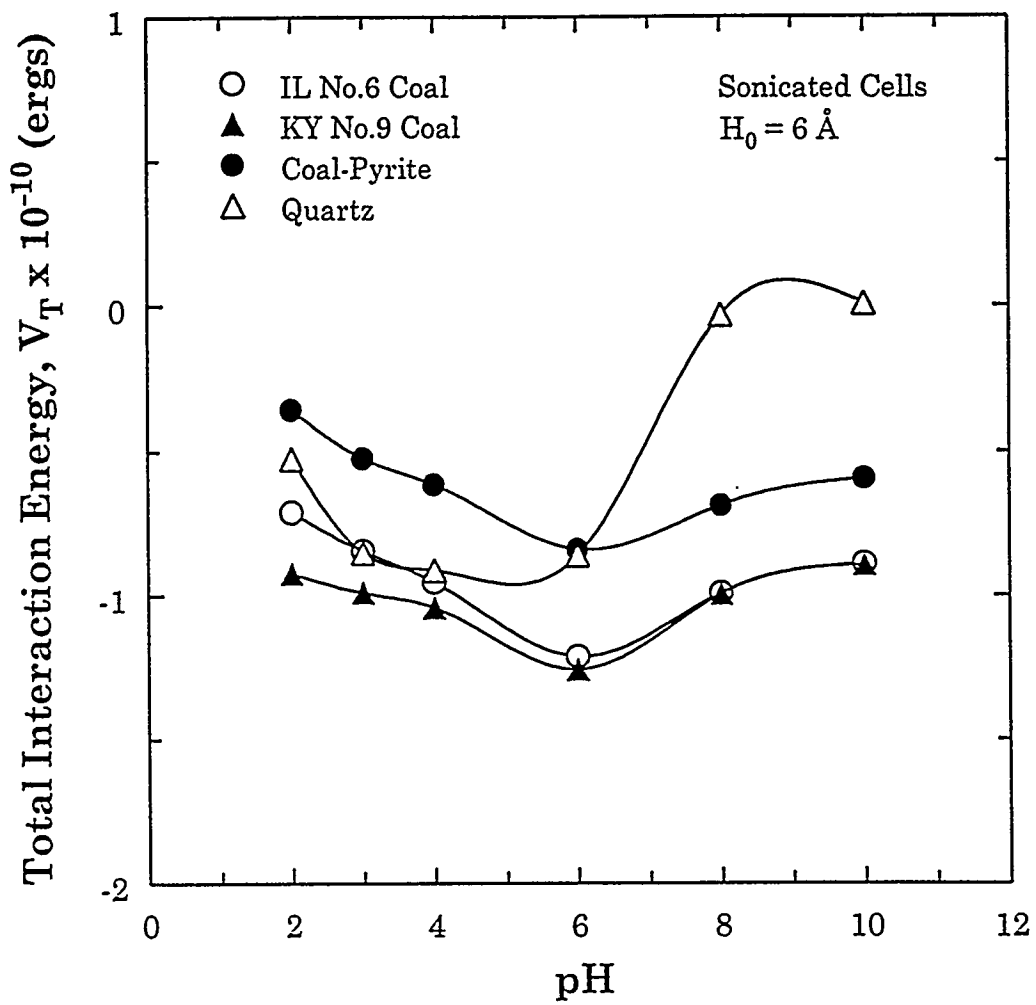


Figure 4.45 Comparison of total interaction energies for coal, coal-pyrite and quartz with sonicated cells of *M. phlei* as a function of pH



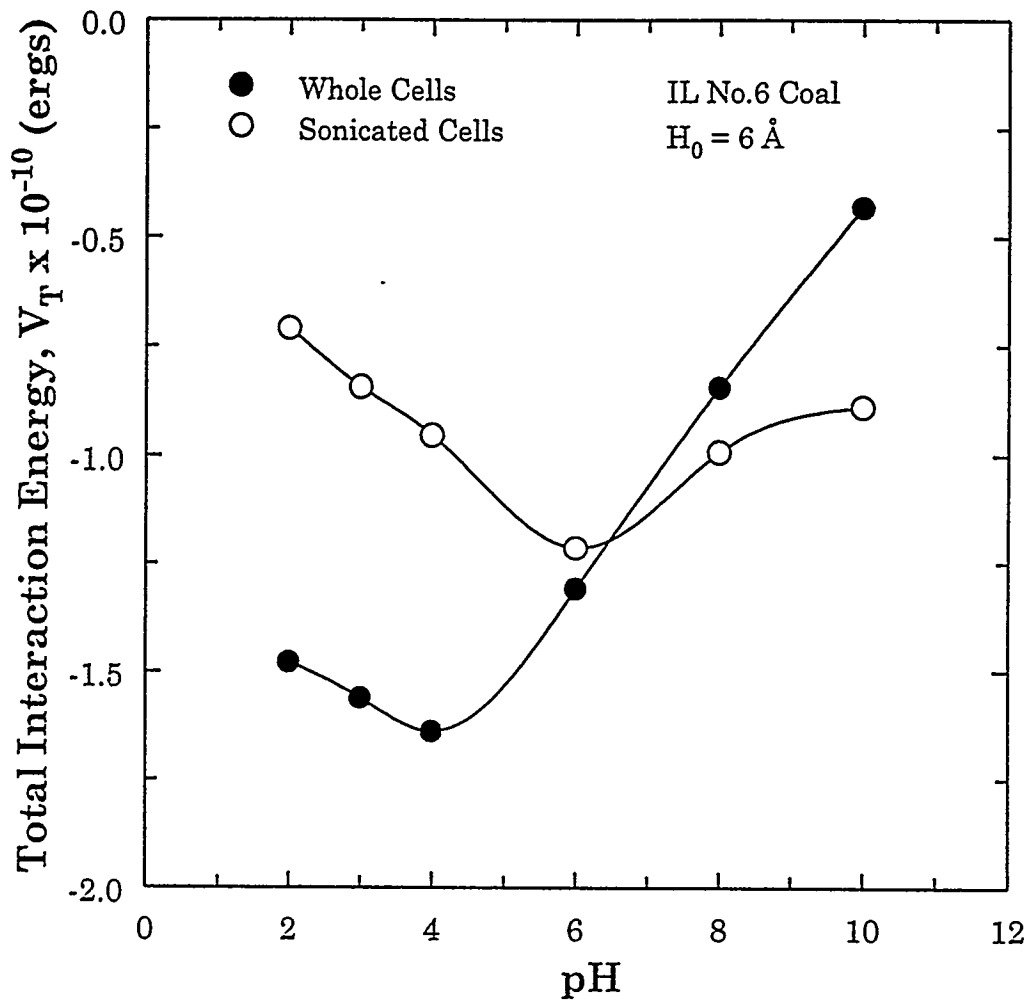


Figure 4.46 Comparison of interaction energies for whole cell/coal and sonicated cells/coal interface for IL No.6 coal

surface of the bacterial cell becomes less hydrophobic and more positively charged. This leads to a substantial decrease in interaction energy when compared with whole cells, which in turn decreases the amount of sonicated cells adhering to the coal surface. Similar results were also observed with other minerals and are shown in Figures 4.47-4.49. These results demonstrate that an increase in interaction energy results in less adhesion of sonicated cells when compared to whole cells.

From the above calculations (Figure 4.44), it is clear that if columbic interactions were the determining factor (according to the DLVO theory) then the same interactions would not distinguish between the coal and pyrite samples in terms of adhesion and their flocculation efficiency. But, adhesion tests showed that *M. phlei* attaches preferentially to coal in comparison to coal-pyrite. Also, the amount of *M. phlei* adhering to IL No.6 coal is much greater than that adhering onto KY No.9 coal. Therefore, the results of adhesion and flocculation tests cannot be explained adequately by DLVO theory. However, a more reasonable explanation can be offered from the consideration of hydrophobic interactions.

The importance of hydrophobic interactions becomes apparent from the examination of contact angle data of the two coal samples. Contact angle

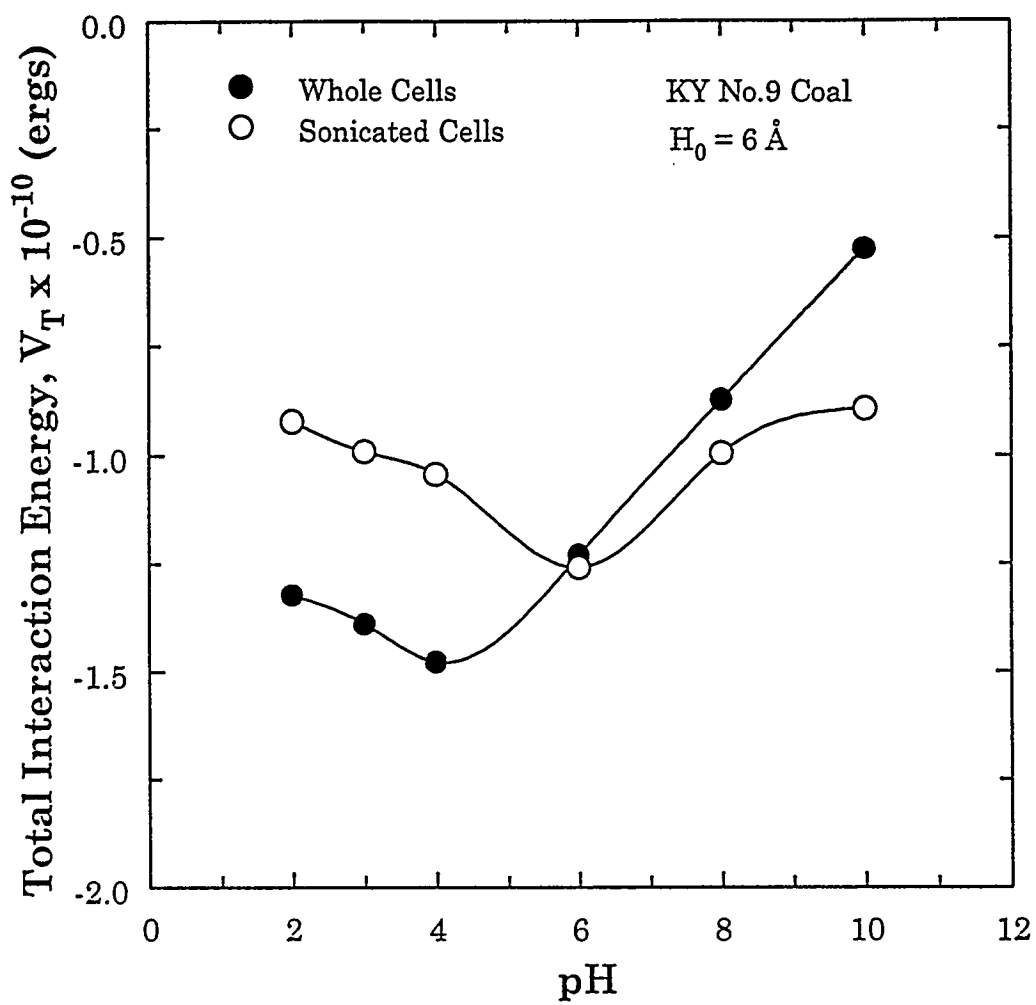


Figure 4.47 Comparison of interaction energies for whole cells/coal and sonicated cells/coal interface for KY No.9 coal

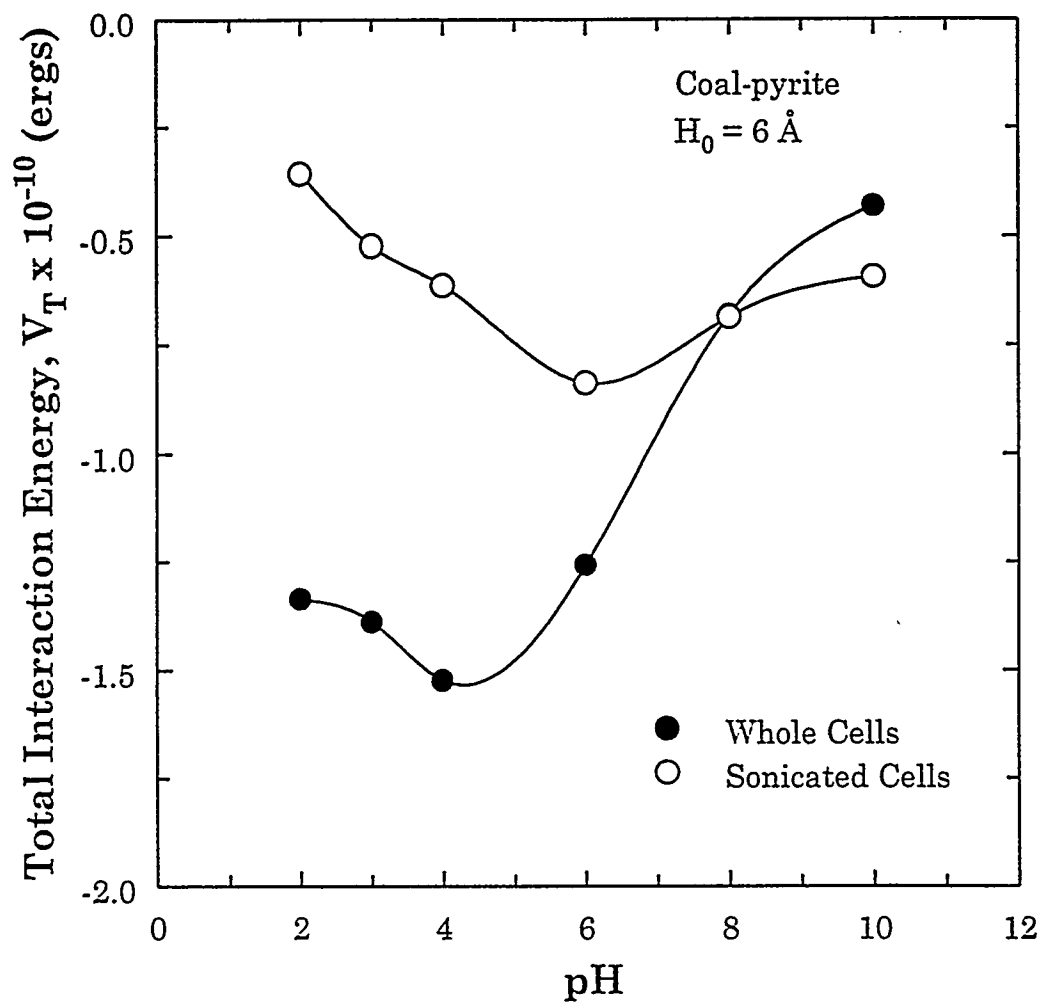


Figure 4.48 Comparison of interaction energies for whole cell/coal-pyrite and sonicated cells/coal-pyrite interface

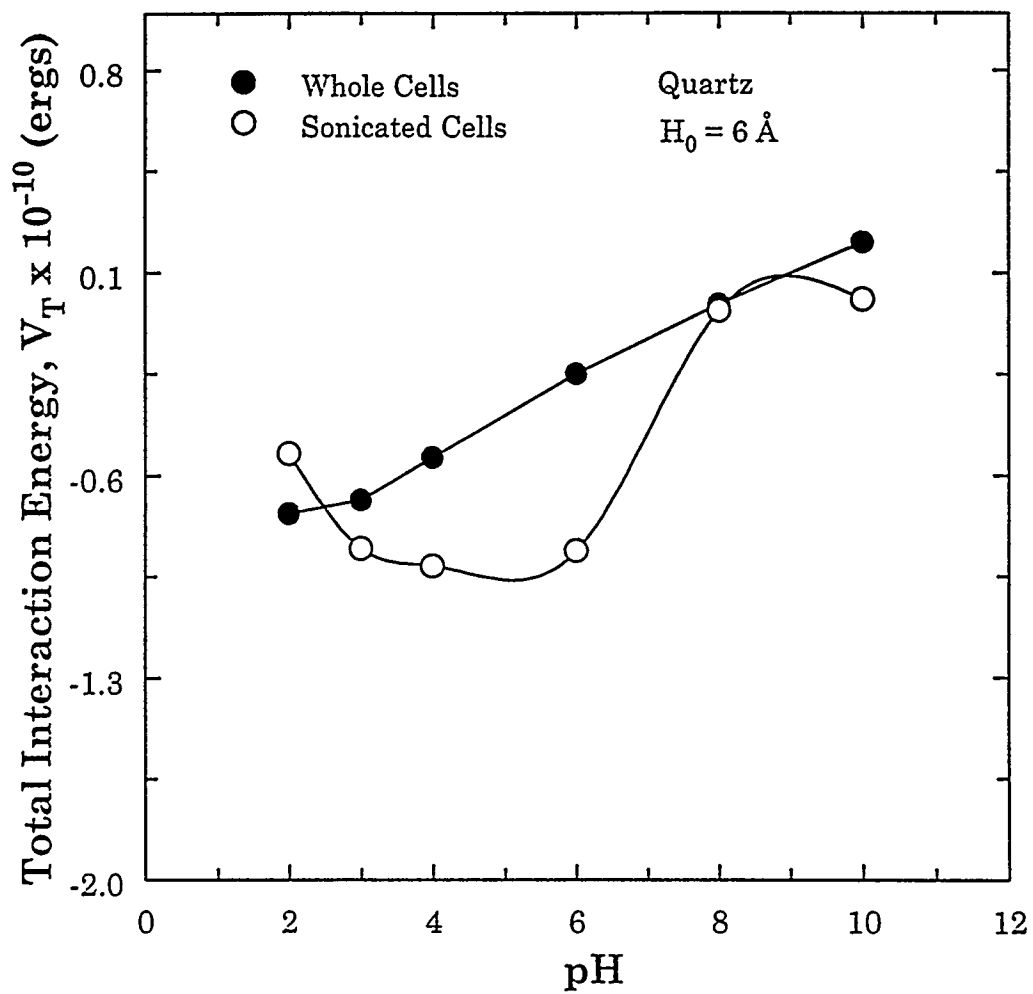


Figure 4.49 Comparison of interaction energies for whole cells/quartz and sonicated cells/quartz interface

measurements clearly indicate that IL No.6 coal is relatively more hydrophobic than KY No.9 coal. Hydrophobic interactions between IL No.6 coal and *M. phlei* are probably responsible for the differential adhesion of bacteria. At this time, there is no convincing theory or method which can be used to estimate the energy due to hydrophobic interactions. Only one method exists which can be used to obtain an approximation for the hydrophobic interaction energy. The theory of this method and the results obtained are discussed in the following section.

#### 4.8.2 *Hydrophobic Interaction Energy*

Hydrophobic interaction between hydrophobic surfaces immersed in water, which is largely entropic, arises mainly from the configurational rearrangement of water molecules around the surfaces, and forces the hydrophobic particles to come together. It is believed that hydrophobic interaction energies cannot be accounted for by conventional theories of van der Waals forces. Despite several recent attempts (Eriksson et al., 1989; Attard, 1989; and Ruckenstein and Churaev, 1991) to provide a theoretical model or explanation for hydrophobic interaction, i.e., the phenomenological theory on the basis of experiments and the hydrodynamic theory, the origin of hydrophobic interaction remains unknown.

In the early 1980s, Israelachvili and his colleagues (1984) directly measured the hydrophobic interaction force acting between two mica surfaces rendered hydrophobic by the cationic surfactant hexadecyltrimethylammonium bromide in aqueous solution and presented an empirical expression of the force,

$$F_{HI} = -0.14 \alpha \exp(-h/1.0) \quad (4.13)$$

where  $\alpha$  is the radius of the spherical particle (in m),  $h$  is the shortest distance between the particles (nm), and  $F_{HI}$  is the hydrophobic interaction force (N).

In recent years, many researchers have studied the direct measurement of hydrophobic force (Claesson and Christenson, 1988; Rabinovich and Derjaguin, 1988; and Christenson et al., 1992). All of them have shown that the hydrophobic force obeys an exponential relationship to separation distance, and can be expressed as

$$F_{HI} = \alpha C \exp(-h/h_0) \quad (4.14)$$

where

$$C = 2.51 \times 10^{-3} \text{ Nm}^{-1}$$

$$h_0 = 12.2 \pm 1.0 \text{ nm}$$

They also pointed out that the interaction force and decay length depend on the

degree of hydrophobicity. After direct measurement of attractive force between the hydrophobic silica filaments ( $\theta=100$ ) and silica filaments immersed in water, Rabionvich and Derjaguin (1988) modified equation 4.14 by introducing a coefficient of incomplete surface hydrophobicity  $k_1$ . Hence, equation 4.14 becomes

$$F_{HI} = -2.51 \times 10^{-3} \alpha k_1 \exp(-h / h_0) \quad (4.15)$$

$$h_0 = k_1 (12.2 \pm 1.0) \text{ nm} \quad (4.16)$$

where  $0 \leq k_1 \leq 1$ .

Song and Lu (1994) have shown that the hydrophobic adhesion force is an exponential function of the hydrophobicity represented by the contact angle of up to  $\theta = 60^\circ$ . In the case of the *M. phlei*/coal system, the maximum contact angle is in the range of  $65-70^\circ$ . Therefore, it is reasonable to assume that the exponential function is valid for the case of *M. phlei*/coal system. Consequently,  $k_1$  can be expressed as follows:

$$k_1 = \frac{\exp(\theta/100) - 1}{e - 1} \quad (4.17)$$



According to equation 4.17,  $k_1$  will equal 1 if  $\theta = 100^\circ$ , and if the particles are hydrophilic ( $\theta = 0^\circ$ ),  $k_1 = 0$  and  $F_{HI} = 0$ . In other words, there is no hydrophobic interaction force between hydrophilic particles. The final equation for the hydrophobic interaction potential energy ( $V_H$ ) between hydrophobic particles is as follows:

$$V_H = -2.51 \times 10^{-3} a k_1 h_0 \exp(-h / h_0) \quad (4.18)$$

If two particles of different radii and hydrophobicities are interacting, then the values of  $a$  and  $k_1$  can be estimated by using the harmonic mean of the two values.

From equation 4.18, the hydrophobic interaction energies for *M. phlei* whole cells/coal and *M. phlei* whole cells/coal-pyrite interface were calculated as a function of separation distance and the results are tabulated in Tables 4.8-4.10. The values for  $V_R$  and  $V_A$  have also been tabulated for comparison purposes.

Table 4.8 Potential energies of interaction for IL No.6 coal and  
*M. phlei* whole cells ( $10^{-10}$  ergs)

$H_0$ (nm)	$V_R$	$V_A$	$V_R + V_A$	$V_H$
1	-0.296	-0.7112	-1.131	-571.7
6	-0.0348	-0.1185	-0.1741	-234.57
11	-0.0063	-0.06466	-0.0823	-96.25
21	-0.00023	-0.03387	-0.0400	-16.20
51	0	-0.01394	-0.01683	-0.0773
71	0	-0.01001	-0.0118	-0.00219
100	0	-0.00741	-0.0087	-0.000025

Table 4.9 Potential energies of interaction for KY No.9 coal and  
*M. phlei* whole cells ( $10^{-10}$  ergs)

$H_0$ (nm)	$V_R$	$V_A$	$V_R + V_A$	$V_H$
1	-0.1797	-0.7113	-0.891	-271.54
6	-0.0206	-0.1185	-0.139	-78.00
11	-0.0037	-0.0646	-0.068	-22.41
21	-0.00014	-0.0339	-0.034	-1.85
51	0	-0.0139	-0.0139	-0.00104
71	0	-0.01001	-0.0100	-0.00
100	0	-0.00741	-0.0074	-0.00

Table 4.10 Potential energies of interaction for Coal-pyrite and *M. phlei* whole cells ( $10^{-10}$  ergs)

$H_0$ (nm)	$V_R$	$V_A$	$V_R + V_A$	$V_H$
1	-0.3506	-0.6	-0.9506	-492.47
6	-0.04103	-0.1	-0.141	-189.73
11	-0.00745	-0.0545	-0.0619	-73.09
21	-0.00027	-0.0285	-0.0288	-10.85
51	0	-0.0118	-0.01176	-0.0354
71	0	-0.00845	-0.00845	-0.0078
100	0	-0.00625	-0.00625	-0.00

From the above calculations, it is clear that the hydrophobic interaction energies are much greater than the interaction energies due to van der Waals forces. In all three cases, the hydrophobic interaction energies were found to be at least three orders of magnitude greater than the attractive energy. These results clearly point out the importance of hydrophobic interactions in determining the adhesion behavior of *M. phlei*.

When the hydrophobic interaction energies of the two coal samples are compared, the hydrophobic interaction energy of IL No.6 coal is twice that of KY No.9 coal. This can be attributed to the fact that IL No.6 coal is more hydrophobic than KY No.9 coal. This explains the fact that greater quantities of *M. phlei* adhere to IL No.6 coal than onto KY No.9 coal.

However, in the case of coal-pyrite, the hydrophobic interaction energy is close to that of IL No.6 coal, which means that *M. phlei* should adhere to coal-pyrite equally well. But, the experimental results obtained from adhesion tests (Figure 4.13) are contradictory to these results. Therefore, hydrophobic interaction energy calculations cannot adequately explain the adhesion behavior of *M. phlei* onto coal-pyrite. The exact reason is not clear at this time. It appears that along with the surface charge and hydrophobicity, the surface chemical composition might be a determining factor in controlling the adhesion of *M. phlei* onto coal and its associated impurities. Hence more experiments will be necessary to confirm the role of surface chemical composition in controlling the adhesion behavior of *M. phlei*.

## CHAPTER 5

### CONCLUSIONS

Based on the results obtained in the present study, the following conclusions were made :

- 1) The bacterium, *Mycobacterium phlei*, was found to be very hydrophobic and negatively charged above pH 2. The microorganism was of coccial shape with a diameter of about 1  $\mu\text{m}$ . Further, *M. phlei* was found to grow very rapidly.
- 2) Characterization studies of the cell wall revealed the presence of various functional groups (such as hydroxyl, carboxylic and phosphate) which are responsible for the negatively charged surface.
- 3) Sonication of the cells showed that about 40% of the cell is composed of extracellular surfactant. Fatty acid analysis of the released fraction

indicated the presence of 14 to 20 carbon chain length fatty acids. The fatty acids are primarily responsible for the hydrophobicity of the microorganism.

- 4) Also, sonication changed the surface charge of the organism. The IEP of the organism was shifted to a higher value (around pH 6) and this can be attributed to the loss of various functional groups during sonication.
- 5) Electrokinetic measurements of the coal samples, coal-pyrite, mineral pyrite and quartz showed that coal and coal-pyrite exhibited similar zeta potential-pH profiles with IEP's around pH 6. However, mineral pyrite exhibited a different trend with an IEP at pH 7. Quartz, as expected, had an IEP at pH 1.9.
- 6) Intrinsic hydrophobicity measurements showed that IL No.6 coal was more hydrophobic compared to KY No.9 coal. The lower hydrophobicity of KY No.9 coal might be due to its higher ash and lower carbon content. Similarly, coal-pyrite was found to be more hydrophobic than mineral pyrite which could be due to the presence of coal/carbonaceous material in the coal-pyrite matrix. All the minerals studied showed a maximum in the neutral pH range.

- 7) Adhesion of *M. phlei* to different mineral surfaces was found to be highly dependent on pH and concentration of the microorganism. Maximum adhesion of whole cells onto coal occurred in the pH range of 3.5-4.5 at a concentration of 200 ppm. Also, adhesion was found to be dependent on the hydrophobicity of the coal.
- 8) However, the amount of sonicated cells adhering to coal was significantly less when compared with whole cells. This could be due to the loss of extracellular surfactant from the cell wall of sonicated cells, which leads to lower hydrophobicity and hence lesser adhesion.
- 9) Upon adhesion of *M. phlei* whole cells, both the coal samples became more hydrophobic and the maximum contact angle shifted to lower pH values around pH 3-4. On the other hand, minimal or no increase in hydrophobicity was observed in the case of coal-pyrite, mineral pyrite and quartz. However, adhesion of sonicated cells had little effect on the surface hydrophobicity of coal.
- 10) Flocculation studies with IL No.6 and KY No.9 coal showed that flocculation was dependent on concentration of the microorganism and pH. Both whole cells and the released extracellular surfactant flocculated coal efficiently

and rapidly. Flocculation efficiencies on the order of 0.98 were obtained with extracellular surfactant over a wider pH range in comparison with whole cells. Further, the amount of extracellular surfactant required for flocculation was significantly less compared to whole cells.

11) Flocc separation was conducted using column flotation. These studies showed that flocculation followed by flotation with extracellular surfactant produced a better quality coal, with a combustible recovery of about 90% and pyritic and ash rejection of 78% and 59% respectively. In the case of whole cells the above numbers were slightly less, but still superior in comparison with conventional flotation using kerosene.

12) Interaction energy calculations using the extended DLVO theory showed that a minimum in interaction energy occurred for the mineral/whole cell interface at pH 4. This corresponds to the maximum in adhesion, contact angle and flocculation efficiency observed with both coal samples. However, the interaction energies could not provide an adequate explanation for the differential adhesion and flocculation behavior of *M. phlei* with the two coal samples.

13) Hydrophobic interaction energy calculations were performed for the coal



samples, coal-pyrite and *M. phlei*. Results showed that the contribution of hydrophobic interaction is significantly greater compared to the interaction energy due to van der Waal's forces. Also, the hydrophobic interaction for IL No.6 coal was greater than that for KY No.9 coal, indicating that the surface hydrophobicity of the sample plays a major role in determining the adhesion of *M. phlei* and hence flocculation of coal.

## REFERENCES

- Agarwal, J. C., Giberti, R. A. and Petrovich, L. J., 1976, U. S. Patent No. 3,960,513.
- Andrews, G. F. and Maczuga, J., 1984, "Bacterial Removal of Pyrite from Coal," *Fuel*, Vol. 63, pp. 297-302.
- Attard, P., 1989, *Journal of Physical Chemistry*, Vol. 93, p. 6441.
- Attia, Y. A. and Fuerstenau, D. W., 1982, "Feasibility of Cleaning High Sulfur Coal Fines by Selective Flocculation," *14th International Mineral Processing Congress*, Toronto, ON, Canada.
- Attia, Y. A., 1985, "Cleaning and Desulfurization of Coal Suspensions by Selective Flocculation," *Processing and Utilization of High Sulfur Coals*, Y. A. Attia, (Ed.), Elsevier, Amsterdam, pp. 267-285.
- Attia, Y. A., Yu, S. and Vecchi, S., 1987, "Selective Flocculation Cleaning of Upper Freeport Coal with a Totally Hydrophobic Flocculant," in *Flocculation in Biotechnology and Separation Systems*, Y. A. Attia, (Ed.), Elsevier, Amsterdam, pp. 547-564.
- Attia, Y. A., Bavarian, F. and Driscoll, K. H., 1988, "Use of Polyxanthate Dispersant for Ultra-fine Pyrite Removal from High Sulfur Coal by Selective Flocculation," *Coal Preparation*, Vol. 6, pp. 35-52.
- Attia, Y. A., Elzeky, M. and Ismail, M., 1993, "Enhanced Separation of Pyrite from Oxidized Coal by Froth Flotation Using Biosurface Modification," *International Journal of Mineral Processing*, Vol. 37, pp. 61-71.
- Ballester, A., González, F. and Blázquez, M. L., 1988, "Biolixiviación de Menas Naturales. Posibilidades Actuales de Utilización," *Revista de Metalurgia Madrid*, Vol. 24, No. 2, pp. 91-101.

Bensley, C. N., Swanson, A. R. and Nicol, S. K., 1977, "The Effect of Emulsification on the Selective Agglomeration of Fine Coal," *International Journal of Mineral Processing*, Vol. 4, pp. 173-184.

Bishop, J. P. and White, M. E., 1976, "Study of Particle Entrainment in Flotation Froths," *Proceedings of Institute of Mining and Metallurgy*, Vol. 85, pp. 191-194.

Blaschke, Z. and Sanak, S., 1975, "Separation of Silty Fractions from Coal Slimes by Selective Flocculation," *Zeszyty Naukowe Akademii Gorniczo-Huntniczeu, Cracow, Poland*, Vol. 66, pp. 191-194.

Bos, P. and Kuenen, J. G., 1990, "Microbial Treatment of Coal," in *Microbial Mineral Recovery*, H. L. Ehrlich and C. L. Brierley, (Eds.), McGraw Hill Publication Co., New York, pp. 343-377.

Brookes, G. F. et al., 1982, "The Selective Flocculation of Coal/Shale Mixtures Using Commercial and Modified Polyacrylamide Polymers," *14th International Mineral Processing Congress*, Toronto, ON, Canada.

Buchanan, R. E. and Gibbons, N. E., 1974, *Bergey's Manual of Determinative Bacteriology*, 8th Edition, The Williams and Wilkins Co., Baltimore, pp. 693-694.

Capes, C. E., 1989, "Liquid Phase Agglomeration : Process Opportunities for Economic and Environmental Challenges," *Challenges in Mineral Processing*, K. V. S. Sastry and M. C. Fuerstenau, (Eds.), SME, Littleton, CO, pp. 237-251.

Capes, C. E. et al., 1973, "Bacterial Oxidation in Upgrading Pyritic Coals," *CIM Bulletin*, pp. 1-4.

Chapelle, F. H., 1992, *Ground-Water Microbiology and Geochemistry*, John Wiley and Sons, New York.

Cheh, C. H., Glass, R. W. and Sehgal, R., 1982, "Solvent Recovery for the Oil Agglomeration Coal Cleaning Process," Preprint No. 82-48, SME-AIME Annual

Meeting, Dallas, TX, Feb. 14-18.

Chen, S., 1992, M. S. Thesis, University of Nevada, Reno.

Chi, S. -M., Morsi, B. I., Klinzing, G. E. and Chiang, S. -H., 1989, "LICADO Process for Fine Coal Cleaning," *Coal Preparation*, Vol. 6, pp. 241-263.

Christenson, H. K., Claesson, P. M., and Parker, J. L., 1992, *Journal of Physical Chemistry*, Vol. 96, p. 6725.

Claeson, P. M. and Christenson, H. K., 1988, *Journal of Physical Chemistry*, Vol. 92, p. 1650.

Couch, G. R., 1987, "Biotechnology and Coal," *IEA Coal Research*, London.

Derjaguin, B. V. and Landau, L. D., 1941, "Theory of the Stability of Strongly Charged Lyophobic Sols and of the Adhesion of Strongly Charged Particles in Solution of Electrolytes," *Acta Physicochim USSR*, Vol. 14, pp. 633-662.

Dixon, B., 1985, "Bacterial Remedy for Acid Rain," *Biotechnology*, Vol. 3, No. 9, p. 113.

Dugan, P. R. and Apel, W. A., 1978, "Microbial Desulfurization of Coal," in *Metallurgical Applications of Bacterial Leaching and Related Microbiological Phenomena*, L. A. Murr, A. E. Torma and J. A. Brierly, (Eds.), Academic Press, New York, pp. 223-250.

Eligwe, C. A., 1988, "Microbial Desulfurization of Coal," *Fuel*, Vol. 67, pp. 451-458.

Elzeky, M. and Attia, Y. A., 1987, "Coal Slurries Desulfurization by Flotation using Thiophilic Bacteria for Pyrite Depression," *8th International Symposium on Coal Slurry Fuels Preparation and Utilization*, Orlando, FL.

Engelbrecht, J. A. and Woodburn, E. T., 1975, "The Effects of Froth Height,

Aeration Rate and Gas Precipitation on Flotation," *Journal of South African Institute of Mining and Metallurgy*, Vol. 76, pp. 125-132.

Eriksson, K., Ljunggren, S. and Claesson, P. M., 1989, *Journal of Chemical Society of Faraday Transactions*, Vol. 85, p. 163.

Finch, J. A. and Dobby, G. S., 1990, *Column Flotation*, Pergamon Press, London.

Fowkes, F. M., 1967, "Attractive Forces at Interfaces," *Industrial Engineering and Chemistry*, Vol. 56, No. 12, pp. 40-52.

Friedman, S., LaCount, R. B. and Warzinski, R. P., 1977, "Chemical Desulfurization," in *Chemical and Physical Methods of Desulfurization*, T. D. Wheelock, (Ed.) ACS, Washington, DC, pp. 164-172.

Good, R. J., Srivatsa, N. R., Islam, M., Huang, H. T. L. and van Oss, C. J., 1990, "Theory of the Acid-Base Hydrogen Bonding Interactions, Contact Angles, and the Hysteresis of Wetting: Application to Coal and Graphite Surfaces," *Journal of Adhesion Science and Technology*, Vol. 4, No. 8, pp. 607-617.

Groppo, J., 1986, "Column Flotation Shows Higher Recovery with Less Ash," *Mining Engineering*, August, p. 36.

Hucko, R., 1977, "Beneficiation of Coal by Selective Flocculation : A Laboratory Study," Report of Investigations 8234, USBM.

Hucko, R., Gala, G. B. and Jacobsen, P. S., 1988, "Status of DOE-Sponsored Advanced Coal Cleaning Processes," in *Industrial Practice of Fine Coal Cleaning*, R. R. Klimpel and P. T. Luckie, (Eds.), SME, Littleton, CO, pp. 159-210.

Isibister, J. D. et al., 1985, "Companion Processes for Removal of Sulfur and Ash from Coal," *Proceedings of 2nd Annual Pittsburgh Coal Conference*, Pittsburgh, PA.

Israelachvili, J. N. and Pashley, R. M., 1984, *Journal of Colloid and Interface Science*, Vol. 98, p. 500.

James, A. M., 1991, in *Microbial Cell Surface Analyses; Structural and Physicochemical Methods*, N. Mozes, P. S. Handley, H. J. Busscher and P. G. Rouxhet, (Eds.), VCH Publishers, New York, p. 21.

Kargi, F., 1986, "Microbial Methods for Desulfurization of Coal," *Trends in Biotechnology*, Vol. 4, pp. 293-297.

Kempton, A. G. et al., 1980, "Removal of Pyrite from Coal by Conditioning with *Thiobacillus Ferroxidans* Followed by Oil Agglomeration," *Hydrometallurgy*, Vol. 5, pp. 117-125.

Kim, C. W., Kim, S. -K., Rha, C. and Robinson, E., 1987, "Removal of Cell and Cell Debris by Electrostatic Adsorption of Positively Charged Polymeric Particles," in *Flocculation in Biotechnology and Separation Systems*, Y. A. Attia, (Ed.), Elsevier, Amsterdam, pp. 429-440.

Luttrell, G. H., Weber, A. T., Adel, G. T. and Yoon, R. -H., 1988, "Microbubble Flotation of Fine Coal," *Column Flotation '88*, K. V. S. Sastry, (Ed.), SME, Littleton, CO, pp. 205-211.

Lynch, A. J., 1981, *Mineral and Coal Flotation Circuits : Their Simulation and Control*, Elsevier, Amsterdam.

Markuszewski, R., Wei, C. -K. and Wheelock, T. D., 1980, "Oxydesulfurization of Coal Treated with Methyl Iodide - Implications on Removal of Organic Sulfur," *Division of Fuel Chemistry, ACS*, Vol. 25, pp. 187-194.

Meyers, R. A., 1989, U. S. Patent No. 3,768,988.

Miller, J. D. and Misra, M., 1985, "Carbon Dioxide Flotation of Fine Coal," *Coal Preparation*, Vol. 2, pp. 69-73.

Miller, J. D., Ye, Y. and Jin, R., 1989, "Improved Pyrite Rejection by Chemically-Modified Fine Coal Flotation," *Coal Preparation*, Vol. 6, pp. 151-166.

Miller, K. J., 1988, "Novel Flotation Technology: A Survey of Equipment and Processes," in *Industrial Practice of Fine Coal Cleaning*, R. R. Klimpel and P. T. Luckie, (Eds.), SME, Littleton, CO, pp. 347-363.

Minneken, D. E., 1982, "Lipids, Complex Lipids, their Chemistry, Biosynthesis and Roles," in *The Biology of Mycobacteria*, C. Ratledge and J. L. Stanford, (Eds.), Academic Press, London, Vol. 1, p. 95.

Misra, M., Smith, R. W. and Dubel, J., 1991, "Bioflocculation of Finely Divided Solids," in *Mineral Bioprocessing*, R. W. Smith and M. Misra, (Eds.), TMS, Warrendale, PA, pp. 91-103.

Misra, M., Chen, S. and Smith, R. W., 1991, "Kerogen Aggregation using a Hydrophobic Bacterium," in *Mineral Bioprocessing*, R. W. Smith and M. Misra, (Eds.), TMS, Warrendale, PA, pp. 133-140.

Murphy, J. et. al., 1985, "Coal Desulfurization by Microbial Processing," *Processing and Utilization of High Sulfur Coals*, Y. A. Attia, (Ed.), Elsevier, Amsterdam, pp. 643-652.

Ohmura, N. and Saiki, H., 1994, "Desulfurization of Coal by Microbial Column Flotation," *Biotechnology and Bioengineering*, Vol. 44, pp. 125-131.

Olson, G. J. and Brinkmann, F. E., 1986, "Bioprocessing of Coal," *Fuel*, Vol. 65, pp. 1638-1646.

Palmes, J. R. and Laskowski, J. S., 1993, "Effect of the Properties of Coal Surface and Flocculant Type on the Flocculation of Fine Coal," *Minerals and Metallurgical Processing*, Vol. 10, No. 4, pp. 218-221.

Parekh, B. K., Slotts, W. F., and Groppo, J. G., 1990, "Column Flotation Studies of Ultra-fine Coals," *Processing and Utilization of High Sulfur Coals III*, R.

- Markuszewski and T. D. Wheelock, (Eds.), Elsevier, Amsterdam, pp. 197-208.
- Pratt, D., 1952, "Nutrition of *Mycobacterium phlei*, I. Requirements for Rapid Growth," *Journal of Bacteriology*, Vol. 64, p. 651.
- Rabinovich, Y. and Derjaguin, B. V., 1988, *Colloids and Surfaces*, Vol. 30, p. 243.
- Raichur, A. M., 1992, M. S. Thesis, University of Kentucky, Lexington, KY.
- Reddy, H. P., Burra, S. S. and Murthy, P. S., 1992, "Correlation Between Calmodulin-like Protein, Phospholipids, and Growth in Glucose-grown *Mycobacterium phlei*," *Canadian Journal of Microbiology*, Vol. 38, p. 339.
- Richardson, C. K. et al., 1986, "Chemical Cleaning of Illinois No.6 Coal Using a Microwave/Caustic Treatment," *Proceedings of 3rd Annual Pittsburgh Coal Conference*, Pittsburgh, PA, pp. 130-141.
- Ruckenstein, E. and Churaev, N., 1991, *Journal of Colloid and Interface Science*, Vol. 147, p. 535.
- Schubert, R. M., 1974, "Method for the Treatment of Coal Washery Wastes," U. S. Patent No. 3,856,668.
- Silverman, M. P., Rogoff, M. H. and Wender, I., 1963, "Removal of Pyritic Sulfur from Coal by Bacterial Action," *Fuel*, Vol. 42, pp. 113-124.
- Song, S. and Lu, S., 1994, "Hydrophobic Flocculation and Fine Hematite, Siderite, and Rhodochrosite Particles in Aqueous Solution," *Journal of Colloid and Interface Science*, Vol. 166, pp. 35-42.
- Suuatri, M. and Laakso, S., 1993, "Effect of Growth Temperature on the Fatty Acid Composition of *Mycobacterium phlei*," *Archives of Microbiology*, Vol. 159, p. 119.
- Torma, A. E., 1977, "The Role of *Thiobacillus ferrooxidans* in Hydrometallurgical



Process," *Advances in Biochemical Engineering*, Vol. 6, pp. 1-37.

van Loosdrecht, M. C. M., 1988, Bacterial Adhesion, Doctoral Dissertation, The Agricultural University, Wageningen, The Netherlands.

Verwey, E. J. W. and Overbeek. J. Th. G., 1946, "Long Distance Forces Acting Between Colloidal Particles," *Transactions of the Faraday Society*, 42B, pp. 117-123.

Viser, J., 1972, "On Hamaker Constants: A Comparison Between Hamaker Constants and Lifschitz-van der Waals Constants," *Advances in Colloid and Interface Science*, Vol. 3, pp. 331-363.

Yoon, R. -H. and Luttrell, G. H., 1989, "The Effect of Bubble Size on Fine Particle Flotation," *Mineral Processing and Extractive Metallurgy Review*, Vol. 5, pp. 101-122.

Yoon, R. -H., 1991, "Advanced Coal Cleaning," in *Coal Preparation*, J. W. Leonard (Ed.), 5th edition, pp. 966-1005.

Zavitsanos, P. D., 1980-82, "Coal Desulfurization by Microwave Process," Technical Progress Reports, DOE Contract No. DE-AC22-80PC30142.

Zurubina, N. N., Lyalikova, N. N. and Shmuk, E. I., 1959, "Investigation of Microbial Oxidation of Coal Pyrite," *Invest. Akad. Nank. SSR. Oteadl, Tekh, Mauk. Me. Toplivo.*, Vol. 1. pp. 117-119.